Identification and characterization of secreted stage-related proteins from the nematode *Strongyloides ratti* with putative relevance for parasite-host relationship: small heat shock proteins 17 and a homologue of the macrophage migration inhibitory factor

DISSERTATION

zur Erlangung der Würde des Doktors der Naturwissenschaften

des Fachbereiches Biologie, der Fakultät für Mathematik, Informatik

und Naturwissenschaften, der Universität Hamburg

vorgelegt von

Abuelhassan Elshazly Ahmed Younis

aus Aswan, Ägypten

Hamburg, Juli 2011

Genehmigt vom Fachbereich Biologie
der Fakultät für Mathematik, Informatik und Naturwissenschaften
an der Universität Hamburg
auf Antrag von Priv. Doz. Dr. N. BRATTIG
Weitere Gutachterin der Dissertation:
Frau Prof. Dr. I. BRUCHHAUS
Tag der Disputation: 15. Juli 2011

Hamburg, den 30. Juni 2011

Professor Dr. Axel Temming
Leiter des Fachbereichs Biologie

Language Certificate

As a native English speaker, I have read and corrected the present PhD thesis and hereby confirm that it complies with the rules of the English language.

Hamburg, 10 May 2011

(Dr. Kathleen E. Rankin)

DEDICATION

To the brave Egyptian heroes of the 25th of January in El-Tahrir place, in Cairo and all over Egypt, you taught us how to be the revolution.

To the Egyptian army who saved its people until they got their freedom.

CONTENTS

ACKNOWLEDGEMENTS

Nobody can work independently and the completion of a thesis is a challenge. Many people from multiple universities and departments have assisted me in developing various aspects of this research project and guiding me.

First and foremost, I need to thank my supervisor, PD Dr. Norbert Brattig. I have the pleasure to get his acceptance to work in his laboratory in the Bernhard Nocht Institute for Tropical Medicine (BNI), Hamburg, and work with him. He provided me guidance and assistance when I needed it most, but also allowed me to figure things out on my own and work with him to develop this project. I am very thankful that everything turned out as it has.

My sincere appreciation is also expressed to PD Dr. Klaus Erttmann for his advice and discussions.

Without Prof. Eva Liebau (Department of Molecular Physiology, Muenster University), finishing my work at times would not have been possible. She allowed me to use part of her lab for two months and gave me many helpful tips and guidance, both on this project and for my future. I want to thank her and everyone there for making me feel so welcome, especially her doctoral student Irene Ajonina-Ekoti who introduced me to the secrets of protein expression and purification.

Many thanks to Prof. Dr. Iris Bruchhaus (BNI) for her kind interview introducing me to the biology department in my first days in the BNI and to Prof. Dr. Lothar Renwrantz (Zoology Institute, Hamburg University) for his comments and suggestions throughout my thesis research.

My sincere appreciation I point out for Prof. Dr. Thorsten Burmester (Zoology Institute, University of Hamburg) and the Biology Department committee for the evaluation of my master's thesis and for giving me the opportunity to perform a doctoral thesis at the University of Hamburg. I would also like to acknowledge all the Ph.D committee members, for taking time from their busy schedule to co-evaluate my thesis.

I would also like to thank the teaching staff of the graduate molecular biology course, especially PD Dr. Irm Hermans-Borgmeyer and Thomas Tilling (ZMNH, Hamburg University), who introduced me to molecular biology.

Thanks to the present and former members of the Brattig/Erttmann laboratory: Frank Geisinger, Hanns Soblik, Silke van Hoorn, Yasmina Tazir, Vera Steisslinger and Kerstin Krausz, who showed me many methods and techniques. Many thanks for the useful discussions and the lab support. The veterinary team of the Bernhard Nocht Institute for

Tropical Medicine is also acknowledged. I want to thank all the BNI members, including those not mentioned here by name. I have many great memories from my time here at the BNI and I am going to miss the friendly and stimulating environment I have found here.

I am grateful to the Faculty of Science at Aswan, Egypt and the Egyptian Ministry of Higher Education for generously providing me a PhD scholarship and the fund for me and my family. My sincere appreciation is also expressed to the Culture and Mission Department in the Egyptian embassy in Berlin for their continuous help through the four years.

I would like to thank Dr. Kathleen Rankin (BNI) for the evaluation of the English language of this thesis.

I would like to thank my family for their support throughout the length of this journey, especially my mother, my brothers and sisters as well as my extended family - friends back home - who were crucial to my success and praying for me daily.

No words are enough to thank my wife, Safaa, what to say? She left the home, family and friends to be with me and to care for me and our children Hind and Ahmed who are also acknowledged because they are the reason to continue. You are the most important in my life. Thank you.

ABBREVIATIONS

%	Percentage
(v/v)	Volume per volume
(w/v)	Weight per volume
mRNA	Messenger RNA
nm	Nanometer
RNase	Ribonuclease
rpm	Rotations per minute
v	Volt
w	Watt
µl	Microlitre
µm	Micromolar
°C	Celsius
aa	Amino acid
Ab	Antibody
ABC	Human alpha-B- crystallin protein
ACD	Alpha-crystallin domain
APS	Ammonium persulfate
BLAST	Basic local alignment search tool
BNI	Bernhard Nocht Institute
bp	Base pair
BSA	Bovine serum albumin
CD	Cluster of differentiation
cDNA	Complementary DNA
cm	Centimetre
conc.	Concentrated
C-terminal	Carboxy-terminal
d	Day
da	Dalton
DEPC	Diethylpyrocarbonate
DMEM	Dulbecco's modified Eagles's medium
DNA	Deoxyribonucleic acid
DNase	Deoxyribonuclease
dNTP	Deoxyribonucleotide triphosphate

DTT	Dithiothreitol
EDTA	Ethylenediaminetetraacetic acid
ELISA	Enzyme-linked immuno-sorbent assay
ESP	Excretory-secretory proteins
EST	Expressed sequence tag
et al.	Et alii
EtBr	Ethidium bromide
EU	Endotoxic Unit(s)
FCS	Fetal calf serum
Fig.	Figure
FITC	Fluorescein isothiocyanate
FLs	Free-living stages
g	Gram
g	Acceleration of gravidity
Gal	Galectin
h	Hour(s)
HBSS	Hanks balanced salt solution
HPP	p-hydroxyphenylpyruvate
HRP	Horseradish peroxidase
HSP	Heat shock protein
Hu	Human
IBD	Inflammatory bowel disease
IEC	Intestinal epithelial cells
IFN-gamma	Interferon-gamma
Ig	Immunoglobulin
IL	Interleukin
iL3	Infective third stage larvae
IPTG	Isopropyl-D-thiogalactopyranoside
kb	Kilo base pair
kDa	Kilodalton
l	Liter
LAL	Limulus amoebocyte lysate
LB	Lysogeny broth
LB	Luria broth
LC-MS/MS	Liquid chromatography tandem mass spectrometry

LDME	L-dopachrome methyl ester
LPS	Lipopolysaccharide
M	Molar
MDH	Malate dehydrogenase
MIF	Macrophage migration inhibitory factor
min	Minute
ml	Milliliter
mM	Millimolar
MNC	Mononuclear cells
MØ	Macrophages
MOPS	3-n(morpholino) propane sulfonic acid
NCBI	National Center for Biotechnology Information
ng	Nanogram
N-terminal	Amino-terminal
OD	Optical density
ORF	Open reading frame
PBL	Peripheral blood lymphocytes
PBS	Phosphate buffered saline
PCR	Polymerase chain reaction
PF	Parasitic females
pH	H+- concentration
PHA	Phytohaemagglutinin
PMB	Polymyxin B sulfate
PMN	Polymorphonuclear cells
POP	Prolyl oligopeptidase
qPCR	Quantitative PCR
RNA	Ribonucleic acid
RPMI	Roswell Park Memorial Institute medium
rRNA	Ribosomal RNA
RT	Reverse transcription
SDS PAGE	Sodium-dodecylsulfate polyacrylamide gel electrophoresis
sec	Seconds
sHSP	Small heat shock protein
Taq	Thermophilus aquaticus

TBS	Tris buffered saline
TE	Tris-EDTA-buffer
TEMED	Tetramethylethylenediamine
TGF-beta	Transforming growth factor beta
Th1/2	T-helper cell type 1 or 2
TNF-alpha	Tumor necrosis factor alpha
TPOR	Thiol-protein oxidoreductase
Treg	Regulatory T cell
Tris	Tris(hydroxymethyl)amino- methane
Tween	Polyoxyethylenglycolsorbitol-monooleate
u	Unit
X-Gal	5-bromo-4-chloro-3-indoyl- ß-d-galactopyranosid
µg	Microgram
µmol	Micromole

LIST OF FIGURES

LIST OF TABLES

1. ZUSAMMENFASSUNG

Eine große Anzahl von Biomolekülen, darunter viele Proteine, werden von Helminthen freigesetzt und tragen zur erfolgreichen Etablierung der Parasiten, zu deren Überleben und Vermehrung in einem zum Teil ungünstigen Lebensraum bei. Exkretorisch/sekretorische (E/S) Proteine wirken an der Interphase zwischen Parasit und Wirt und stellen potenzielle Ziele für eine Intervention dar. Der intestinale Nematode *Strongyloides* spp. weist eine außergewöhnliche Plastizität in seinem Lebenszyklus auf, der parasitisch und frei lebende Generationen umfasst. Dieser Parasit ist daher besonders gut geeignet, für die parasitische Lebensweise relevante Moleküle und das Wirtssystem beeinflussende Moleküle zu identifizieren.

In der vorliegenden Studie wurde zunächst die differentielle Expression von Genen, die exkretorisch/sekretorische Proteine kodieren, mit Hilfe der quantitativen RT-PCR untersucht. Dabei wurden Transkripte von infektiösen Larven (iL3), parasitären Weibchen (PW) und frei lebenden Weibchen (FW) des Rattenparasiten *Strongyloides ratti* analysiert, der ein genetisch nahverwandter Nematode des menschlichen Parasiten *Strongyloides stercoralis* ist. Diese Ergebnisse bestätigten die frühere Proteomanalyse der Arbeitsgruppe über stadien-spezifischen E/S Proteine von *S. ratti* (http://www.chemie.uni-hamburg.de/bibliothek/2009/DissertationSoblik.pdf). Die ausgewählten 19 Gene der untersuchten Stadien, die in der quantitativen RT-PCR analysiert wurden, waren:

(i) iL3: eine Astacin Metalloproteinase, Kohlenhydrat-bindende Proteine, ein Homolog des menschlichen Zytokins Makrophagen-Migrations-Inhibitionsfaktor

(ii) PW: eine Prolyloligopeptidase, kleine Hitzeschockproteine und Kohlenhydrat-bindende Proteine

(iii) FW: ein Protein der Lysozymfamilie und Kohlenhydrat-bindende Proteine

Im Rahmen der Untersuchungen über *Strongyloides*-Proteine, die von parasitären Weibchen im Darm freigesetzt werden, wurden weiterhin zwei kleine Hitzeschockproteine nachgewiesen. Die vollständigen Gensequenzen von *Sr*-HSP17a (cDNAs - 483 bp; ~19 kDa) und *Sr*-HSP17b (cDNAs - 474 bp; ~ 18 kDa) wurden identifiziert und zeigten eine 49% Übereinstimmung in der Aminosäuresequenz. Die genomische Organisation der Gene wurde analysiert. Beide Gene wiesen eine konservierte alpha-Kristallindomäne und einen variablen N-Terminus auf. Die *Sr*-HSP17-Proteine zeigten die höchste Homologie mit der abgeleiteten Hitzeschockproteinsequenz von *S. stercoralis*. Zur weiteren Charakterisierung wurden die HSPs rekombinant exprimiert und gereinigt. Nach Infektion sowie nach Immunisierung von

Ratten liess sich eine starke Immunogenität beider Proteine feststellen. Mit Hilfe gereinigter polyklonaler Antikörper konnten die nativen HSP17a,b-Proteine in Extrakten sowie E/S-Produkten von PW nachgewiesen werden und deren Stadienassoziation bestätigt werden. Durchflusszytometrische Analysen zeigten eine hemmbare Bindung von *Sr*-HSP17s an Monozyten/Makrophagen, jedoch keine Bindung an Lymphozyten oder neutrophile Granulozyten. Erstmalig konnte eine dosisabhängige Bindung von *Sr*-HSP17a, aber nicht von *Sr*-HSP17b an Epithelzellen des Rattendünndarms nachgewiesen werden. *Sr*-HSP17-exponierte Monozyten setzten außerdem das immunsuppressiv wirkende Zytokin IL-10 aber nicht das inflammatorische Zytokin TNF-alpha frei, was auf eine mögliche Wirkung des sekretierten Proteins bei lokalen Immunantworten hinweist.

In der vorliegenden Studie wurde weiterhin ein 13,5 kDa Homolog des Zytokins Makrophagen-Migrations-Inhibitionsfaktor (MIF) von *S. ratti* charakterisiert, der vor allem von iL3 freigesetzt wird, dessen Transkript auch in geringem Ausmaß in parasitären und frei lebende Weibchen nachweisbar war. Die komplette 372 bp cDNA wurde identifiziert und die Genstruktur analysiert. Die Sequenzanalyse zeigte erneut die höchste Homologie zu dem humanpathogenen *S. stercoralis*. Das rekombinant exprimierte und aufgereinigt *Sr*-MIF-Protein wies keine *in vitro* Tautomeraseaktivität auf. Eine Wirkung von *Sr*-MIF auf das Immunsystem des Wirtes zeigte sich an hohen IgG-Titern infizierter oder immunisierter Tiere. Durchflusszytometrische Analysen ergaben, daß *Sr*-MIF an Monozyten/Makrophagen nicht aber an Lymphozyten bindet. *Sr*-MIF induzierte die Freisetzung von IL-10 aber kaum von TNF-alpha aus peripheren Monozyten, was auf eine Wirkung des sekretierten Proteins auf das Wirtsimmunsystem hinweist.

In der vorliegenden Arbeit wurden zwei Hitzeschockproteine (*Sr*-HSP17s) und ein Zytokinhomolog, der Makrophagen-Migrations-Inhibitionsfaktor (*Sr*-MIF), molekular charakterisiert und eine Analyse ihrer biologischen Aktivität initiiert. Die Freisetzung der HSPs aus PW in den Dünndarm wie des Zytokinhomologs aus iL3 im Gewebe, deren Interaktion mit Zellen des natürlichen Abwehrsystems sowie die Bildung spezifischer Antikörper gegen die Parasitenproteine lassen deren Einfluß auf das intestinale mukosale Immunsystem bzw. das Gewebe annehmen, in das die iL3 eindringen, wobei sie möglicherweise beteiligt sind, die Etablierung der Parasitenstadien und deren Evasion zu fördern sowie möglicherweise auch zur lokalen Immunmodulation beitragen und die Homöostase der Gewebe beeinflussen.

2. SUMMARY

A wide range of biomolecules, including proteins, are excreted/secreted from helminths that contribute to parasites' successful establishment, survival and reproduction in an adverse habitat. Excretory/secretory proteins are active at the interface between parasite and host comprising potential targets for intervention. The intestinal nematode *Strongyloides spp.* exhibits an exceptional developmental plasticity in its life cycle characterized by parasitic and free-living generations. This parasite is therefore a good candidate for the exploration of parasite-host-relationships.

In the present study the differential expression of genes encoding the excretory/secretory proteins has been investigated by quantitative RT-PCR from infective larvae (iL3), parasitic females (PF) and free-living females (FF) of the rat parasite *Strongyloides ratti,* genetically very similar to the human pathogen *Strongyloides stercoralis*. This study confirms the previous proteomic analysis of the stage-specific ESP from *S. ratti* (http://www.chemie.uni-hamburg.de/bibliothek/2009/DissertationSoblik.pdf). The selected 19 genes from the investigated stages analysed in qRT-PCR included proteases, heat shock proteins, carbohydrate-binding proteins and a cytokine homologue. The stage-related transcripts comprised:

(i) iL3: an astacin metalloproteinase, carbohydrate-binding proteins and a homologue of the human cytokine macrophage migration inhibitory factor

(ii) PF: a prolyl oligopeptidase, small heat shock proteins and carbohydrate-binding proteins

(iii) FF: a lysozyme family member and carbohydrate-binding proteins

In search of proteins involved in the interaction of intestinal nematodes with the mammalian mucosal host cells, two small *Sr*-HSPs secreted by PF were investigated. The full-length gene sequences of *Sr*-HSP17a (cDNAs - 483 bp ; ~19 kDa) and *Sr*-HSP17b (cDNAs - 474 bp; ~18 kDa) were identified showing 49% amino acid identity and the genomic organization was analysed. The analysis of DNA and amino acid sequences showed that the two genes share a conserved alpha-crystallin domain and a variable N-terminus. The *Sr*-HSP17 proteins displayed the highest homology to the deduced small heat shock protein of the human parasite *S. stercoralis.* For further characterization, the proteins were recombinantly expressed and purified. We observed a strong immunogenicity of both proteins leading to high IgG responses following infection or immunization of rats. By applying the

purified polyclonal antibodies, both native *Sr*-HSP17s could be detected in the extract as well as the E/S products from PF, confirming their stage-associated expression. Flow cytometry analysis indicated the inhibitable binding of *Sr*-HSP17s to the monocytes/macrophage lineage but neither to peripheral lymphocytes nor neutrophils. A rat intestinal epithelial cell line also, showed dose-dependent binding of *Sr*-HSP17a but not of *Sr*-HSP17b. Exposed monocytes released IL-10 but not TNF-alpha in response to *Sr*-HSP17s, suggesting a possible involvement of the secreted female proteins in local host immune responses.

In addition, the 13.5 kDa *S. ratti* homologue of the human cytokine macrophage migration inhibitory factor (MIF) was characterized as primarily secreted from iL3 - while the transcript was also found at lower levels in parasitic and free-living females. The full-length 372 bp-cDNA was identified and the gene structure analyzed. Again, the sequence analysis showed the highest homology to the human pathogen *S. stercoralis* and both are related to the nematode MIF type-2. The recombinantly expressed and purified *Sr*-MIF exhibited no *in vitro* tautomerase activity. The exposure of *Sr*-MIF to the host immune system is indicated by demonstration of high IgG reactivities in hosts' sera following infection or immunization. Flow cytometry analysis revealed the inhibitable binding of *Sr*-MIF to the monocytes/ macrophage lineage but not to peripheral lymphocytes. After exposure to *Sr*-MIF, monocytes released significant levels of IL-10 but not TNF-alpha suggesting the involvement of the secreted parasite MIF in host immune responses.

In the present work two *Strongyloides* small heat shock proteins (*Sr*-HSP17s) and a cytokine homologue (*Sr*-MIF) have been identified, molecularly characterized and analyzed for their biological activity. The release of the small HSPs from PF into the host's intestine suggests their link to the mucosal host immune defense system. Further, the release of the MIF from iL3 may suggest a possible role of the *Sr*-MIF in their survival after invasion into host tissues. The exposure of *Sr*-HSP17s and *Sr*-MIF to the host's environment, verified by humoral and cellular reactions, displays their involvement in local parasite-host-interactions, improving their establishment and evasion mechanisms or contributing to immunomodulation and intestinal homeostasis.

3. INTRODUCTION

3.1. Intestinal parasitic nematodes

Nematodes are multicellular soft-body vermiform invertebrates which have successfully adapted to nearly every ecosystem, occupying both terrestrial and mostly aquatic habitats. They encompass the class Nematoda (thread) in the phylum Nemathelminthes (roundworms). Nematodes include a vast number of species; some 20,000 species have been described, including the completely sequenced genetic model organism *Caenorhabditis elegans.* Common predatory forms of the nematodes consume microorganisms including bacteria, fungi or algae. A supposed 30% of the nematodes has developed a parasitic life style, mainly of animals including humans but also of plants (Anderson, 2000; Burglin *et al*., 1998; Stone *et al*., 1983). Parasitic worm infections, including nematode infections, represent one of the most prevalent problems in human and veterinary medicine with an estimated cost of more than 1.2 billion Euro per annum attributed to parasitism (Newton and Munn, 1999).

Soil-transmitted helminths commonly known as intestinal worms, are the most common infections worldwide affecting the most deprived communities where infected people generally cannot afford treatment. More than 2 billion humans are infected by gastrointestinal or tissue nematodes and 3.5 billion are exposed to them, which results in tremendous health and economic problems (Chan, 1997; Hotez, 2008). Since infections tend to be chronic, they are destructive to severely infected children, causing anaemia, growth retardation, impaired cognitive function and lowered educational accomplishment (Cooper and Bundy, 1988; Guyatt, 2000; Nokes *et al*., 1992).

3.2. Helminth immunomodulation

Every infection represents a competition between the parasite and the host (Playfair and Bancroft, 2008).The important difference between a free-living organism and a parasite of vertebrates is that the parasite must survive and reproduce in the face of a complicated immune response directed against it (Wakelin, 1996; Wakelin and Walliker, 1996). The first test for any parasite is to invade its host and to migrate to its final destination, a process that often requires passing through host tissue, extracellular matrices, basement membranes, and blood or lymph vessel walls. Parasites have generated an array of molecules that interfere with the host´s defense system endeavor to eliminate the unwanted lodger (Nagaraj *et al*., 2008). The ability of helminths to modulate the immune system supports their longevity in the

mammalian host (Behnke *et al*., 1992; Maizels and Yazdanbakhsh, 2003). This modulation is most likely caused by the release of soluble mediators which ligate, degrade or otherwise interact with host immune cells (Hewitson *et al*., 2009; Lightowlers and Rickard, 1988). Molecules expressed and secreted by nematodes that might modulate host immune responses include proteases, protease inhibitors, antioxidants and orthologs of host cytokines and their receptors (Bungiro and Cappello, 2004).

A characteristic feature of parasitic helminths is their ability to survive within their hosts for long time periods through suppression of the host's immune system. Even though the infected hosts strongly initiate inflammatory immune responses to the invading pathogens, most helminths have the ability to polarize the immune response toward a strong CD4+ T-helper-2 (Th2) cell response and establish a chronic infection (Sher *et al*., 2003). In evolutionary terms, long-lasting interaction between intestinal parasitic nematodes and mammalian hosts has led to increased adaptation and co-evolution (Woolhouse *et al*., 2002).

The „old friend" hypothesis assumes that the presence of certain helminths and microbes chronically colonizing the intestine stimulates the host´s immunoregulatory system to tolerate these rather "harmless," yet foreign organisms. It is currently hypothesized that increases in chronic inflammatory disorders in developed countries, such as inflammatory bowel diseases and allergies, are partially attributable to diminished exposure to organisms that were part of mammalian evolutionary history (Rook, 2007, 2009, 2010; Rook and Lowry, 2008).

Moreover, it has been reported that regulatory T cells (Tregs) play an important role by suppressing inflammatory Th1/Th17 responses and pathology, while permitting a contained Th2 response (Hewitson *et al*., 2009). Interestingly, such responses are beneficial for both the host and the parasite; host pathology is reduced, and the parasites have a better chance to survive in such a "modified Th2" environment (Smits *et al*., 2010; Smits and Yazdanbakhsh, 2007; van Riet *et al*., 2007).

3.3. Strongyloides

3.3.1. History

In 1876 Louis Normand, physician to the Naval Hospital in Toulon, France, discovered *Strongyloides stercoralis* in the feces of soldiers who were dangerously ill of Cochin-China diarrhea, believed to be caused by *Anguillula intestinalis* (the first name given to the parasitic generation). In the same year Bavay described the nematode for the first time.

Extensive, careful work and interesting publications then followed describing *Strongyloides* biology, for example Grassi and Parona in 1878 and 1979, Perroncito in 1881and Leuckart 1883. In 1902 Stiles and Hassall pointed out that the parasite should in fact be denoted *Strongyloides stercoralis*; for old references and reviews see (Grove, 1989; Grove, 1996).

3.3.2. Unique features and epidemiology

The genus *Strongyloides* comprises some 50 species of intestinal parasites of vertebrates like mammals, birds, reptiles and amphibians (Grove, 1989; Viney and Lok, 2007). Nematodes of the genus *Strongyloides* infect a wide range of mammalian species, including humans and livestock. *Strongyloides stercoralis* - the major human pathogen species – is an enteric nematode that has the capability to escape host immune attack and survive within the human small intestine for decades and infects at least 100 million people (Concha *et al*., 2005; Liu and Weller, 1993). This prevalence is likely underestimated since the diagnostic tests are insensitive, and the development of accurate and sensitive methods is needed (Kramme *et al*., 2010; Montes *et al*., 2010).

The *Strongyloides* spp. belongs to the phylum nematoda in the order Rhabditida and family Strongyloididae, whose members inhabit the intestinal mucosa (Fig. 1).

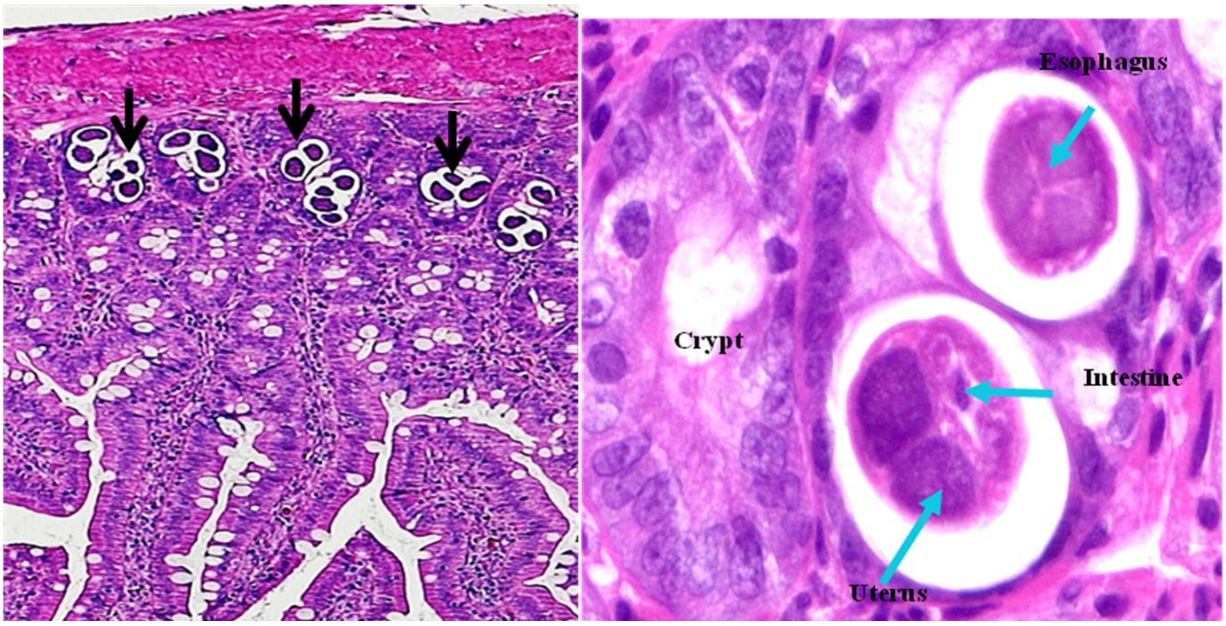

Fig. 1. *Strongyloides ratti* PF embedded in the rat intestinal mucosa. The photos were captured in our lab by Inga Toborg. Magnifications are: left 40X and right 100X, (H&E).

Strongyloides shows several fundamental differences to the other helminths:

(i) In contrast to other soil-transmitted helminths, the unique life cycle of *S. stercoralis* encompasses both, direct (asexual) and, optionally, indirect (sexual) development of infective larvae(iL3) (Fig. 2), which invade into the host by skin penetration followed by migration through tissues *via* the blood stream, through the lung, trachea and oesophagus to the small intestine. In this final habitat the nematodes evolve into the parasitic female stage (PF) producing eggs by mitotic parthenogenesis (Viney, 1994, 1999). In contrast to e.g. *Ascaris* and hookworm, the *Strongyloides* larvae can develop *ex vivo* into adults resulting in sexual reproduction and egg formation; iL3 hatch from these eggs thereby completing the complex life cycle.

(ii) *S. stercoralis* exhibits the ability to complete its life cycle within the human host. Accordingly, larvae can develop to the infective third stage within the gastrointestinal tract, traverse the intestinal mucosa, migrate through the tissues, and again establish an infection in the small intestine (Grove, 1996). Such cycles of autoinfection can lead to repeated re-infection that can persist for several decades without apparent symptoms.

(iii) No other human parasitic nematode has been associated with such a broad spectrum of manifestations and clinical syndromes as *S. stercoralis*. Chronic infections with *S. stercoralis* are often associated with no or mild cutaneous, gastrointestinal, or pulmonary symptoms. In immune-competent hosts, the disease is generally not life-threatening. However, in immunocompromised patients – e.g. after treatment with immunosuppressive drugs like glucocorticoids, after co-infection with HTLV-1 or tuberculosis, in case of hematologic malignancies, or protein-caloric malnutrition syndrome - an accelerated autoinfection (hyperinfection) normally occurs, leading in ≥87% of the cases to threatening disseminated infections and death (Keiser and Nutman, 2004; Olsen *et al*., 2009). Recent reports have indicated the underestimation of strongyloidiasis and its hyperinfection syndrome, which is now considered an emerging global infectious disease that has migrated from developing regions to industrialized areas (Marcos *et al*., 2008).

Helminth infections, especially strongyloidiasis, are generally considered to be a disease found in tropical and sub-tropical areas (Grove, 1989; Grove, 1996). In the last decades, however, a shift has been observed, attributed in part by the import of tropical diseases by infected immigrants or travelers coming from endemic areas. Presently, strongyloidiasis has been described in many temperate countries, such as the USA, Italy and France (Junod, 1987; Lim *et al*., 2004; Sampson and Grove, 1987; Scaglia *et al*., 1984; Sprott *et al*., 1987; Walzer *et al*., 1982). Moreover, *S. stercoralis* infections are, together with hookworm infections, the

only officially recognized occupational parasitic health hazard for miners in Germany (*Bundesanstalt für Arbeitsschutz und Arbeitsmedizin (BauA). Berufskrankheiten-Verordnung (BKV) vom 31. Oktober 1997 (BGBl. I S. 2623), zuletzt geändert durch die Verordnung vom 5. September 2002 (BGBl. I S. 3541). Dortmund: BauA; 23 March 2004* (http://www.baua.de/de/Themen-von-A-Z/Berufskrankheiten/Rechtsgrundlagen/BKV.html).

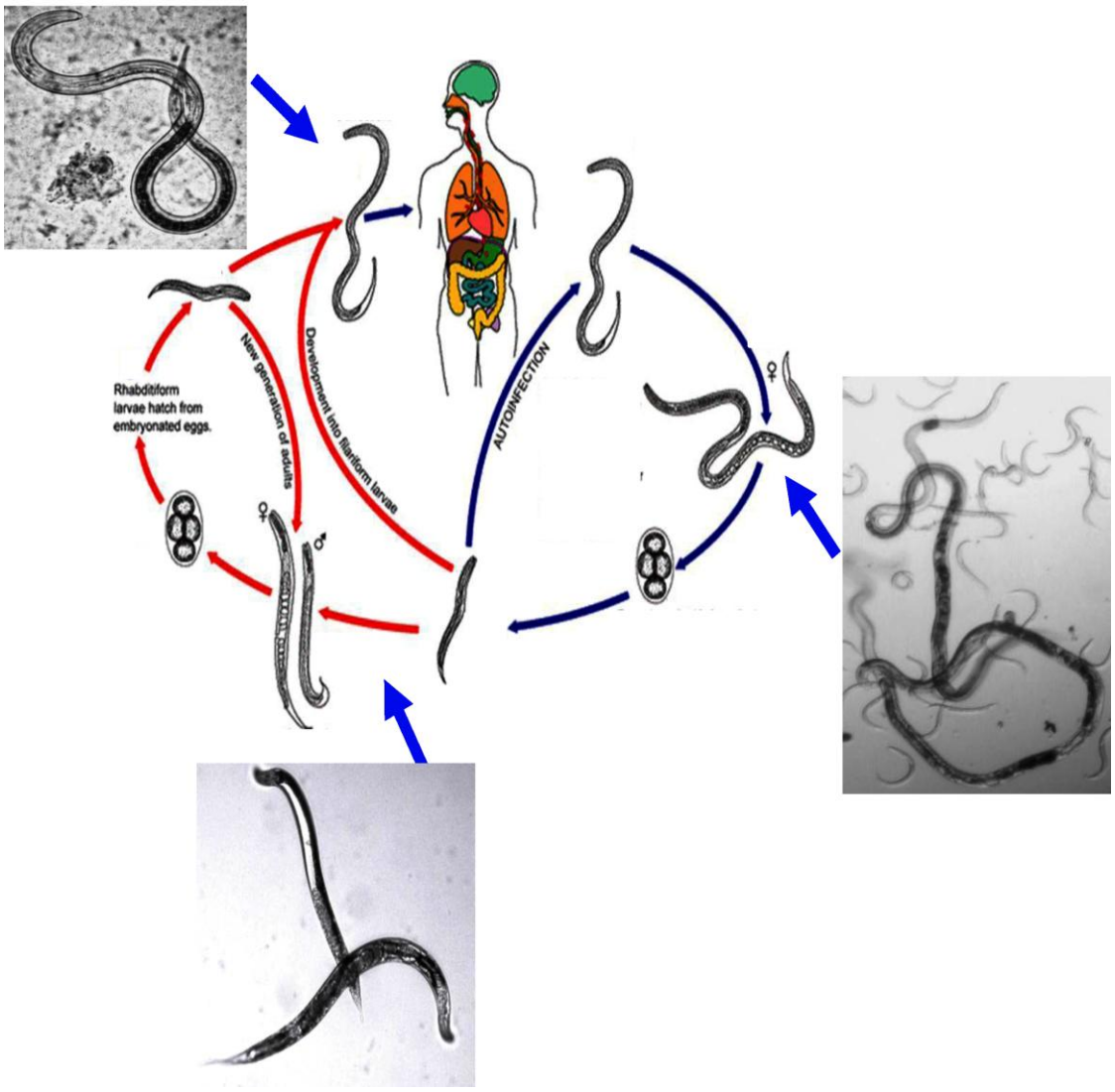

Fig. 2. The life cycle of *S. stercoralis* modified from the CDC (Centers for Disease Control and Prevention, Division of Parasitic Diseases, http://www.dpd.cdc.gov/dpdx/).

3.3.3. Transcriptome and proteome

The expressed sequence tag (EST) libraries, collections of small pieces of sequenced cDNA derived from mRNA isolated from an organism or tissue of interest, have been generated for many nematodes, by researchers from The Washington University Nematode EST Project, Genome Sequencing Center, Washington University School of Medicine, St. Louis, USA. Approximately 530,000 ESTs from 40 nematode species, including *S. stercoralis* (11,335 ESTs collected in 3311 clusters) and *S. ratti* (14,761 ESTs collected in 4152 clusters) has been submitted (Martin *et al*., 2009; Wylie *et al*., 2004). Recently, 3,688 distinct transcripts were estimated on the microarray analysis of *S. ratti* stages and about half of the transcripts exhibited a gender-based transcription (Evans *et al*., 2008).

The stage-related excretory/secretory proteins (ESP) from *S. ratti* were investigated in our laboratory by Hanns Soblik (BNI, Hamburg, http://www.chemie.uni-hamburg.de/bibliothek/2009/DissertationSoblik.pdf). Proteomic mass spectrometric analysis of ESP followed by protein identification and sequence analysis revealed 586 proteins. The largest number of stage-specific ESP (Fig. 3) were found in infective third stage larvae (196) followed by parasitic females (79) and free-living stages (35). 140 proteins were identified in all studied stages including anti-oxidative enzymes, heat shock proteins and carbohydrate-binding proteins. Examples of the stage-related ESP of (i) iL3 included an astacin metalloproteinase, the L3 Nie antigen and a fatty acid retinoid-binding protein; (ii) PF included a prolyl oligopeptidase, small heat shock proteins, and a secreted acidic protein; and (iii) FlS included a lysozyme family member, a carbohydrate-hydrolyzing enzyme and a saponin-like protein.

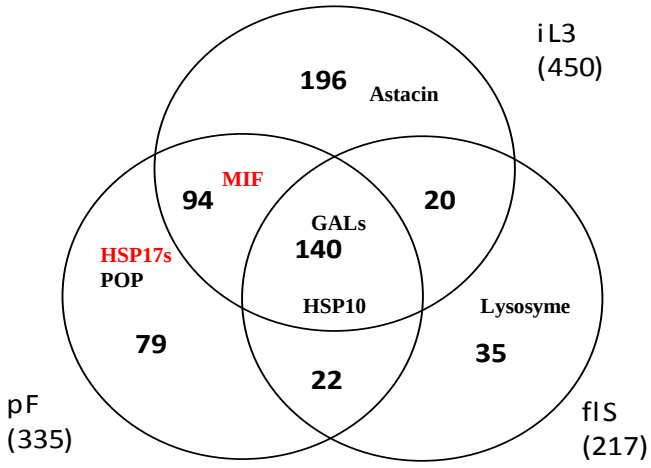

Fig. 3. Venn diagram showing the distribution of the identified *S. ratti* E/S proteins of the studied developmental stages: iL3, pF and flS. The numbers in brackets show the quantities of the proteins in each stage(s) total.

3.3.4. Immunity

The body surface is the first line of defense against a wide variety of infections. When this defense mechanism is penetrated, the innate immune system becomes activated. Innate immunity, which involves dendritic cells, monocytes/macrophages, polymorphonuclear leukocytes as well as the humoral and complement system, reacts within hours after the appearance of foreign antigens and is based on the recognition of a pathogen-associated molecular pattern (PAMP). A PAMP consists of microbial components characteristic for certain microbes, e.g. lipopolysaccharides from Gram-negative bacteria, lipoproteins from Gram-positive bacteria or mannans for fungi. The PAMPs of helminths are rarely identified and may include glycans. Innate immunity is evolutionarily conserved and can be traced back to the earliest forms of life. Innate immunity, also denoted as non-adaptive or native immunity, is particularly important in immuno-compromised patients who lack activated, adaptive immune responses. The agents of the innate immune system are phagocytic cells, mast cells, natural killer cells, cytokines and the complement system. While microbial antigens can be removed *via* phagocytosis, the effector cells can only adhere to the multicellular worms and degranulate toxic compounds ("frustrated phagocytosis") including oxygen radicals, proteinases and other enzymes. Massive adhesion and release of toxins by the effector cells, however, can result in the killing of worm larvae. Next, the adaptive immune responses will ensue, initiating an amplification of activated cells and cytokines, including T and B lymphocytes and their products (Janeway, 2001).

Formation of a marked protective immunity against a challenge infection was found in rats immunized with enteral antigenic stimuli (Korenaga *et al*., 1983) and the excretory/secretory products (ESP) of *S. ratti* adult worms (Mimori *et al*., 1987). In addition, *Strongyloides* interacts and is in close contact with the intestinal epithelial cells belonging to the innate mucosal immune system and secondarily with the adaptive mucosal defense system. *S. ratti* infection was shown to induce a transient nematode-specific Th2 response. This is characterized by the generation of interleukin-4, -5, and -13 which foster eosinophilic granulocytes and mast cells and also induce IgG4 and IgE antibody isotype production involved in effector responses (Eschbach *et al*., 2010). Recently, it was reported that the *S. ratti* infection induces expansion of Foxp3+ regulatory T cells in mice (Blankenhaus *et al*., 2011).

3.4. Heat shock proteins

Heat shock protein (HSP; stress protein) families are widely distributed in nature and are among the most highly conserved molecules of the biosphere as they have been reported in various organisms ranging from prokaryotic *E. coli* to eukaryotic mammalians (Feder and Hofmann, 1999). Originally, HSPs expression has been reported to be induced by a wide range of potentially deleterious stimuli, including bacterial and viral infections (Collins and Hightower, 1982), ethanol treatment (Plesset *et al*., 1982), glucose analogues (Pouyssegur *et al*., 1977) and oxidative stress (Currie, 1987). Many reports revealed that HSPs have cytoprotective effects and facilitate protein folding of nascent or damaged proteins, prevent protein aggregation, mediate solubilization of protein aggregates and target damaged proteins for degradation (Liu *et al*., 2010; Young *et al*., 2004). HSPs were classified into families on the basis of sequence homology and typical molecular weight: HSP110, HSP100, HSP90, HSP70, HSP60, HSP40, HSP10 and small HSP families (Gething, 1997).

The small heat shock proteins (sHSPs) are ubiquitous, ATP-independent stress response chaperones. They have the smallest monomeric masses of the HSP classes, ranging from 12 kDa to 42 kDa, yet they usually associate *in vitro* into large polydisperse oligomers (Jehle *et al*., 2010; Laganowsky *et al*., 2010). By their originally described chaperone activity they prevent an irreversible aggregation of non-native proteins and deliver them to the ATP-dependent chaperone systems. *In vivo* the HSPs maintain other proteins that are liable to unfold or disassemble (Van Montfort *et al*., 2001).

During infection, both host and pathogen are confronted with dramatic physiological alterations. An induction of HSP synthesis can be vital for the survival of a pathogen. Although immune responses to HSP have been observed in various experimental infection models, the exact role of HSPs in immunity to microbial infection is poorly understood (Zugel and Kaufmann, 1999).

3.5. Macrophage migration inhibitory factor (MIF)

MIF is one of the first described cytokines, originally identified as an inhibitor for the random migration of macrophages. MIF is expressed in a wide variety of cell types including lymphocytes, monocytes and macrophages, endothelial cells and fibroblasts (Calandra and Roger, 2003). MIF has multiple functions in the mammalian immune system including the influence on the innate and adaptive immune responses and appears to be involved in pathogenesis of inflammatory diseases (Calandra *et al*., 2000; Kobayashi *et al*., 2006; Leech

et al., 2003; Morand, 2005; Ogawa *et al*., 2000). The exact mechanism of its action remains unresolved. One possible pathway represents the cell surface binding to the CD74–CD44 receptor complex (Leng and Bucala, 2006; Shi *et al*., 2006).

MIF was reported to express two catalytic activities *in vitro*, namely a tautomerase (Flaster *et al*., 2007) and thiol-protein oxidoreductase (TPOR) activity (Kleemann *et al*., 1998). Homologues of two types of MIF proteins have been identified in several nematodes based on homology to *C. elegans* MIFs (*Ce*-MIF-1 and *Ce*-MIF-2), where the nematode MIF-1 homologues have a higher extent of amino acid similarity with the mammalian hosts MIFs than the MIF-2 homologues (Vermeire *et al*., 2008).

3.6. Objectives of the study

The first objective of the presented investigation was the validation of the stage relationship of the proteins identified earlier, in our group, in the E/S products from various stages of *S. ratti* by quantification of transcripts from different stages using qRT-PCR. Transcripts associated with iL3 may comprise novel transcripts involved in the transition to parasitic lifestyle, or gene products with relevance for intervention strategies; those associated with PF may comprise gene products involved in the establishment and reproduction of the parasite, but also in evasion or host mucosal immunmodulation.

The second objective was the characterization of two novel low molecular heat shock proteins secreted by PF, *Sr*-HSP17s, and one protein released by iL3, *Sr*-MIF. The experiments comprise: (i) the identification of the full length gene sequences, (ii) bioinformatic analyses, (iii) analysis of the genomic organization, (iv) recombinant expression and purification of the proteins, (v) evaluation of biochemical activities, (vi) the production of polyclonal antibodies and their application in neutralization and immune recognition experiments, (vii) examination of antibody reactions with the recombinant proteins by infected hosts, and (viii) exploration of possible binding of the expressed proteins to host innate immune cells and induction of cytokine release.

These investigations should help to identify putative relevant stage-related E/S proteins in order to elucidate their biological role in parasite-host interaction.

4. MATERIALS AND METHODS

4.1. Materials

2.1.1 Animals

4.1.1.1. Rats

All animal experiments were approved by and conducted in accordance with guidelines of the appropriate Animal Protection Board of the City of Hamburg (G 21131/591-00.33). Four to six weeks-old Wistar rats (*Rattus norvegicus*) from Charles River were used to maintain the cycle. There was no systematic bias in terms of weight. The Wistar rats were housed singly in stainless steel cages with food and water available *ad libitum*.

4.1.1.2. Parasites

The *S. ratti* life cycle has been held at the Bernhard Nocht Institute for Tropical Medicine (BNI, Hamburg) since January 2006. The iL3 for the initial infection were kindly supplied for Hanns Soblik (BNI, Hamburg) by Prof. Dr. Gerd Pluschke (Swiss Tropical Institute, Department of Medical Parasitology and Infection Biology Basel, Switzerland).

2.1.2 Equipment and instruments

Type	Manufacturer / Supplier
7000 Sequence detection system	Applied Biosystems
95 mm culture plates	Ilmabor GmbH
Amicon Ultra-4/-15 Ultracel-10k	Millipore
Beckmann Coulter Avanti J-26 XP	Beckmann (Krefeld)
Blood collection tubes containing 0.106 mol/l trisodium citrate solution and 1 ml citrate solution	Sarstedt (Nuembrecht)
Branson Sonifier-250	Bandelin (Berlin)
Cellstar tissue culturing flasks 25 cm^2	Greiner Bio-one GmbH (Nuertingen)
Cellstar tissue culturing Multidish wells	Sarstedt (Nuembrecht)

Charcoal, 2.5 mm granules	Merck (Darmstadt)
Chromabond 30 ml resevoir columns	Macherey-Nagel (Dueren)
Citrate tube for blood collection S-Monovette	Sarstedt (Nuembrecht)
CO2 Incubator (37 °C) Excella Eco-17	New Brunswick Scientific (Nuertingen)
Cooling centrifuge Rotanda/RP	Hettich (Tuttlingen)
Electrophoresis chamber Perfect Blue Mini	Peqlab
F96 Maxisorp Nunc-Immunoplate	Nunc (Roskilde)
F96 Nunclon sterile microtiter plate	Nunc (Roskilde)
FACSCalibur	Becton Dickinson
Incubator	Memmert
Incubator shaker Innova 4400	New Brunswick Scientific (Nuertingen)
Magnetic stirrer Ikamag RO	Ika-Werk (Staufen)
Microcentrifuge 5415 C	Eppendorf (Hamburg)
Microplate reader Dynex MRX I	Dynex (Chantilly)
Microscope Axiovert 25	Zeiss (Jena)
Microwave MW736	Ciatronic
Mini-centrifuge/vortex	Neolab
MultitempII thermostatic circulator	LKB Bromma
Non-pyrogenic sterile filter 0.2 µm	Sarstedt (Nuembrecht)
Omnfix-F 1 ml syringes	B. Braun (Melsungen)
pH meter CG 480	Schott (Mainz)
Photometer 1101M CKE 6455	Eppendorf (Hamburg)
Power supply unit Power Pac 300	Bio Rad (Munich)

Powershot A640	Canon (Krefeld)
Precellys steel beads	Peqlab (Erlangen)
Refrigerators/freezers	Liebherr
Roller mixer SRT6	Stuart
Rotator SB3	Stuart
Safety bench LaminAir HB 2448	Heraeus
Sonifer Sonopuls HD 60	Bandelin (Berlin)
Sorvall Superspeed RC2-B centrifuge	Sorvall (Newtown)
Spectra/Por dialysis tubing MWCO 6000-8000	Spectrum Medical Industries (Houston)
Stereozoom microscope Wild M8	Leica (Wetzlar)
Sterican hypodermic needles, 0.40 x 25 mm	B. Braun
Sterile working bench Microflow	Nunc (Wiesbaden)
Thermocycler Primus 25	Peqlab
Thermomixer 5436	Eppendorf (Hamburg)
UV/VIS ultrospec 2000 Spectrophotometer	Pharmacica Biotech. LabX
Vortex MS 1 Minishaker	IKA (Staufen)

2.1.3 Buffers, solutions and supplements

Buffers, solutions and supplements	**Composition/description**	**Application**
APS	10% ammonium peroxodisulphate (Amersham) in ddH_2O	Protein gel
Alum/PBS	1:1 aluminum hydroxide gel in 1X PBS	Rats immunization
Ampicillin	ampicillin trihydrate [D-(-)-α-aminobenzyl penicillin]; stock conc. 100	LB-medium and LB-plate additives

	m/ml ddH_2O	(selection)
Antibody diluting medium	2.5% milk/PBS/0.05% Tween-20	Western blot
Antibody elution medium	1 ml of 0.2 M glycine (pH 2.6)/0.05% Tween-20	Antibody purification
Antibody storage medium	PBS/ 0.1% BSA (pH 7.5)	Antibody purification
B1	8 M urea, 50 mM Tris, 10 mM imidazole, 500 mM NaCl, 10 % glycerol, 0.1 % Triton X-100	Protein purification
B2	8 M urea, 50 mM Tris, 10 mM imidazole, 500 mM NaCl, 10 % glycerol, 0.4 % Triton X-114	Protein purification
B3	8 M urea, 50 mM Tris, 20 mM imidazole, 500 mM NaCl, 10 % glycerol, 0.1 % Triton X-100, 250 µg/ml PMB	Protein purification
B4	8 M urea, 50 mM Tris, 250 mM imidazole, 500 mM NaCl, 10 % glycerol, 0.1 % Triton X-100	Protein purification
B5	2 M urea, 20 mM Tris, 150 mM NaCl, 0.1 % Triton X-100, 30 µg/ml PMB	Protein purification
B6	PBS, 30 µg/ml PMB or TBS, 30 µg/ml PMB	Protein purification
Blocking Buffer	5% BSA	ELISA
Blocking milk	5% dry milk (Bio-Rad) in 1X PBS	Western blot
Blotting buffer (Bjerrum-Schoefer-Nielsen Buffer)	48 mM Tris, 39 mM glycine, 20% methanol	Western blot
Bradford - Solution	AppliChem (Darmstadt)	determination of protein conc.
chloro-1-naphthol stock	0.150 g in 50 ml methanolRoche	Western blot

Coating buffer	NaHCO3, Na2CO3, pH 9,5	ELISA
Coomassie blue destaining solution	40% ethanol; 10% ice acetic acid 50% ddH_2O	Protein gel staining
Coomassie blue staining solution	0.05% (w/v) Coomassie brilliant-blue R-250; 40% ethanol; 10% ice acetic acid; 50% ddH_2O	Protein gel staining
CS	Citrate synthase, from porcine heart in 2.2 M $(NH_4)_2SO_4$, pH 7.0, 6 mM phosphate, 0.5 mM citrate(Sigma)	Chaperone assay
DEPC- ddH_2O	0.1% diethylpyrocarbonate in ddH_2O; autoclaved (ROTH)	Nucleic acids preparations
DNA-Loading buffer	Fermentas	DNA gel electrophoresis
DTT stock	1M Dithiothreitol in dd H_2O	Chaperone assay
Ethidium bromide (EtBr)	1 g/100 ml ddH_2O; stored shaded	Staining of nucleic acids
Ficoll-hipaque discontinuous density	3 ml Mono-Poly Resolving Media (density of 1.114 g/ml), 3 ml Lymphoflot (density of 1.077 g/ml)	Separation of MNC and PMN blood cells
HAES-steril® 6%	6% Poly(O-2-hydroxyethyl starch in 0.9% NaCl	Sedimentation of Erythrocytes
Highly pure steralized water	Aqua B. Braun, Melsungen AG, Germany	Buffers preparation
Homogenization buffer	1X PBS, 0.1 mM EDTA, 25 mM HEPES	Worm extract
HPP	p-hydroxyphenylpyruvate dissolved in 50 mM ammonium acetate pH 6.0	Tautomerase assay
HPP buffer	0.435 M boric acid, pH 6.2	Tautomerase assay
IEC-6 culture media	DMEM, 2 mM glutamine, 5% inactivated fetal calf serum (FCS), 0.1 IU/ml insulin, 100 U/ml penicillin and	Cell culturing

	100 µg/ml streptomycin	
Insulin stock	10 µg/µl in HEPES (pH 8.2); Sigma	Chaperone assay
IPTG stock solution	1M Isopropyl-beta-D-thiogalactopyranoside (Fermentas) in ddH_2O	Protein expression and blue white selection
LB-Agar	Bacto agar 15 g/l, LB medium 20g/l; autoclaved	E. coli - medium (solid)
LB-medium	10 g/l trypton, 5 g/l hefeextract, 5 g/l NaCl (Lennox L Broth Base) in ddH_2O; autoclave	E. coli - medium (fluid)
LDME	L-dopachrome methyl ester (4 mM L-3,4-dihydroxyphenylalanine methyl ester (Sigma), 8 mM sodium periodate)	Tautomerase assay
LDME buffer	25 mM potassium phosphate buffer pH 6, 0.5 mM EDTA	Tautomerase assay
LPS	1 mg/ml Lipopolysaccharide	Cytokine ELISA
Lymphoflot	Biotest	peripheral blood cells preparation
MDH	malate dehydrogenase, from porcine heart in ammonium sulfate (Sigma)	Chaperone assay
MNC and MØJ774 culture media	RPMI 1640, 2mM L-Glutamine, 5% Fetal Calf Serum, 100 U/ml Penicillin, 100 µg/ml Streptomycin, 25 mM HEPES	Cell culturing
Mono-Poly Resolving Media	MP Biomedicals, Sweden	peripheral blood cells preparation
MOPS 10X	200 mM MOPS [3-(N-morpholino)propanesulfonic acid], pH 7.0, 80 mM Sodium Acetate, and 10 mM EDTA, pH 8.0 in ddH_2O	RNA formaldehyde/agarose gels electrophoresis
PBS	Dulbeccos phosphate buffered saline (GIBCO)	Physiological buffer

Phenol	phenol, saturated with equivalent volume 0.5 mM Tris pH 7.8	Nucleic acid purification
Phytohaemagglutinin	Phytohaemagglutinin (HA 16; 2 µg/ml; Murex Diagnostics Ltd, Dartford, England)	Cytokine ELISA
PMB	Polymyxin B (sigma)	Protein purification and cytokine ELISA
Polyacrylamide solution	0.8% N'N'-methylbisacrylamide; 30% acrylamide; in ddH_2O (Rotiphorese® Gel 30; Carl Roth)	Protein gel preparation
Ponceau-red S	2% ponceau-red S; 30% sulfoacyl acid; 30% sodium deoxycholate aqueous; in ddH_2O	Western blot
Proteinase K buffer	Qiagen	gDNA isolation
rHu-MIF	1mg/ml recombinant human MIF in PBS; Applichem, GmbH, Darmstadt, Germany	Cross reaction
Roti®-RNA Loading buffer	ROTH	RNA gel electrophoresis
SDS-PAGE running buffer (10 x)	1.92 M glycine; 250 mM Tris; 10% (w/v) SDS; ddH_2O ad 1 l (pH 8.3; to be adjusted before SDS addition)	Protein gel preparation
SDS-PAGE sample buffer	8 ml glycerin; 4 ml ß - mercaptoethanol; 12 ml 20% SDS; 16 ml 4 x staking gel buffer; (if necessary 4% bromphenol-blue)	Protein gel preparation
SDS-PAGE separation buffer (4 x)	1.5 M Tris (pH 8.8); 0.4% SDS	Protein gel preparation
SDS-PAGE stacking gel buffer (4 x)	0.5 M Tris (pH 6.8); 0.4% SDS	Protein gel preparation
SOC-medium	Invitrogen	E. coli - medium
Stop solution	2 M H_2SO_4	ELISA

Substrate: Tetramethylbenzidine	50% BD OptEIA Substrate Reagent A and 50% BD OptEIA Substrate Reagent B	ELISA
TAE-buffer (50 x)	2 M Tris, 50 mM EDTA, 5.71% glacial acetic acid pH 8.0	DNA gel electrophoresis
TBS	20 mM Tris, 150 mM NaCl	Physiological buffer
TEMED	Tetramethylethylenediamine (Amersham Biosciences)	Protein gel preparation
TRIzol®-Reagenz	Phenyl, guanidine-isothiocyanate (Invitrogen)	Nucleic acids isolation
Visualization buffer	10% chloro-1-naphtol stock in PBS + 0.001 H_2O_2	Western blot
Washing buffer	PBS 1x + 0.05% Tween-20	ELISA and Western blot
Washing solution	Hanks Balanced Salt Solution (HBSS), 100 U/ml penicillin, 100 µg/ml streptomycin	Worm washing
Worm culture medium	RPMI-1640, penicillin 100 U/ml, streptomycin 100 µg/ml, HEPES 10 mM	Excretory/secretory products
X-Gal	5-bromo-4-chloro-3-indolyl-ß-D-galactopyranoside; stock conc. 2% in dimethylformamide; end conc. 0.004%	Blue-white selection

2.1.4 Commercially available kits

Kit	**Manufacturer / Supplier**
Enterokinase cleavage capture kit	Novagen, USA
EZ-Link® Sulfo-NHS-Biotinylation kit	Thermo Scientific, USA
GeneRacer kit	Invitrogen
Human IL10 ELISA	eBioscience and R&D Systems

Human TNF-alpha ELISA	eBioscience and R&D Systems
Limulus Amebocytes Lysate, QCL-1000	Lonza, Walkersville
Profinity ^{TM} IMAC Ni–NTA resin	Bio-RAD Laboratories, Germany
QIAprep® Miniprep kit	Qiagen (Hilden)
QIAquick® gel extraction kit	Qiagen (Hilden)
QIAquick® PCR purification kit	Qiagen (Hilden)
qPCR Core kit for SYBR®Green I	Eurogentec S.A.
RNeasy® MinElute® Cleanup kit	Qiagen (Hilden)
Streptavidin-Alexa Fluor 647 Labeling kit	Invitrogen
SuperScript™ III Reverse Transcriptase kit	Invitrogen

2.1.5 Enzymes

Enzyme	**Company/Origin**	**Description**
DNase I	Qiagen	RNase-free DNase I
Proteinase K	Qiagen	Cystein-protease
Restriction enzymes	New England Biolabs, Fermentas, Roche	Type II restriction endonuclease
Reverse transcriptase	Invitrogen	SuperScriptIII
RNaseA	Roche	DNase-free RNase
RNaseH	Invitrogen	Digestion of the excess of RNA after cDNA synthesis
T4-DNA-Ligase	New England Biolabs	DNA ligation

Taq-polymerase	New England Biolabs	DNA-Polymerase

2.1.6 Antibodies

Antibody	**Description**	**Source**
anti-his peroxidase	monoclonal, mouse	Roche (Mannheim)
Anti-human peroxidase	Horseradish peroxidase conjugated goat anti-human IgG (affinity purified)	Roche (Mannheim)
Anti-human-MIF	Polyclonal rabbit anti-human-MIF	BioVision (CA, USA)
Anti-rat peroxidase	Horseradish peroxidase conjugated goat anti-rat IgG (affinity purified)	Dianova (Hamburg)
FITC Mouse Anti-Human CD14	Monoclonal Ab reacts with the 53-55 kDa glycosylphosphatidylinositol (GPI)-anchored single chain glycoprotein expressed at high levels on monocytes/MØ	BD Biosciences
Mouse ICAM-1	Monoclonal Ab binds to intercellular adhesion molecule 1 (ICAM-1), also known as CD54	BD Biosciences
PE Mouse Anti-Human CD16	Monoclonal Ab specifically binds to CD16 expressed on the neutrophils	BD Biosciences

2.1.7 Molecular weight standards

Marker	**Origin**	**Description**
1 KB DNA ladder	Fermentas	250-10,000 bp
Low Range DNA ladder	Fermentas	25-700 bp
Precision Plus Protein Dual Color Standards	Bio-Rad	Consists of ten proteins standards, 10, 15, 20, 25, 37, 50, 75, 100, 150 and

		250 kDa
Precision Plus Protein prestaind Standards	Bio-Rad	Consists of ten proteins standards, 10, 15, 20, 25, 37, 50, 75, 100, 150 and 250 kDa
RNA Marker High	Abnova Corporation (Heidelberg)	consists of nine single-stranded RNAs, 200, 500, 1,000, 1,500, 2,000, 3,000, 4,000, 5,000 and 8,000 bases
RNA Marker Low	Abnova Corporation (Heidelberg)	Consists of seven single-stranded RNAs, 20, 50, 100, 200, 300, 400 and 500 bases

2.1.8 Plasmids

Plasmid	**Description**	**Origin**
pGem-T easy	Cloning vector	Promega
pJC45	Expression vector	Kindly provided by Dr. J. Clos, BNI, Hamburg

2.1.9 Bacteria strains

Bacterial strain	**Description**
One Shot® TOP10	*E. coli* cells for cloning (Invitrogen)
BL21	*E. coli* cells for recombinant expression
Star BL21 DE3	*E. coli* for recombinant expression

2.1.10 Primers

All primers were ordered from Eurofins MWG / Operon https://ecom.mwgdna.com/services/home.tcl

Primer name	Sequence (5´ - 3´)	Application
oligodT-T7I	GAGAGAGGATCCAAGTACTAATACGACTCACTATAGGGAGATT24	cDNA synthesis
10f (forward)	TGGTGGAAATAAAGTTGTTATGGAC	*Sr*-HSP10 qRT-PCR
10r (reverse)	CAAACTACAATATCAACTATGCAAAAA	*Sr*-HSP10 qRT-PCR
60f (forward)	GCCATTGCTACAGGAGCTAAA	*Sr*-HSP60 qRT-PCR
60r (reverse)	TTGTTCAGCATCACCTTTTCC	*Sr*-HSP60 qRT-PCR
af1 (forward)	ATGAACGACCGTTGGATGA	*Sr*-HSP17a 3´end (full length)
af2 (forward)	AACGACAAGGAATTCAGAGTCAA	*Sr*-HSP17a 3´end (partial)
af3 (forward)	AACGACAAGGAATTCAGAGTCAA	*Sr*-HSP17a qRT-PCR
af4 (forward)	AAGCTTgatgatgatgataaaATGAACGACCG	*Sr*-HSP17a recombinant expression
ar1 (reverse)	TTATTTTCTATATTCAATTGGGAC	*Sr*-HSP17a 5´start (full length)
ar2 (reverse)	ACGGACGAAACTTCTTTGGA	*Sr*-HSP17a 5´start (partial)
ar3 (reverse)	ACGGACGAAACTTCTTTGGA	*Sr*-HSP17a qRT-PCR
ar4 (reverse)	GGATCCTTATTTTCTATATTCAATTGGGAC	*Sr*-HSP17a recombinant expression
astf (forward)	TTGATACAGGAGTAAATGAAACTACAG	*Sr*-AST qRT-PCR
astr (reverse)	CCAACATATGATCGACAACCA	*Sr*-AST qRT-PCR
bf1 (forward)	ATGTTTGACAACCACATGATGACACC	*Sr*-HSP17b 3´end (full length)
bf2 (forward)	CCATTCACTCGTATGCCACTT	*Sr*-HSP17b 3´end (partial)

bf3 (forward)	CCATTCACTCGTATGCCACTT	*Sr*-HSP17b qRT-PCR
bf4 (forward)	CATATGgatgatgatgataaaATGTTTG ACAAC	*Sr*-HSP17b recombinant expression
br1 (reverse)	TTACTTAAACTTGATAGGAATA TTTTTTCCC	*Sr*-HSP17b 5´start (full length)
br2 (reverse)	TGGGTGGGTGTCAGCAAAT	*Sr*-HSP17b 5´start (partial)
br3 (reverse)	TGGGTGGGTGTCAGCAAAT	*Sr*-HSP17b qRT-PCR
br4 (reverse)	GGATCCTTACTTAAACTTGATA GG	*Sr*-HSP17b recombinant expression
calumf (forward)	TGATGGTAAATTAGATCGTGAT GAGA	*Sr*-CALUM qRT-PCR
calumr (reverse)	CATAATGTTGGATAATCTCTTCT GGTGA	*Sr*-CALUM qRT-PCR
cbpf (forward)	ATGATACTAAGAAACCTTTTAC TCAAG	*Sr*-CBP qRT-PCR
cbpr (reverse)	GTATTGACCATCAGGACATGAA CTG	*Sr*-CBP qRT-PCR
gal-1f (forward)	CAAGCTGGAGAATGGGGTAATG AGG	*Sr*-GAL-1 qRT-PCR
gal-1r (reverse)	ATCACAACGATGAGCAAAAGTG CAG	*Sr*-GAL-1 qRT-PCR
gal-2f (forward)	GGAATGCCTGAAAAAAAAGGTA AACG	*Sr*-GAL-2 qRT-PCR
gal-2r (reverse)	CTCTCTCTTCATTACCCCATTCA CC	*Sr*-GAL-2 qRT-PCR
gal-3f (forward)	TGAGCATCGTGTACCACTTTC	*Sr*-GAL-3 qRT-PCR
gal-3r (reverse)	ATAAGACTTTTTCCAGGAACTA ACC	*Sr*-GAL-3 qRT-PCR
gal-5f (forward)	TTGAAACTCCATATACTGCTCTT GC	*Sr*-GAL-5 qRT-PCR
gal-5r (reverse)	AGCTGATTCACCATATCTAATTG AGAC	*Sr*-GAL-5 qRT-PCR
gapdhf (forward)	GTACCACTAACTGTTTAGCTCC	*Sr*-GAPDH (houskeeping gene)

		qRT-PCR
gapdhr (reverse)	GCACCTCTTCCATCTCTCC	*Sr*-GAPDH (houskeeping gene) qRT-PCR
lysf (forward)	TTACTGGATTCGATGCCATTGGAA	*Sr*-LYS-5 qRT-PCR
lysr (reverse)	ACCAGCTTTCACAGCATTTTTTATATT	*Sr*-LYS-5 qRT-PCR
mf1 (forward)	ATGCCATATGTTCGTTTGTTCTC	*Sr*-MIF 3´end (full length)
mf2 (forward)	CACAATTTACCGATTTATTAGCTGAA	*Sr*-MIF 3´end (partial)
mf3 (forward)	CTGATGCTTTTTGTACAGAATTTACCG	*Sr*-MIF qRT-PCR
mf4 (forward)	AAGCTTgatgatgatgataaaATGCCATATGT	*Sr*-MIF recombinant expression
mfpf (forward)	ATGCCAAATCTTAAACCAGCTAAAGAAG	*Sr*-MFP2b qRT-PCR
mfpr (reverse)	AGCTCTTCCATGAATTGGTTTTCCAT	*Sr*-MFP2b qRT-PCR
mr1 (reverse)	TTATTTTAAACCAGCAATTGATTCAG	*Sr*-MIF 5´start (full length)
mr2 (reverse)	GCGACCATATCAGGTGACATAT	*Sr*-MIF 5´start (partial)
mr3 (reverse)	GTCCAACGTTATTTATCTCAATCCAA	*Sr*-MIF qRT-PCR
mr4 (reverse)	GGATCCTTATTTTAAACCAGCAATTGATTCAG	*Sr*-MIF recombinant expression
oligodT-T7II	GAGAGAGGATCCAAGTACTAATACGACTCACTATAGG	3´end
phrtf (forward)	GGAACTGATTCAACTGGACATTTAC	*Sr*-PhRT qRT-PCR
phrtr (reverse)	TTGATGCTCCATTGTCATTAACTGT	*Sr*-PhRT qRT-PCR
pjc45f (forward)	ATACGACTCACTATAGGGGAATTG	PJC45 forward primer (sequencing)
popf (forward)	GTTCTAATGGTGGACTTTTGACA	*Sr*-POP qRT-PCR

	G	
popr (reverse)	CAGGATCTCCATATTCAGATTTCC	*Sr*-POP qRT-PCR
SL-1 (spliced leader)	GGTTTAATTACCCAAGTTTGAG	5´start
tilf (forward)	CTTCCAACTGTCCAACAACTCAAA	*Sr*-TIL qRT-PCR
tilr (reverse)	CAGAAATACACTCACATTTTGGTGGT	*Sr*-TIL qRT-PCR
y51ff (forward)	TCTCAAGGATTAGTACTTCCAAAAAC	*Sr-Sr*-Y51F10.7 qRT-PCR
y51fr (reverse)	TCCTTTATCATCAGTAATTTGAGCTTT	*Sr-Sr*-Y51F10.7 qRT-PCR
zkf (forward)	TTGTAGATTTGCCATTGCTCATCC	*Sr*-ZK qRT-PCR
zkr (reverse)	TCCCAAGCACTTTGAGTCATAATTC	*Sr*-ZK qRT-PCR

2.1.11 Human sera list

Serum	**Origin**	***S. stercoralis* in stool**
S 1	Liberia	Not determined
S 2	Liberia	Not determined
S 3	Liberia	Not determined
S 4	Liberia	Not determined
S 5	Liberia	Not determined
S 6	Liberia	Not determined
S 7	Liberia	Not determined
S 10	Liberia	Not determined
S 15	Liberia	Not determined
S 16	Liberia	Not determined

S 17	Liberia	Not determined
S 18	Liberia	Not determined
ON3 7-3-50	Ghana	Yes
ON3 19-34-202	Ghana	Yes
ON3 30-15-95	Ghana	Yes
ON3 32-08-74	Ghana	Yes
ON3 32-09-77	Ghana	Yes
ON3 33-3-45	Ghana	Yes
ON3 35-1-33	Ghana	Yes
ON3 34-14-98	Ghana	Yes
202015	Ghana	No
201006	Ghana	No
200022	Ghana	No
202004	Ghana	No
201009	Ghana	No
200021	Ghana	No
202009	Ghana	No
202011	Ghana	No
201016	Ghana	No
201031	Ghana	No
201007	Ghana	No
202001	Ghana	No
201008	Ghana	No
201030	Ghana	No
202014	Ghana	No
202007	Ghana	No
202010	Ghana	Yes

200008	Ghana	No
201006	Ghana	No
202009	Ghana	No
201019	Ghana	No
200001	Ghana	No
200019	Ghana	No
200026	Ghana	No
200012	Ghana	No
200007	Ghana	No
200020	Ghana	Yes
201024	Ghana	No
200002	Ghana	No
201011	Ghana	No
EC 1	European	Not determined
EC 2	European	Not determined
EC 3	European	Not determined
EC 4	European	Not determined
EC 5	European	Not determined
EC 6	European	Not determined
EC 7	European	Not determined
EC 8	European	Not determined
EC 9	European	Not determined
EC 10	European	Not determined

4.2. Methods

4.2.1. Maintaining the *S. ratti* life cycle and related preparations

4.2.1.1. Parasite culture and infection

Naïve- male 4-6 week old Wistar rats were used to maintain the cycle by serial passage as described (Keiser *et al*., 2008; Viney and Lok, 2007), by subcutaneous infection on the neck region with about 2,500 freshly harvested iL3 each 3 weeks. Fecal pellets were collected in glass dishes every 24 hours on days 6-16 after subcutaneous infection of rats that were placed on steel mesh lined with towel papers. The charcoal coprocultures were set up by adding ~ 50 ml tap water to fecal pellets and left at room temperature for 1 h. Then the softened stool was thoroughly mixed with charcoal. The dishes were covered and placed into an incubator at 26°C.

4.2.1.2. Isolation of *S. ratti* stages

For the isolation of the third stage infective larvae (iL3) and the free-living females (FF), the culture dishes were incubated for 6 days for the collection of newly generated iL3 and 24 - 27 h to collect the free-living stages (FLS). The FF were isolated from other FLS by carefully pipetting under the light microscope. For the recovery of iL3 and FLS the standard Baermann (Fig.4) isolation technique was used. In brief, warm water (39-42°C) was filled in a funnel which was closed at the bottom with a clamp. A steel sieve was placed on top of the funnel. About ¼ of the steel sieve had to be covered with water. A piece of cotton was laid into the sieve and the charcoal culture was carefully transferred above the cotton. A lamp was placed directly next to the funnel to maintain warm temperatures.

The migrating larvae were collected from half of the water in the funnel and then concentrated in a ceramic sieve (Filternutsche, Roth). The larvae were then used freshly, stored at 4 °C, at -20 °C or at – 70 °C until further use. For the recovery of parasitic females (PF), the rats were infected with about 2,500 iL3. On day 7 post-infection the rats were sacrificed and the PF recovered from the small intestine, which was opened longitudinally after cleaning and then applied to a Baermann funnel (without cotton) for 3 h.

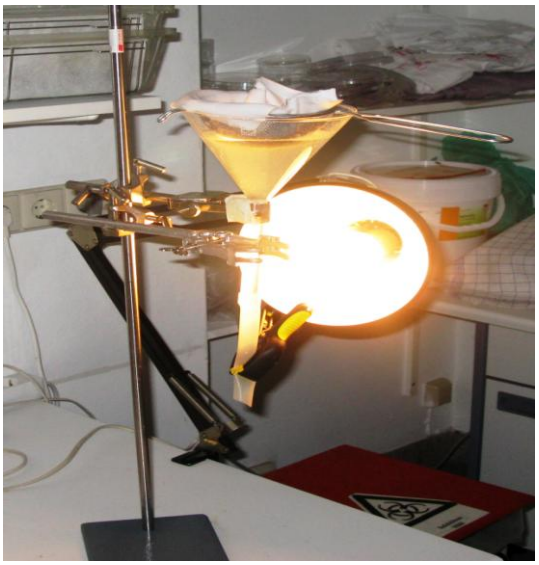

Fig. 4. Setup of the Baermann funnel routinely used at the BNI for isolation of *S. ratti* stages from faecal cultures

4.2.1.3. Somatic extracts and excretory/secretory proteins (ESP) preparation

The freshly harvested iL3, PF and FF were extensively washed in sterile Hanks Balanced Salt Solution (HBSS) supplemented with 100 µg/ml penicillin and 100 units/ml streptomycin (Sigma–Aldrich Chemie, Steinheim, Germany). Somatic extracts were prepared by fast agitation of the worms in the presence of a single steel ball (2.8 mm diameter) using a Precellys Steel Kit (PeqLab Biotech., Erlangen, Germany) in cold phosphate buffer (4 ºC) supplemented with 0.1 mM EDTA and 25 mM HEPES for 10 min.

The ESP from the same stages (iL3 (4×10^4/ml), PF (200/ml) and FF (200/ml)), which were cultured at 37 °C under the laminar flow hood, were prepared as described before (Maruyama *et al*., 2003). The culture medium was RPMI-1640 (Sigma-Aldrich) supplemented with penicillin and streptomycin (same concentration as washing solution) and 10 mM HEPES (Sigma-Aldrich). The incubation times were 24 h for the iL3 and FF and 72 h for PF with changes of media every 24 h. After the incubation period, vitality and sterility were checked under the microscope. An additional test for sterility was performed by placing 5 µl of each culture medium on blood agar plates and subsequently incubating the plates at 37 °C for 24 h. Only sterile cultures were used for further experiments. The larvae were pelleted by centrifugation, extracts and ESP were supplemented with fresh protease inhibitors (Complete protease inhibitor cocktail, Roche Diagnostics, Mannheim, Germany) and were then concentrated about 200-fold (Amicon Ultra 10.000 MWCO filters; Millipore GmbH, Schwalbach, Germany). For the inhibition of an active astacin metalloprotease, 10 mM phenanthroline solution was added to the preparations prior to centrifugation.

4.2.2. General bioinformatic procedures

4.2.2.1. Data search

The mass spectrometry analyses of the ESP from the *S. ratti* stages were performed by Hanns Soblik (Bernhard-Nocht Institute) supervised by Hanno Steen, from the Proteomics Center, Department of Pathology, Children's Hospital, Harvard Medical School in Boston by liquid chromatography–tandem mass spectrometry (LC–MS/MS). All MS datasets were searched against a combined protein sequence database containing EST sequences from *S. ratti* and *S. stercoralis* as well as the RefSeq protein sequences for *C. elegans* and *C. briggsae*. Searches were performed using ProteinPilot™ (v.2.0.1; AB/Sciex).

4.2.2.2. Computer-based sequence analysis

The ESTs constituting clusters identified were screened for more sequence information to get the longest possible nucleotide sequences representing partial genes structures. The EST database used for this search is available at www.nematode.net (Martin *et al*., 2009). Homology searching on the nucleotide and protein database was carried out using the BLAST program with default settings at NCBI (http://www.ncbi.nlm.nih.gov/). Thereafter, to compare identity and for further bioinformatic analysis, sets of software available at the Expert Protein Analysis System (ExPASy) proteomics server (http://expasy.org/tools/) of the Swiss Institute of Bioinformatics were used.

4.2.2.3. Selection criteria of candidate proteins

To select proteins from the identified ESP lists, for the determination of stage-related genes expression, for the quantitation of the transcriptional level and for further characterization the following criteria were followed:

- Stage-specificity for the highest scoring proteins of E/S products from the previous MS/MS analysis and their abundance in the different stages
- Knowledge of interesting functional activities of homologues
- Novel, hypothetical, small sized, presence of a signal peptide and uncharacterized proteins
- Bioinformatic & computational analysis (clusters/ESTs); to get a suitable length sequence of the open reading frame (ORF) and to design primers.

- Data evaluation and confirmation: the genes should give specific signals to be confirmed by dissociation curves and ethidium bromide gel analysis. In addition, gene efficiencies should be > 90% for reliable data evaluation.

Accordingly, various genes encoding the abundant and highly scored secreted proteins (MS/MS) were chosen for quantitative RT-PCR investigation, and the following 19 genes which encode the ESP proteins are listed in Table 1.

4.2.3. General molecular biological methods

4.2.3.1. RNA isolation

Total RNA was extracted from the freshly prepared iL3, PF and FF or stored at -70 °C, after 7 days of infection as described (Tazir *et al*., 2009). Briefly, after collection, ~ 0.1 g of separated stages was washed extensively in PBS, then homogenized by fast agitation (vortexed at highest speed) of the worms, suspended in 750 µl Trizol LS buffer (Invitrogen) in the presence of a single steel ball (2.8 mm diameter) using a Precellys Steel Kit (PeqLab Biotech., Erlangen, Germany) for 15 min. 200 µl chloroform (per 750 µl of Trizol LS) were added and vortexed for 15 seconds. After incubation at RT, the entire sample including smashed worms, Trizol LS, and chloroform, but without the bead, was transferred to a clean Eppendorf tube and centrifuged at 4°C for 15 min at 13,000 g. The aqueous phase (top phase) was transferred to a fresh tube and kept on ice. To precipitate the RNA sample, 500 µl ice-cold isopropanol (Merck) per 750 µl of Trizol LS were added, followed by vortexing. After 10 min incubation at RT, the sample was centrifuged at 4°C for 15 min at 13,000 g. The supernatant was removed with an RNase-free pipette. Then, the pellet was washed with 1 ml 75% ethanol (Merck) made with DEPC H_2O (Roth) and centrifuged at 4°C for 5 min at 5,300 g. The supernatant was carefully removed; the tube containing the pellet was inverted and air-dried for 5 min. Depending on the yield, the pellet was resuspended with 50-100 µl of DEPC H_2O (Roth). Subsequently, RNA was quantified spectrophotometrically. The quality and integrity of the total RNA was confirmed after staining of 3 µg RNA from all stages by loading buffer (Roti®-RNA, ROTH), following the manufacturer's protocol, on an ethidium bromide-stained gel containing formaldehyde. RNA samples were then treated with RNase-free DNase I (Qiagen, Hilden, Germany) and purified with RNeasy MinElute spin column (Qiagen) following the manufacturer's protocol.

Table 1. Genes and identified clusters used for verification of the stage-related proteins by qRT-PCR. The identification is linked to the nematode.net data base and based on the MS/MS analysis of the stages ESP by ProteinPilot program

Putative/homologe gene name	**Cluster**	**Accession N°**	**Stage ESP abandance**
Sr-astacin	SR11111	AAK55800	iL3
Sr-calumenin	SR00564	NP_001024806	PF
Sr-chitin binding protein	SR04455	XP_001664881	PF
Sr-GAL-1	SS00840	AAD39095	All stages
Sr-GAL-2	SR00627	AAF63405	All stages
Sr-GAL-3	SR00900	XP_001896448	All stages
Sr-GAL-5	SR00857	NP_495163	All stages
Sr-GAPDH	SR00526	NP_508534	Houskeeping gene
Sr-HSP10	SS01752	ABN49241	All stages
Sr-HSP17a	SR00984	HQ848950	PF
Sr-HSP17b	SR03349	HQ848951	PF
Sr-HSP60	SR00728	ABY65231	All stages
Sr-lysozyme-5	SR00671	NP_502193	FLS
Sr-MFP2b	SR00863	AAP94889	FLS
Sr-MIF	SS01459	ACH88456	iL3 and PF
Sr-phosphoribosyl-transferase	SR02118	XP_001895434	PF
Sr-POP	SR01641	NP_971802	PF
Sr-trypsin inhibitor-like protein	SR02054	XP_001866937	PF
Sr-Y51F10.7; CBG22129	SR02091	XP_001667627	FLS
Sr-ZK1073.1	SR02886	XP_001899587	iL3

4.2.3.2. Reverse transcription

To obtain 3'-cDNA ends, 3'-Rapid Amplification of cDNA Ends (RACE) was performed. The 3'-RACE is a method that generates full-length cDNAs by utilising 3'-oligo-dT-containing primers complementary to the poly(A) tail of mRNA during the first strand

cDNA synthesis. A total of ~ 5 µg of purified parasite RNA was used to synthesize the first strand cDNA using SuperScript® III RT and GeneRacer (Invitrogen). The manufacturer's instructions were followed except for the antisense primer, oligo dT-T7I (primer list), which was used at a final concentration of 10 µM.

4.2.3.3. Relative mRNA quantification by qRT- PCR

After 7 days of infection, *S. ratti* iL3, PF and FF cDNAs were synthesized from high quality RNAs as described above. ABI PRISM® 7000 SDS/Relative quantification system (Applied Biosystems, Foster, CA, USA) was used to perform quantitation of gene expression of *S. ratti* ESP selected candidates (see above).

Sr-GAPDH was included as a housekeeping gene and showed a stable and constant expression level in all stages. Specific forward and reverse primers were designed with primer3plus (http://www.bioinformatics.nl/cgi-bin/primer3plus/primer3plus.cgi), or manually to amplify ~150 bp amplicons. The primers used to amplify 154 bp of *Sr*-GAPDH were forward gapdhf and reverse gapdhr. In order to avoid secondary structures such as hairpins and loops, which may affect the final products' specificities, the qualities of primers were analyzed using the Oligonucleotide Properties Calculator (http://www.basic.northwestern.edu/biotools/oligocalc.htmL).

PCR was performed using the qPCR Core kit for SYBR®Green I (Eurogentec S.A.) following the manufacturer's recommendations, under the following conditions:

- 0.1 µg of cDNA (except for HSP10 and HSP60, 0.5 µg cDNA was used in a separate experiment), 3.5 mM MgCl2, 1 µM of each pair of primers, 0.75 µl of SYBR Green I, 0.13 µl of HotGoldStar enzyme and 200 µMdNTP in a final volume of 25 µl.
- Thermocycling included incubations at 50 °C for 2 min and 95 °C for 10 min, followed by 40 cycles of 95 °C for 15 s and 60 °C for 1 min.
- Baseline and threshold for Ct calculation were set automatically with the ABI Prism 7000 SDS software version 1.0, or set manually whenever necessary.
- PCR-efficiency was determined for all PCRs using serial 10-fold dilutions of cDNA (Pfaffl, 2001). Briefly, Serial cDNA dilution curves were produced to calculate the amplification efficiency for all genes (1, 1:10, 1:100, 1:1000, and 1:10000). A graph of threshold cycle (Ct) versus log10 relative copy number of the sample from a dilution series was produced. The slope of the curve was used to determine the amplification efficiency: Efficiency = 10 (-1/slope).

- For measurement of gene expression levels, each sample was tested in triplicate, using positive and template-free controls beside negative reverse transcription controls.
- The specificity and identity of individual amplicons were verified by setting up the 7000 SDS machine to produce melting curve analysis for each gene in each stage (specifically amplified genes should give identical curves). Then the PCR products were evaluated by agarose gel electrophoresis.
- The threshold cycles (Ct) values from real-time PCR instrument were imported into a spreadsheet program (Microsoft Excel), and the mean Ct from two individual experiments (each in triplicate) was calculated for each gene.
- Relative transcriptional differences were calculated from normalized values following the protocol described (Livak and Schmittgen, 2001). Shortly, The fold change in the target genes was performed using the formula:

$2^{-\Delta\Delta CT}$, where $\Delta\Delta CT = (Ct_{,Target} - Ct_{,control})_{Time\ x} - (Ct_{,Target} - Ct_{,control})_{Time\ 0}$; x is any time point and time 0 represents the 1X expression of the target gene normalized to an internal control gene. In case of determining the fold change in the target gene in different stages of *S. ratti* the Eq. will be simply:

$\Delta\Delta CT = (Ct_{,Target} - Ct_{,GAPDH})_{Stage\ x} - (Ct_{,Target} - Ct_{,GAPDH})_{Stage\ 0.}$ The mean Ct values for the target genes were determined at time x (stage x; PF or iL3), normalized to GAPDH and relative to the expression at time 0 (stage 0 or selected stage; FF), was calculated for each sample using the Eq. $2^{-\Delta\Delta CT}$.

4.2.3.4. Genomic DNA isolation

For DNA isolation, a pellet of approximately 250,000 *S. ratti* iL3 was digested for 3-4 h at 56 ºC with 40 µl proteinase K and 200 µl ATL buffer (Qiagen, Hilden, Germany) under constant agitation. RNA free gDNA was extracted by standard phenol/chloroform methods and treated with RNase A (Roche). For precipitation, the salt concentration of the aqueous DNA solution was adjusted by adding 1/10 volume of 3 M sodium acetate (pH 5.2). Cold 96% ethanol (-20 °C, 2.5 volumes) was then added, and the samples were mixed. For optimal purity, the pellet was fished from the tube, washed with 80% ethanol (-20°C), and air dried in a new Eppendorf tube (~ 15 min at RT). The DNA was resuspended in 25 µl or 50 µl DEPC water depending on the pellet size.

4.2.3.5. Agarose gel electrophoresis

Agarose gel electrophoresis was performed as described (Sambrook *et al*., 1989) using TAE buffer and agarose concentrations between 0.8%-1.2% (w/v) depending on the size of the fragments to be separated. DNA was mixed with the DNA-loading buffer (Fermentas) and suitable DNA-ladder (see above) was used to monitor fragment size. 5 μL ethidium bromide per 100 ml agarose solution was added before pouring the gel. The running buffer is 1X TAE and the voltage was set to 80-100 V. For RNA analysis, the method previously described (Farrell, 1993) was used, using 0.8%-1.2% (w/v) agarose prepared in 1X MOPS buffer containing 0.7 M as a final concentration of formaldehyde. RNA was mixed with the RNA-loading buffer, which contains formaldehyde and 0.005 ethidum bromide as described above; a suitable RNA-ladder (see above) was used to monitor fragment size. Gels were run overnight in 1X MOPS as running buffer under 25 V. RNA or DNA bands were visualized using a UV transilluminator and immediately photographed.

4.2.3.6. Identification and characterization of *S. ratti* selected candidates

The proteins detected only in the ESP PF and/or iL3 and showing upregulation in transcription levels in such stages are very interesting molecules because they may be involved in parasite-host interactions. Two small HSPs (HSP17s) and a homologue of the human cytokine macrophage migration inhibitory were selected for further molecular and functional characterization.

4.2.3.6.1. Identification of the full length sequences

4.2.3.6.1.1. Clusters analysis

Two EST clusters from the ESP of the PF, encode homologues for Ce-HSP17s; SR00984 (Contig 767, EST=17) and SR03349 (Contig 820, EST=17) were identified and a third less abundant cluster SR01014 (Contig834, EST=65), was identified to have 98% identity to SR03349. In addition, peptides related to the cluster SS01459 (Contig1459, EST=11) from *S. Stercoralos,* assigned to MIF homologues, were abundantly found in the iL3 and PF ESP but not FF. The ESTs constituting these clusters were processed as described above and aligned to get the possible longest DNA sequence and a deduced amino acid sequence.

4.2.3.6.1.2. Polymerase chain reaction (PCR)

The resulting ESTs were used for the design of forward and reverse primers for the three clusters corresponding to HSP17 and MIF. To obtain 3'-cDNA ends, specific forward primers (af2, bf2 and mf2, see the primer list above) were used for amplification of *Sr*-HSP17a, *Sr*-HSP17b and *Sr*-MIF respectively, and the oligo dT-T7II was used in all cases as the reverse primer. The 5' ends were obtained using the following gene specific reverse primers: ar2 to amplify *Sr*-HSP17a; br2 to amplify *Sr*-HSP17b; and mr2 for MIF using the 5' SL-1, corresponding to the nematode spliced leader sequence (Hunter *et al*., 1997).

The PCR was done as described before (Sambrook *et al*., 1989). In brief, the PCR conditions were: 1x thermo buffer (NEB), forward primer (10-20 pmol), reverse primer (10-20 pmol), dNTP mix (Invitrogen; 10 mM), Taq polymerase (NEB; 0.3 µl), DNA 0.1-0.5 µg and DEPC-H_2O to 50 µl. The denaturation step was set to five minutes at 95°C and the elongation was performed at 72°C between 30–120 seconds depending on the fragment size to be amplified. The annealing temperatures (50-60 °C) are related to the primers' properties and their melting temperatures (Tm), which were calculated using the following formula: Tm = (A+T) x 2 + (G+C) x 4. The annealing time was set to 40-60 seconds and 25-30 cycles were repeated. The results of the amplification were tested on agarose gel.

4.2.3.6.1.3. Cloning and sequencing

Various *Sr*-HSP17s and MIF genes' PCR products were purified by QIAquick® PCR purification Kit (Qiagen, Hilden) and then cloned into pGEM-T Easy vector (Promega Corp.,Madison, USA) according to the manufacturer's protocols. The cloned fragments were subsequently transformed into competent *Escherichia coli* TOP10 cells (Invitrogen) and the recombinant plasmids were purified from the bacterial cultures by QIAprep® Miniprep Kit (Qiagen, Hilden), according to the manufacturer's protocols. The resulting products were sequenced (LGC Genomics GmbH, Germany).

Alignment of the various cloned fragments of each gene resulted in the full length sequences. Subsequently, primers including the 3'- and the 5'-ends were designed (see the primers list above), which included the codon for the initiating methionines and a stop codon. The full length ORFs of the *Sr*-HSP17a, *Sr*-HSP17b and *Sr*-MIF cDNAs were captured by PCR using specific forward primers af1, bf1 and mf1 and reverse primers ar1, br1 and mr1, respectively.

The full length cDNAs were cloned, after purification, into the pGEM-T Easy vector and transformed into TOP10 cells. The results confirmed by restriction digestion by NotI for

the cloned *Sr*-HSP17s and EcoRI for *Sr*-MIF (NEB) according to the supplier's protocol, then observed on ethidium bromide-stained gel. For further sequence confirmation the fragments were sequenced using the M13 forward-, and gene specific primers.

4.2.3.6.2. Genomic organization

The specific primer sets af1, ar1 for HSP17a, bf1, br1 for HSP17b and mf1, mr1 for MIF (see the primer list above), were used to amplify the full length gene sequences using 0.1 µg gDNA as a template. The resulting products were cloned into the pGEM-T Easy vector and sequenced (see above). The cDNA was used as size and sequence control. After sequencing, the gDNA and cDNA clones were compared by sequence alignment and analysed by ethidium bromide-stained gel.

4.2.3.6.3. Expression of the recombinant proteins in *E. coli*

4.2.3.6.3.1. Insert design

A pair of primers was designed to generate a fragment which encodes the full length sequence of the *Sr*-HSP17a. The 5′ sense primer af4 (see primers list above) contained a recognition site for HindIII (upper case), an enterokinase cleavage site to remove the his-tag (lower case) and 11 bp (underlined in the primer sequence) of the cDNA which included the codon for the initiating methionine. The 3′ anti-sense primer ar4 contained a recognition site for BamHI and 24 bp of cDNA, which included a stop codon. To express the *Sr*-HSP17b, the cDNA was amplified by PCR using the forward primer bf4 containing a recognition site for NdeI (upper case), an enterokinase cleavage site (lower case) and 12 bp (underlined in the primer sequence) of the cDNA; and the reverse primer br4, which contained a BamHI recognition site and 18 bp of cDNA. Similarly, primers were designed to express the *Sr*-MIF. The 5′ sense primer, mf4, contained a HindIII recognition site (upper case), an enterokinase cleavage site to remove the his-tag (lower case) and 11 bp (underlined in the primer sequence) of the cDNA including the codon for the initiating methionine. The 3′ anti-sense primer, mr4, contained a recognition site for BamHI and 26 bp of cDNA, which included the stop codon.

4.2.3.6.3.2. Recombinant construction

The amplified fragments were ligated into pGEM-T Easy. The plasmids were then isolated and digested with the corresponding restriction enzymes (mentioned above). The restriction fragments purified from the gel by the QIAquick® gel extraction Kit (Qiagen, Hilden) were subcloned into pJC45 expression vector (Clos and Brandau, 1994), which kindly

provided by Dr. J. Clos (BNI, Hamburg), which was previously digested with the same restriction enzymes corresponding to each case and purified from the gel in the same way as the fragments. The Sequences were confirmed again by restriction digestion and sequenced using a pJC45 specific forward primer pJC45f (see the primer list above).

4.2.3.6.3.3. Recombinant expression

The recombinant plasmids of HSP17s were then transformed into an *E. coli* Star BL21 DE3 and the MIF recombinant construct was transformed into *E. coli* BL21. The expression *E. coli* strains were kindly provided by Prof. Eva Liebau (Department of Molecular Physiology, Muenster). The expression of polyhistidine-recombinant proteins were induced at OD600 ~ 0.25 with 0.2 mM iso-propyl-beta-D-thiogalactopyranosid (IPTG) for 8 h at 30 °C to avoid over expression of the r*Sr*-HSP17s. r*Sr*-MIF was induced at OD600 ~ 0.5 with 1 mM IPTG for 3 h at 37 °C. The induced cells were then processed directly or stored at -20 for further purification.

4.2.3.6.3.4. Purification by affinity chromatography

The induced cells were suspended and lysed in 5x (v/v) in 8 M urea supplemented buffer B1 (see the list of buffers), followed by sonication (Branson Sonifier-250) while kept on ice for four min. The supernatants containing the recombinant *S. ratti* protein products (r*Sr*-HSP17a, r*Sr*-HSP17b and r*Sr*-MIF) were purified by affinity column chromatography using the profinity TM IMAC Ni–NTA resin (Bio-RAD Laboratories, Germany). The bound proteins were washed 3 times, 10 min each, in 5x (v/v) B2 and 3 times, 10 min each, in 5x (v/v) B3. Recombinant proteins were then recovered by elution in two steps, 2 min each, with 2x (v/v) of B4. The eluted fractions were dialyzed in 2 M urea containing buffer (B5) overnight, and then dialyzed against B6 for 2 h. Subsequently samples were dialyzed 3 times for 2 h each in B7 (1 X GIBCO DPBS, Invitrogen) or sterilized TBS, concentrated and stored at 4 ºC or -20 ºC.

All buffers used were chilled on ice before use and prepared using sterile, highly pure water (Aqua B. Braun, Melsungen AG, Germany). Dialysis was carried out in a cooling room at 8 ºC -10 ºC. Enterokinase cleavage capture kit (Novagen, USA) was used to cut the his-tag, followed then by the rapid, affinity-based capture and removal of recombinant enterokinase using the manufacturer's protocol. We used the terms rhis*Sr*-MIF and r*Sr*-MIF for comparison in the enzymatic assay only, other experiments were done using the rhis*Sr*-MIF which was referred to as r*Sr*-MIF.

4.2.3.6.3.5. Endotoxin removal

Bacterial lipopolysaccharides (LPS) were removed by adding Triton X-114 in the washing procedure of the Ni agarose-bound recombinant protein and the antibiotic polymyxin B (PMB), purchased from Sigma–Aldrich (Germany), as part of the purification process (see the list of buffers). Parallel fractions were purified with the same method but without using PMB or Triton X-114. Endotoxin concentrations were quantified by standard *Limulus* amoebocyte lysate chromogenic endpoint assay (LAL assay) according to the manufacturer's protocol (*Limulus* Amebocytes Lysate, QCL-1000, Lonza, Walkersville).

4.2.4. Biochemical methods

4.2.4.1. SDS-PAGE analysis

The purity of the recombinantly expressed proteins was analyzed by sodium dodecylsulfate polyacrylamide gel electrophoresis (SDS-PAGE) using the discontinuous system as described (Laemmli, 1970), which is based on the principle that proteins are separated depending on their molecular mass under denaturing conditions. For all gels performed at the BNI Bio-Rad gel chambers were used. The gels were 8.3 x 7.3 cm in size. The gel concentration was 15%**.** After SDS-PAGE separation, the gel was stained with 0.05% (w/v) Coomassie brilliant-blue (Carl Roth). After destaining (Coomassie destaining solution), protein bands on regular SDS-PAGE gels were visible as blue bands on the clear gel. The his-tagged proteins were detected from identical gels by Western blotting applying standard procedures (see below) onto a nitrocellulose membrane using anti-his POD.

4.2.4.2. Determination of protein concentration by Bradford assay

The proteins concentrations (ESP, extracts and recombinant proteins) were determined spectrophotometrically by standard Bradford assay method. The absorbance maximum for an acidic solution of Coomassie Brilliant Blue G-250 dye shifts from 465 nm to 595 nm when binding to protein occurs. The concentrations of protein solutions can be determined through comparison to a standard curve. All protein concentration measurements were performed using the Bio-Rad Protein Assay according to the manufacturer's protocol.

4.2.4.3. *In vitro* chaperone-like activity assay for the r*Sr*-HSP17s

The chaperone-like activity of recombinant *Sr*-sHsp17s was studied by measuring their ability to prevent the aggregation of the well known substrates citrate synthase (CS) (as described in (Wu et al., 2007)), malate dehydrogenase (MDH) (as described in (Cherepkova et al., 2006) or the activity was also studied by thermal aggregation induction and inhibition of DTT-induced insulin aggregation, as previously described (Liao *et al*., 2009). Aggregation of substrates was measured in the presence of different concentrations of r*Sr*-HSP17a or r*Sr*-HSP17b. The following conditions were applied:

(i) CS from porcine heart, provided in 2.2 M $(NH_4)_2SO_4$, 6 mM phosphate, 0.5 mM citrate (Sigma) was used at a concentration of 75 µg/ml at 45 °C.

(ii) MDH from porcine heart provided in ammonium sulfate (Sigma) was used at a concentration of 41.5 µg/ml at 48 °C. For both substrates (CS and MDH) the molar ratios (HSP/substrate) were 1:10 and 1:20.

(iii) Chemically-induced insulin aggregation at 37 °C in a molar ratio (HSP/insulin) of 1:2.5, 1:5 and 1:10 was determined. The bovine pancreas insulin (250 µg/ml), provided in 25mM HEPES pH 8.2 (Sigma), was induced for aggregation by 0.02 M DTT.

Absorbance was recorded at O.D. 360 nm for insulin and MDH and 320 nm for CS aggregations every 5 min using ultrospec 2000 spectrophotometer (Pharmacia, Biotech.) for 40 min in 1 ml semi microquartz tubes.

4.2.4.4. *In vitro* tautomerase enzymatic assay for r*Sr*-MIF

Tautomerase assays were done as previously described (Swope *et al*., 1998), with slight modifications, using the well known substrates:

(i) L-dopachrome methyl ester (LDME) which was prepared by adding 4 mM L-3,4-dihydroxyphenylalanine methyl ester (Sigma) with 8 mM sodium periodate for 5 min at room temperature and then placed directly on ice for 20 min before use. Activity was determined at ~ 25°C by adding dopachrome methyl ester to 1µg of rhis*Sr*-MIF, r*Sr*-MIF or recombinant human MIF (rHu-MIF) (Applichem GmbH, Darmstadt, Germany) in a cuvette containing 25 mM potassium phosphate buffer pH 6, 0.5 mM EDTA and measuring the decrease in absorbance for 5-100 s at 475 nm.

(ii) HPP (p-hydroxyphenylpyruvate), purchased from Sigma, was dissolved in 50 mM ammonium acetate pH 6.0, allowed to equilibrate at room temperature overnight,

and stored at 4°C. Activity was determined at ~ 25 °C by adding HPP to 1µg of rhis*Sr*-MIF, r*Sr*-MIF or rHu-MIF in a quartz cuvette containing 0.435 M boric acid, pH 6.2, and measuring the increase in absorbance at 330 nm spectrophotometrically by following the increase in absorbance for 5-100 s due to the formation of the borate-enol complex.

In both assays blanks containing only substrate and no MIFs were used.

4.2.5. Immunological methods

4.2.5.1. Generation of antisera, titration and antibody purification

Antibodies against r*Sr*-HSP17s and against r*Sr*-MIF were generated by immunization of 10 weeks, old male Wistar rats with 20 µg recombinant proteins in alum/PBS (1:1 v/v; pH ~ 7.4); rats were injected subcutaneously in the neck and boosted twice in the same way at 14 day intervals as described before (Tazir *et al*., 2009). Sera collected from immunized rats at day 14 post prime and at day 14 post boost were tested with the corresponding r*Sr*-HSP17 or r*Sr*-MIF by enzyme-linked immunosorbent assay **(**ELISA) (see below) and Western blots. Antibodies were affinity-purified using a modified method described before (Muller *et al*., 1992). Briefly, after electrophoretic transfer, nitrocellulose membranes were blocked for 1 h using 5% milk/PBS. A 5 mm wide strip was longitudinally excised with a new razor blade strip and incubated overnight at 4 ºC in 1:5000 anti-his POD diluted in 2.5% milk/PBS/0.05% Tween-20. The rest of the membrane was incubated in a 1:50 dilution of immunized rat sera in 2.5% milk/PBS/0.05% Tween-20 with constant agitation. The clearly visualized band of the excised strip was aligned to the rest of the membrane and the corresponding strip, which contains the antibody bound to protein, was excised and washed 5 times in PBS/0.05% Tween-20 for 5 min each. Subsequently, the pure antibodies were eluted by incubation in 1 ml of 0.2 M glycine (pH 2.6)/0.05% Tween-20 with constant agitation for 10 min on ice, then directly 10X concentrated and the buffer replaced by PBS/ 0.1% BSA (pH 7.5) and stored at – 20 ºC. Purified antibodies were:

(i) Analysed by ELISA for detection of native *S. ratti* proteins in the somatic extracts and ESP of the developmental stages and

(ii) For neutralization experiments in FACS analysis.

4.2.5.2. Detection of native *Sr*-HSP17s and *Sr*-MIF proteins

To test the presence of the native *Sr*-HSP17s and *Sr*-MIF proteins in the extracts and ESP of the *S. ratti* stages, the purified antibodies from the rat sera were used in the ELISA analysis diluted at 1:300. 96-well polystyrene microtiter plates (Maxi-Sorb, Nunc) were coated with 200 ng protein (in coated buffer; see buffer list) either in extracts or ESP per well, blocked with 5% BSA/PBS, and HRP-conjugated goat-anti-rat IgG (Dianova, Hamburg, Germany) was used as a secondary antibody (1:5,000). Sera taken from naïve rats served as the negative controls. Optical density was measured at 450 nm.

4.2.5.3. Immune recognition by ELISAs with rat and human sera

Sera were taken from 5 rats before, 37 days after and 112 days after infection with *S. ratti* iL3. sera were also taken from 50 individuals residing in West African endemic areas for nematode infections including strongyloidiasis as well as from 10 healthy Europeans. Taking of blood samples for research purposes was approved by the Ethics Commission of the Medical Board, Hamburg, and by ethics committees and medical authorities in the respective countries. A semi-quantitative analysis of serum IgG antibody levels was performed with modifications using ELISA as previously described (Liebau *et al*., 2008; Mpagi *et al*., 2000). In brief, polystyrene microtiter plates (Maxi-Sorb, Nunc) were coated with *Strongyloides* recombinant proteins at a concentration of 200 ng/well in carbonate buffer (pH 9.6), sealed with saran wrap and incubated overnight at 4 °C. After removal of unbound protein by washing three times with PBS/0.05% (v/v) Tween-20, the plates were blocked with 5% (w/v) BSA in PBS for one hour at 37 °C. Sera from rats were diluted 1:150, 1:300 and 1:900 and sera from humans were diluted 1:500, 1:1,000 and 1:2,000 in PBS/0.5% BSA; all were incubated at 37 °C for one hour. Unspecifically bound proteins were removed by three washing steps. For detection of bound rat IgG, anti-rat IgG peroxidase–conjugated antibody was applied at a final concentration of 1:5,000. For human sera anti-human IgG1 peroxidase–conjugate antibody was applied to a final concentration of 1:500; tetramethylbenzidine was used as substrate. Data are expressed as endpoint titers derived from titration curves (Liebau *et al*., 2008).

4.2.5.4. Cross-reactivity between human and *Strongyloides* MIF

Immunoblot analysis was performed to detect whether either the generated and purified rat anti-*Sr*-MIF or the rabbit anti-human-MIF (BioVision, CA, USA) will react with the r*Sr*-MIF and/or the recombinant human MIF (rHu-MIF), purchased from Applichem, GmbH,

Darmstadt, Germany. 5 µg of either r*Sr*-MIF or rHu-MIF were separated by 15% SDS PAGE, then transferred onto a nitrocellulose membrane using a mini-Trans Blot Cell in Bjerrum-Schafer-Nielsen transfer buffer for 50 min at 50 V. The membrane was blocked with 5% skim milk in PBS (w/v) overnight with constant agitation at 4 °C. After a wash step with TBS/0.05% Tween-20 for 10 min at room temperature, the nitrocellulose membrane was probed either with a 1:300 dilution (v/v) of the purified anti-*Sr*-MIf or a 0.5 µg/ml concentration of anti-Hu-MIF. As secondary antibodies, horseradish peroxidase-conjugated goat anti–rat IgG or anti-human IgG (Roche) diluted in 5% (v/v) skim milk in PBS were applied. The immunoreactive bands were visualized using 410/3/11chloro-1-naphtol (Roche) according to the manufacturer´s protocol.

4.2.5.5. Cell preparation

Venous blood samples obtained from healthy volunteers in agreement with institutional guidelines served as a source for peripheral blood mononuclear cells (MNC) and polymorphonuclear cells (PMN). Samples were collected in tubes containing 0.106 mol/l trisodium citrate solution and 1 ml citrate solution (Sarstedt, Germany). Erythrocytes were sedimented from blood samples by addition of equal amounts of 6% hydroxyethyl starch for 40 min at room temperature. After washing the buffy-coat cells in PBS for 10 min at 400 ***g***, MNC were separated from PMN by Ficoll-histopaque discontinuous density centrifugation comprised of 3 ml Mono-Poly Resolving Media (MP Biomedicals, Sweden) with a density of 1.114 g/ml overlaid with 3 ml Lymphoflot (Bio-Rad) with a density of 1.077 g/ml, centrifuging at 600 *g* for 30 min. The aspirated MNC and PMN were carefully harvested, washed and resuspended in RPMI 1640 (MNC) and Ca^{++}-containing HBSS (PMN), respectively, at a concentration of $4x10^6$ cells/ml and kept on ice. Murine MØ cell line J774 cells, purchased from the German Collection of Microorganisms and Cell Culture (Braunschweig, Germany), were cultured and passaged in RPMI 1640, 2 mM L-glutamine, 5% inactivated FCS, 25 mM HEPES supplemented with 100 U/ml penicillin and 100 µg/ml streptomycin. The rat small intestinal epithelial cell line (IEC-6) purchased from the European Collection of Cell Cultures (ECACC), UK., was passaged in DMEM, 2 mM glutamine, 5% inactivated fetal calf serum (FCS), 0.1 IU/ml insulin, supplemented with 100 U/ml penicillin and 100 µg/ml streptomycin (Quaroni *et al*., 1979). The confluent cells were detached by treatment with accutase in Dulbecco's PBS (PAA Laboratories, Pasching, Austria).

4.2.5.6. Analysis of cell binding by flow cytometry

To determine the binding properties of the parasite proteins, r*Sr*-HSP17s and r*Sr*-MIF were biotinylated using the EZ-Link® Sulfo-NHS-Biotinylation kit (Thermo Scientific, USA), subsequently purified from the excess of biotin and the biotin conjugation determined according to manufacturer's instructions. 2-5 µg biotinylated r*Sr*-proteins were incubated with 2 x 10^5 cells/100 µl of human MNC, PMN, macrophage cell line J774 or rat intestinal epithelial cell line IEC-6, for 45 min at 4 °C to prevent internalization. Biotinylated r*Sr*-HSP17s were used directly or after pre-incubation with corresponding purified antibodies at a final dilution 1:20 for 15 min at RT, prior to incubation with the respective cells.

Similarly, biotinylated r*Sr*-MIF was used directly or pre-incubated either with the purified antibody (with MØ J774, PMNC and IEC-6) or recombinant human CD74 (with MNC), purchased from ABCAM plc, Cambridge, UK., at a final dilution of 1:20, for 15 min at RT. Competition experiments were performed by preincubation of the cells with non-biotinylated proteins.

After washing with PBS, samples were incubated with streptavidin-Alexa Fluor 647 (Invitrogen) for 30 min on ice. Samples that were incubated only with streptavidin-Alexa Fluor 647 were used as the negative controls. Anti-CD14-FITC, anti-CD16-PE and ICAM-1 were applied to gate the monocytes/macrophages, neutrophils and viable IEC-6, respectively, serving as positive controls. Samples were washed two more times and analyzed by flow cytometry on a FACScalibur cytometer (BD Biosciences), measuring 20,000 events from the gated populations. Flow cytometry data were analyzed with CellQuestPro.

4.2.5.7. Cytokine ELISAs

Freshly prepared MNC were cultured in RPMI 1640 supplemented with 2 mM L-glutamine, 5% inactivated FCS, 25 mM HEPES, 100 U/ml penicillin and 100 µg/ml streptomycin and plated in 96-well culture plates (Nunc). 2x10^5 cells per well were cultured in duplicates with or without addition of 50 µg/ml PMB and exposed to the r*Sr*-HSP17a, r*Sr*-HSP17b and r*Sr*-MIF proteins (2 µg/ml) or to LPS (1 µg/ml) or phytohaemagglutinin (2 µg/ml) (PHA; Murex Diagnostics Ltd, Dartford, England) at 37 °C/5% CO_2 for 72 h. Culture medium was used as negative control. In the cell-free culture supernatants, IL-10 and TNF-alpha levels were determined by ELISA according the manufacturer's instructions (eBioscience and R&D Systems) (Brattig *et al*., 2002). The absorbance of the final reactant

was determined at 450 nm using an ELISA plate reader. Four experiments were performed at different conditions.

2.2.2.1. Small scale experiment of immunization and subsequent infection

To examine the immunogenicity of the *Sr*-HSP17s and *Sr*-MIF, four groups of four male Wistar rats were immunized with r*Sr*-HSP17a, r*Sr*-HSP17b, *Sr*-MIF or alum/PBS. The test groups were immunized as described above. Animals were infected on day 14 post boost with 1,000 *S. ratti* iL3 by subcutaneous injection into the neck. Sera were collected before immunization, post immunization and post immunization/post infection.

To determine the worm burden of the infected rats, faecal pellets were collected quantitatively on days 6, 12 and 18 post infection. The fecal cultures after 18-20 h comprise FLS (F1 generation). At that time, not all the free-living female and males have matured and the second generation of FLS (F2) has not yet developed. To normalize the variation of the faecal output of the animals, the count of F1 output from culture of ~ 10 g faecal pellets was calculated and compared in the test groups.

4.2.6. Statistical analysis

Data were processed and analyzed by Statview software. The log values of the OD data are presented in box plots and whiskers as medians and percentiles (10th, 25th, 50th, 75th, and 90th) (Brattig *et al*., 2002). Statistical differences between groups were analyzed by the Mann-Whitney *U* test. *P* values <0.05 were taken as significant, *P* <0.01 as strong evidence of significance. Additionally, one way ANOVA, by Minitab 14 software was used.

5. RESULTS

5.1. Verification of the stage-specific expression of *S. ratti* proteins by differential gene transcription

High quality RNA from iL3, PF and FF (Fig.5) was used in the quantitative real-time PCR (qRT-PCR) to measure relative expression levels of 19 selected genes (Table 1) whose protein products were found to be stage-related in iL3, PF and free-living stages.

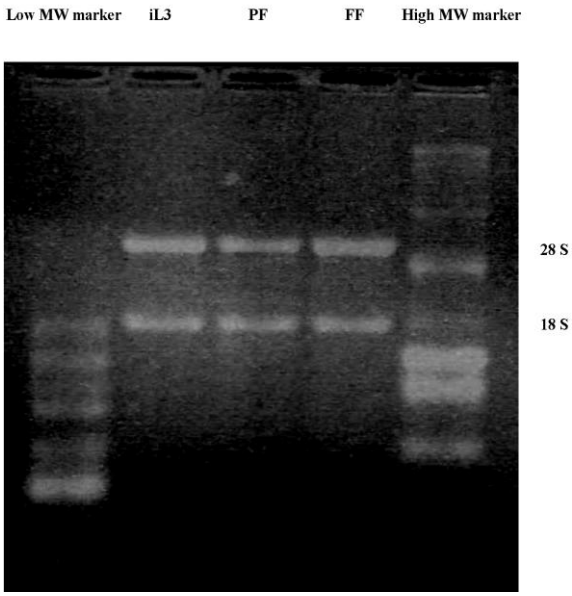

Fig. 5. Total RNA quality and integrity analysis. 3 µg RNA from each stage were analysed by ethidium bromide-stained gel containing formaldehyde after staining by loading buffer (Roti®-RNA, ROTH). The RNA quality was confirmed via the detection of discrete 18 S and 28 S ribosomal RNA bands.

The qRT-PCR results for each transcript were expressed relative to the respective transcript level of the free-living female stage which served as baseline. The efficiency and linearity of qRT-PCR reactions were examined using 10-fold serial dilutions indicating efficient amplification and the threshold cycles were recorded (Table 2). Furthermore, each qRT-PCR reaction was performed in two biological replicates. The qRT-PCR reactions corroborated the findings of the proteomics experiments done by Hanns Soblik (BNI, Hamburg), since increased transcript levels were observed for those proteins that showed exclusive presence in the respective E/S proteome (Fig. 6).

Table 2. Mean Ct (threshold cycle) of tested *S. ratti* transcripts compared to the housekeeping control gene, *Sr*-GAPDH in iL3, parasitic and free-living *S. ratti* female stages. The data are shown for two independent experiments from two separately prepared biological samples. Ct values are mean±S.D.

	iL3	**PF**	**FF**
GAPDH	15,365±0,1341	15,4±0,0782	15,3767±0,304
AST	19,9367±0,0225	32,11±0,0713	31,8567±0,0361
ZK	16,2867±0,1629	21,425±0,2417	19,8817±0,0915
MIF	17,7033±0,0635	18,97±0,0456	18,9533±0,045
GAL-2	17,1433±0,0821	18,1±0,0506	18,1233±0,0985
POP	28,1133±0,0763	16,1333±0,0547	28,02±0,0141
HSP17a	20,5433±0,0273	15,6233±0,0121	18,04±0,041
HSP17b	26,8967±0,0103	19,1833±0,0288	22,06±0,0434
GAL-3	18,1333±0,1162	17,0883±0,0637	18,1467±0,1268
HSP10	27,34 ± 0.47	21,62 ± 0.36	22,81 ± 0.8
HSP60	16,03 ± 0.04	13,22 ± 0.09	14,36 ± 0.08
CBP	30,51±0,2495	19,21±0,1423	20,0267±0,6413
CAUM	21,4667±0,0403	18,1867±0,0615	18,9867±0,0225
TIL	22,7067±0,5601	18,16±0,1088	18,73±0,2418
MFP2B	30±0,019	24,8617±0,0783	18,185±0,2195
Y51F10	27,2267±0,1971	28,465±0,2509	22,1733±0,2491
Lys-5	24,7733±0,3974	25,9733±0,0665	21,4617±0,264
GAL-1	18,7333±0,0216	18,76±0,0335	17,63±0,26
GAL-5	18,1167±0,065	19,3467±0,0266	18,03±0,02
PhRT	20,7767±0,0327	20,7867±0,0946	20,7267±0,0163

The tested stage-specific ESPs for transcription included:

(i) *Sr*-astacin (SR11111), and ZK1073.1 (SR02886), detected only in the ESP of the iL3 stage. Also, the results of the transcripts showed exclusive expression of *Sr*-AST (Metalloproteinase) in the iL3, which was absent in both PF and FF. Similarly, the *Sr*-ZK (homologue of *Brugia malayi* hypothetical 35.6 kDa protein) was highly upregulated (~ 11-fold higher) compared to its expression in the FF, while it was downregulated in the PF.

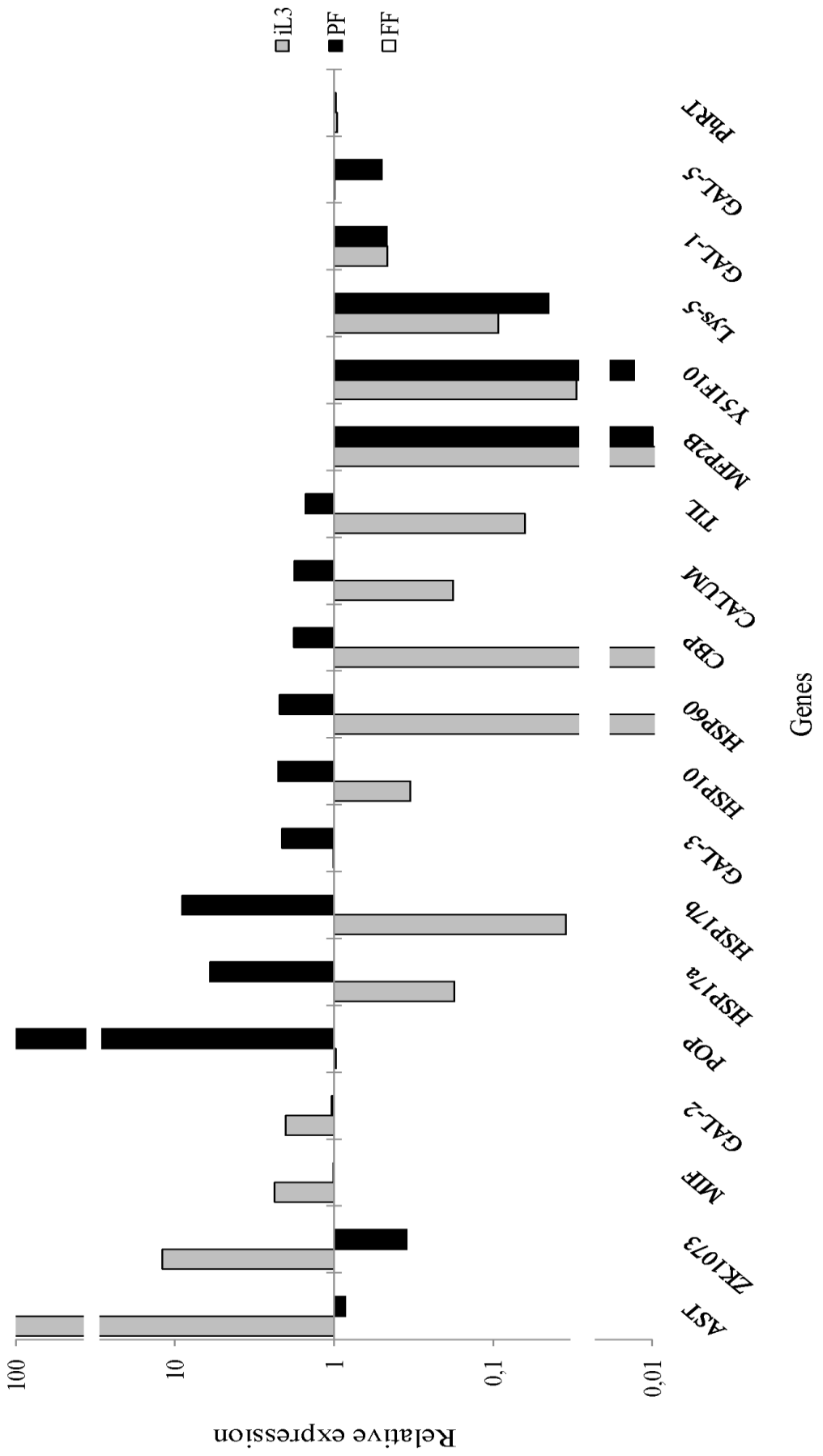

Fig. 6. Stage-specific gene expression confirming stage-related occurrence of secreted proteins. cDNA from infective larvae, parasitic and free-living females were used as a template in real-time quantitative PCR, applying a SYBR Green assay with gene-specific primers. Data are expressed as relative quantity of gene-specific transcription levels of free-living female stage as baseline (value = 1). The results of all samples were normalized to the expression levels of the constitutively expressed gene GAPDH.

(ii) *Sr*-POP (SR01641), *Sr*-HSP17a (SR00984), *Sr*-HSP17b (SR03349), *Sr*-calumenin (SR00564), *Sr*-chitin-binding protein (SR04455), *Sr*-trypsin inhibitor-like protein (SR02054), and *Sr*-phosphoribosyl-transferase (SR02118) were detected in the ESP of the pF stage only. qRT-PCR results confirmed the exclusive transcription of the *Sr*-POP (Prolyl oligopeptidase) and its absence in in both the iL3 and FF. In addition, the transcription levels of the *Sr*-HSP17a and *Sr*-HSP17b were concomitantly elevated more than 6-fold and 9-fold, respectively, in adult PF (Fig. 6) and highly down-regulated in iL3 stage when compared to expression levels in the FF. Furthermore, the differences in the threshold cycle (Ct) values (Table 2) indicated independent *Sr*-HSP17s transcription. Moderate transcriptional upregulation of ~ 1.76-, 1.79- and 1.5-fold was observed in the PF stage for *Sr*-calumenin (*Sr*-CALUM), *Sr*-chitin-binding protein (*Sr*-CBP) and *Sr*-trypsin inhibitor-like protein (*Sr*-TIL), respectively. These genes were downregulated in the iL3 when compared to the transcriptional level in the FF. At the transcript level, for phosphoribosyltransferase (*Sr*-PhRT), which was previously identified as ESP PF-specific, no differential abundance could be measured, indicating that the secretion of this protein may be post-transcriptionally regulated either at the translational or post-translational levels. The transcript levels for *Sr*-PhRT, although found as protein only in PF, showed such little variation that it can serve as a control, in addition to *Sr*-GAPDH.

(iii) *Sr*-MIF (SS01459) was one of the proteins detected in the ESPs of the PF and iL3 but not in the FF. The transcription level of *Sr*-MIF was elevated > 2-fold in the iL3 stage (Fig. 6) when compared to expression levels in the FF.

(iv) MFP2B (SR00863; *Ascaris suum* putative homologue or P40 putative protein of *B. malayi*), *Sr*-Y51F10.7 (SR02091; *C. elegans* putative uncharacterized protein) a *Sr*-lysozyme family protein (SR00671; homologue of Lys-5 from *C. elegans*) represented the free-living stage ESP. The transcripts were, observed to be highly downregulated in both iL3 and PF compared to levels in the FF.

(v) *Sr*-galectin-1 (SS00840), *Sr*-galectin-2 (SR00627), *Sr*-galectin-3 (SR00900), *Sr*-galectin-5 (SR00857), *Sr*-HSP10 (SS01752) and *Sr*-HSP60 (SR00728), which were detected in the ESP of all stages (iL3, PF and FLS), showed a weak to moderate differential transcription between the stages. The expression levels of *Sr*-GAL-3, *Sr*-HSP10 and *Sr*-HSP60 were ~ 2-fold higher in the PF than those in the FF (Fig. 6). Interestingly, *Sr*-HSP10 and *Sr*-HSP60 were 2-fold upregulated in the PF. Because

they showed different Cts (Table 2), this means that they are independently transcribed.

Additionally, the expression levels of *Sr*-GAL-1 and *Sr*-GAL-5 showed a slight upregulation in the FF. Finally, *Sr*-GAL-2 was 2.1-fold upregulated in the iL3 and showed the same level in PF when compared to FF (Fig. 6).

5.2. Identification and characterization of of selected *S. ratti* candidates upregulated in PF or iL3

5.2.1. Identification of full-length cDNAs

5.2.1.1. PF-related *Sr*-HSP17s

Peptides (characterized by the EST cluster numbers SR00984 (Contig 767, EST=17) and SR03349 (Contig 820, EST=17)) related to sHSPs were abundantly found only in the PF ESP. The two sequences were homologues of HSP-17 from *C. elegans* (E-value 2e-20). In addition, a less abundant cluster SR01014 (Contig834, EST=65) with 98% identity to SR03349 was also identified (Fig. 7A).

The partial sequences of the genes represented by the two clusters SR00984 and SR03349 were used to obtain the full-length clone of the *S. ratti* sHSPs. The gene products were denoted *Sr*-HSP17a and *Sr*-HSP17b, respectively, according to their nearest *C. elegans* homologues *Ce*-HSP17a (450 bp) and *Ce*-HSP17b (447 bp). Whereas the *Ce*-HSP17s are nearly identical isoforms with only one amino acid difference (Fig. 7B), the *Sr*-HSP17s are likely two different homologous genes with only 64% identity (Fig. 7C). The full length cDNAs of *Sr*-HSP17a and *Sr*-HSP17b were amplified and resulted in 483 bp and 474 bp, respectively. The translated protein products have no signal peptides for secretion.

7A

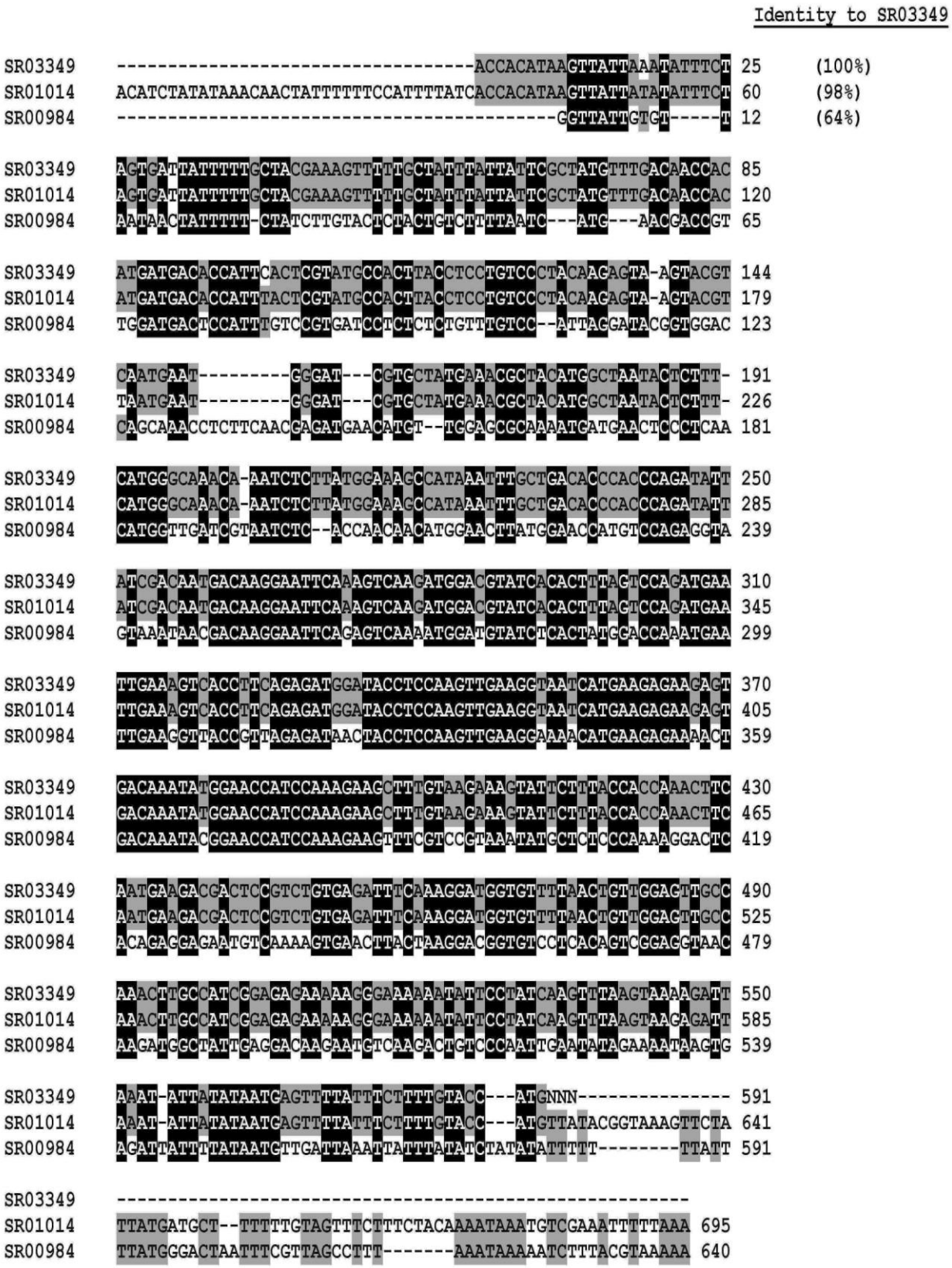
Identity to SR03349
SR03349 ----------ACCACATAAGTTATTAAATATTTCT 25 (100%)
SR01014 ACATCTATATAAACAACTATTTTTTCCATTTTATCACCACATAAGTTATTATATATTTCT 60 (98%)
SR00984 ----------GTTATTGTGT-----T 12 (64%)
SR03349 AGTGATTATTTTTGCTACGAAAGTTTTTGCTATTTATTATTCGCTATGTTTGACAACCAC 85
SR01014 AGTGATTATTTTTGCTACGAAAGTTTTTGCTATTTATTATTCGCTATGTTTGACAACCAC 120
SR00984 AATAACTATTTTT-CTATCTTGTACTCTACTGTCTTTTAATC---ATG---AACGACCGT 65
SR03349 ATGATGACACCATTCACTCGTATCCCACTTACCTCCTGTCCCTACAAGAGTA-AGTACGT 144
SR01014 ATGATGACACCATTTACTCGTATCCCACTTACCTCCTGTCCCTACAAGAGTA-AGTACGT 179
SR00984 TGGATGACTCCATTTGTCCGTGATCCTCTCTCTGTTTGTCC--ATTAGGATACGGTGGAC 123
SR03349 CAATCAAT---------GGGAT---CGTGCTATGAAACGCTACATGCGCTAATACTCTTT- 191
SR01014 TAATCAAT---------GGGAT---CGTGCTATGAAACGCTACATGCGCTAATACTCTTT- 226
SR00984 CAGCAAACCTCTTCAACCAGATGAACATGT--TGGAGCGCAAAATCATGAACTCCCTCAA 181
SR03349 CATGGGCAAACA-AATCTCTTATGCAAAGCCATAAATTTGCTGACACCCACCCAGATATT 250
SR01014 CATGGCGCAAACA-AATCTCTTATGCAAAGCCATAAATTTGCTGACACCCACCCAGATATT 285
SR00984 CATGGTTGATCGTAATCTC--ACCAACAACATGGAACTTATGGAACCATGTCCAGAGGTA 239
SR03349 ATCGACAATGACAAGGAATTCAAAGTCAAGATGGACGTATCACACTTTAGTCCAGATGAA 310
SR01014 ATCGACAATGACAAGGAATTCAAAGTCAAGATGGACGTATCACACTTTAGTCCAGATGAA 345
SR00984 GTAAATAACGACAAGGAATTCAGAGTCAAAATGGATGTATCTCACTATGGACCAAATGAA 299
SR03349 TTGAAAGTCACCTTCAGAGATGGATACCTCCAAGTTGAAGGTAATCATGAAGAGAAGAGT 370
SR01014 TTGAAAGTCACCTTCAGAGATGGATACCTCCAAGTTGAAGGTAATCATGAAGAGAAGAGT 405
SR00984 TTGAACGTTACCGTTAGAGATAACTACCTCCAAGTTGAAGGAAAACATGAAGAGAAAACT 359
SR03349 GACAAATATGGAACCATCCAAAGAACCTTTGTAAGAAAGTATTCTTTACCACCAAACTTC 430
SR01014 GACAAATATGGAACCATCCAAAGAAGCTTTGTAAGAAAGTATTCTTTACCACCAAACTTC 465
SR00984 GACAAATACGGAACCATCCAAAGAAGTTTCGTCCGTAAATATGCTCTCCCAAAAGGACTC 419
SR03349 AATGAAGACGACTCCGTCTGTGAGATTTCAAAGGATGGTGTTTTAACTGTTGGAGTTGCC 490
SR01014 AATGAAGACGACTCCGTCTGTGAGATTTCAAAGGATGGTGTTTTAACTGTTGGAGTTGCC 525
SR00984 ACAGACGAGAATGTCAAAAGTGAACTTACTAAGGACGGTGTCCTCACAGTCGGAGGTAAC 479
SR03349 AAACTTGCCATCGGAGAGAAAAACGGAAAAAATATTCCTATCAACTTTAAGTAAAAGATT 550
SR01014 AAACTTGCCATCGGAGAGAAAAACGGAAAAAATATTCCTATCAACTTTAAGTAAGAGATT 585
SR00984 AAGATGGCTATTGAGGACAAGAATGTCAAGACTGTCCCAATTGAATATAGAAAATAAGTG 539
SR03349 AAAT-ATTATATAATGAGTTTTATTTCTTTTGTACC---ATGNNN--------------- 591
SR01014 AAAT-ATTATATAATGAGTTTTATTTCTTTTGTACC---ATGTTATACGGTAAAGTTCTA 641
SR00984 AGATTATTTTATAATGTTGATTAAATTATTTATATCTATATATTTTT--------TTATT 591
SR03349 ----------
SR01014 TTATGATGCT--TTTTTGTAGTTTCTTTCTACAAAATAAATGTCGAAATTTTTAAA 695
SR00984 TTATGGGACTAATTTCGTTAGCCTTT-------AAATAAAAATCTTTACGTAAAAA 640

7B

```
Ce-HSP17a       ATGGATCGTCGTTTTCCACCATTCTCCCCATTCTTTAACCATGGCCGCAGATTCTTCGAT 60
Ce-HSP17b       ATGGATCGTCGTTTTCCACCATTCTCCCCATTCTTTAACCATGGCC---GATTCTTCGAT 57
                ********************************************   ***********

Ce-HSP17a       GACGTCGACTTTGATCGCCACATGATCCGACCATACTGGGCCGATCAAACAATGCTCACT 120
Ce-HSP17b       GACGTCGACTTTGATCGCCACATGATCCGACCATACTGGGCCGATCAAACAATGCTCACT 117
                ************************************************************

Ce-HSP17a       GGACACCGAGTAGGAGATGCTATTGATGTTGTGAACAACGATCAAGAATACAATGTATCT 180
Ce-HSP17b       GGACACCGAGTAGGAGATGCTATTGATGTTGTGAACAACGATCAAGAATACAATGTATCT 177
                ************************************************************

Ce-HSP17a       GTAGATGTTTCACAGTTTGAACCAGAAGAGTTGAAAGTGAACATTGTTGATAATCAGCTA 240
Ce-HSP17b       GTAGATGTTTCACAGTTTGAACCAGAAGAGTTGAAAGTGAACATTGTTGATAATCAGCTA 237
                ************************************************************

Ce-HSP17a       ATCATCGAAGGAAAGCATAACGAGAAGACTGATAAATATGGACAGGTAGAGCGTCACTTT 300
Ce-HSP17b       ATCATCGAAGGAAAGCATAACGAGAAGACTGATAAATATGGACAGGTAGAGCGTCACTTT 297
                ************************************************************

Ce-HSP17a       GTCCGGAAGTATAACCTTCCAACAGGGGTCCGTCCAGAACAAATCAAGTCCGAATTGAGC 360
Ce-HSP17b       GTCCGGAAGTATAACCTTCCAACAGGGGTCCGTCCAGAACAAATCAAGTCCGAATTGAGC 357
                ************************************************************

Ce-HSP17a       AACAATGGAGTGCTCACTGTCAAATATGAGAAGAATCAGGAACAGCAGCCAAAATCCATT 420
Ce-HSP17b       AACAATGGAGTGCTCACTGTCAAATATGAGAAGAATCAGGAACAGCAGCCAAAATCCATT 417
                ************************************************************

Ce-HSP17a       CCAATCACAATTGTGCCAAAGAGAAACTGA 450
Ce-HSP17b       CCAATCACAATTGTGCCAAAGAGAAACTGA 447
                ******************************
```

7C

```
Sr-HSP17a       ATG---AACGACCGTTGGATGACTCCATTTGTCCGTGATCCTCTCTCTGTTTGTCC--AT 55
Sr-HSP17b       ATGTTTGACAACCACATGATGACACCATTCACTCGTATGCCACTTACCTCCTGTCCCTAC 60
                ***    ** ***    ****** *****    ***   ** **  *    *****  *

Sr-HSP17a       TAGGATACGGTGGACCAGCAAACCTCTTCAACGAGATGAACATGTT--GGAGCGTAAAAT 113
Sr-HSP17b       AAGAGTA-AGTACGTCAATGAAT---------GGGAT---CGTGCTATGAAACGCTACAT 107
                 **  **  **    **   **          * ***   * ** *  * * **  * **

Sr-HSP17a       GATGAACTCCCTCAACATGGTTGATCGTAATCTC--ACCAACAACATGGAACTTATGGAA 171
Sr-HSP17b       GGCTAATACTCTTT-CATGGGCAAACA-AATCTCTTATGGAAAGCCATAAATTTGCTGAC 165
                *   **  * **   *****   * *  ******  *   * * *    ** **   **

Sr-HSP17a       CCATGTCCAGAGGTAGTAAATAACGACAAGGAATTCAGAGTCAAAATGGATGTATCTCAC 231
Sr-HSP17b       ACCCACCCAGATATTATCGACAATGACAAGGAATTCAAAGTCAAGATGGACGTATCACAC 225
                 *    *****  *  *  * ** ************* ****** ***** ***** ***

Sr-HSP17a       TATGGACCAAATGAATTGAAGGTTACCGTTAGAGATAACTACCTCCAAGTTGAAGGAAAA 291
Sr-HSP17b       TTTAGTCCAGATGAATTGAAAGTCACCTTCAGAGATGGATACCTCCAAGTTGAAGGTAAT 285
                * * * *** ********** ** *** * ******   ***************** **

Sr-HSP17a       CATGAAGAGAAAACTGACAAATACGGAACCATCCAAAGAAGTTTCGTCCGTAAATATGCT 351
Sr-HSP17b       CATGAAGAGAAGAGTGACAAATATGGAACCATCCAAAGAAGCTTTGTAAGAAAGTATTCT 345
                *********** * ********* ***************** ** **  * ** *** **

Sr-HSP17a       CTCCCAAAAGGACTCACAGAGGAGAATGTCAAAAGTGAACTTACTAAGGACGGTGTCCTC 411
Sr-HSP17b       TTACCACCAAACTTCAATGAAGACGACTCCGTCTGTGAGATTTCAAAGGATGGTGTTTTA 405
                 * ***  *    ***  ** **  *   *    ****  ** * ***** *****  *

Sr-HSP17a       ACAGTCGGAGGTAACAAGATGGCTATTGAGGACAAGAATGTCAAGACTGTCCCAATTGAA 471
Sr-HSP17b       ACTGTTGGAGTTGCCAAACTTGCCATCGGAGAGAAAAAGGGAAAAAATATTCCTATCAAG 465
                ** ** **** *  ***  * ** ** * **  ** ** ** *  ** * * * ** **  *

Sr-HSP17a       TATAGAAAATAA 483
Sr-HSP17b       TTTA---AGTAA 474
                * **   * ***
```

Identity (64%)

Fig. 7. Sequence identification of *Sr*-HSP17s. (A) Alignment of the two HSP17 clusters identified by ProteinPilot search engine v2.0.1 from the ESP of the PF (SR00349 and SR00984) and a third alternative cluster SR01014. Identical residues are shaded in black blocks, conserved residues in two clusters are shaded in grey. (B) Alignment of *Ce*-HSP17a (acc. No Q20660) and *Ce*-HSP17b (acc. No Q7JP52) isoforms (differ nucleotides bounder in red). (C) Alignment of the identified full length cDNAs of *Sr*-HSP17a and *Sr*-HSP17b. Identical residues are underlined with asterisks.

5.2.1.2. *Sr*-MIF

Peptides (characterized by the EST from *Strongyloides stercoralis* cluster number SS01459 (Contig1459, EST=11)) related to MIF were abundantly found in the iL3 and PF ESP but not FF. The partial sequence of the gene represented by the cluster SS01459 was used to obtain the full-length of the *S. ratti* MIF. The full length of *Sr*-MIF cDNA was amplified and resulted in 372 bp (Fig. 9).

5.2.2. Sequence and phylogenetic analyses

5.2.2.1. *Sr*-HSP17s

Both *Sr*-HSPs have an HSP20/alpha-crystallin domain (ACD). Structurally, the sHSP family members share a sequence of about 80-100 residues in the C-terminal region that is homologous to ACD from the vertebrate eye lens (Kim *et al*., 1998). The protein sequences of both *Sr*-HSP17s were aligned with the human alphaB-crystallin (ABC; Fig. 8A). The homology between the *Sr*-HSP17s was 49%, but increased in their ACDs to 67% (Fig. 8A). The ACDs are covered by residues 61 – 143 and 59 – 141 in *Sr*-HSP17a and *Sr*-HSP17b, respectively. The comparison of the deduced complete amino acid sequences of *Sr*-HSP17a (160 aa, ~18 kDa) and *Sr*-HSP17b (157 aa, ~ 19 kDa) with other nematode members of the sHSP protein family (Fig. 8B) showed 39 highly conserved residues, with 19 invariant residues located in the central part (ACD) and the C-terminal regions of the 14 aligned nematode sHSPs.

8A

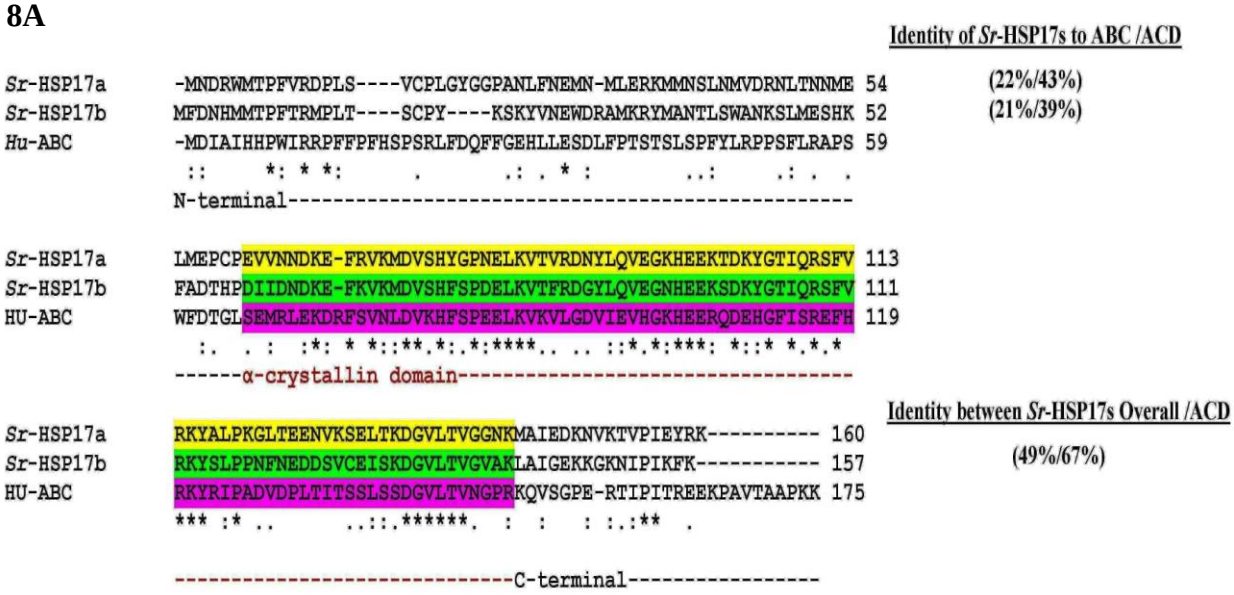

8B

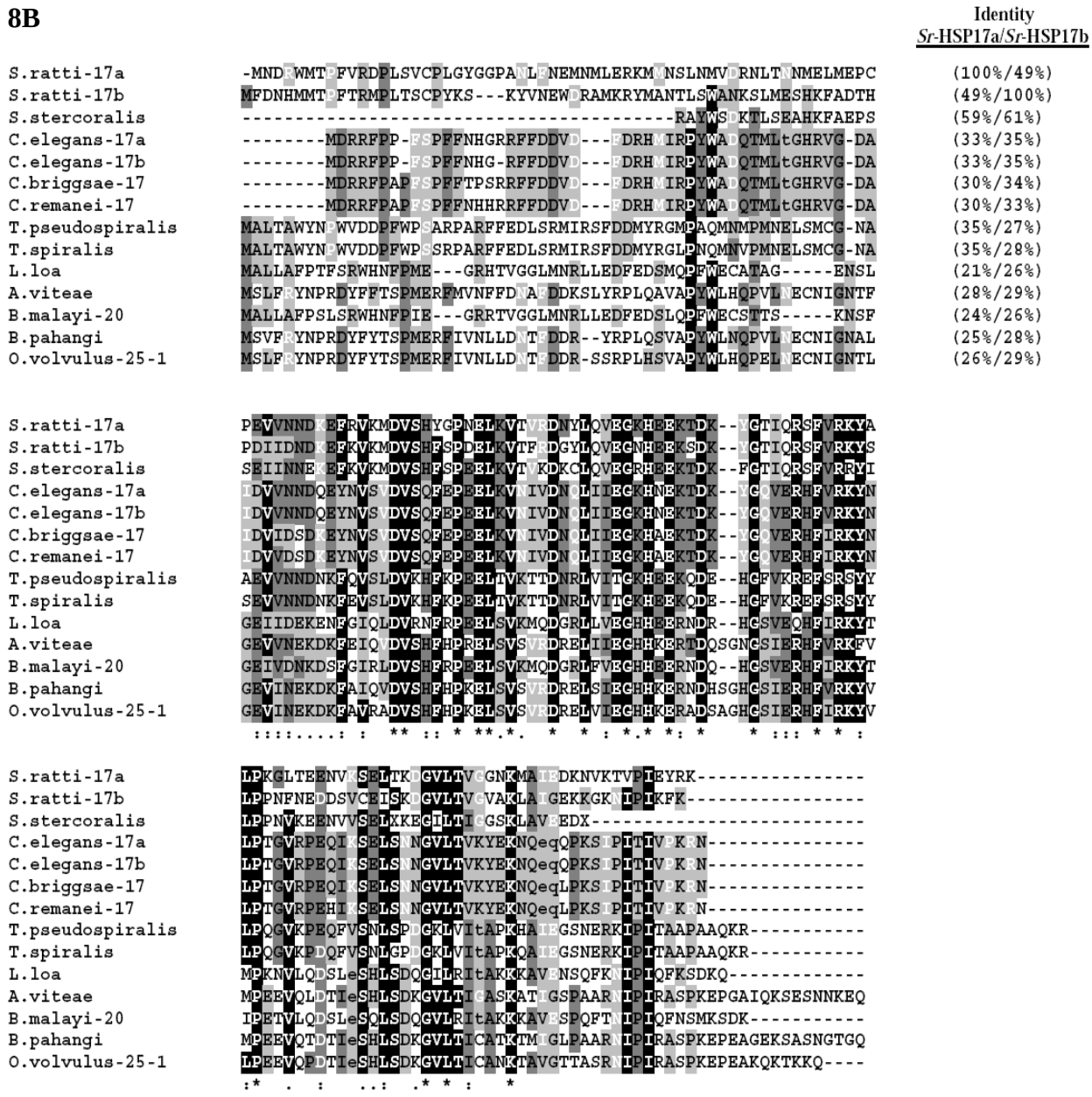

Clear variation was observed in the N-terminal region of the proteins. The aligned amino acid sequences of all free-living species of the genus *Caenorhabditis* are highly homologous (≥ 93%) and differ from the parasitic nematodes. Both *Sr*-HSP17s were different from the other nematodes sHSPs, especially in their N-terminal regions, with low overall sequence identities ranging between 21% and 35%. In contrast, the deduced sequence of *S. stercoralis* sHSP (accession no. N21794; *Ss*-HSP17) showed 59 and 61% identity to *Sr*-HSP17a and *Sr*-HSP17b, respectively, which was even higher than the homology between both *Sr*-HSP17s (49%).

Phylogenetic analysis for both DNA and protein sequences produced similar results, of which the latter is displayed in Fig. 8C. Identities and phylogenetic distances of the selected sHSPs showed that the *Sr*-HSP17s are very closely related to that of the human pathogen *S. stercoralis*. Similar trunks in the phylogenetic tree are built by the HSP17s of the four *Caenorhabditis* species, of the five filariae species and of the two *Trichinella* species.

8C

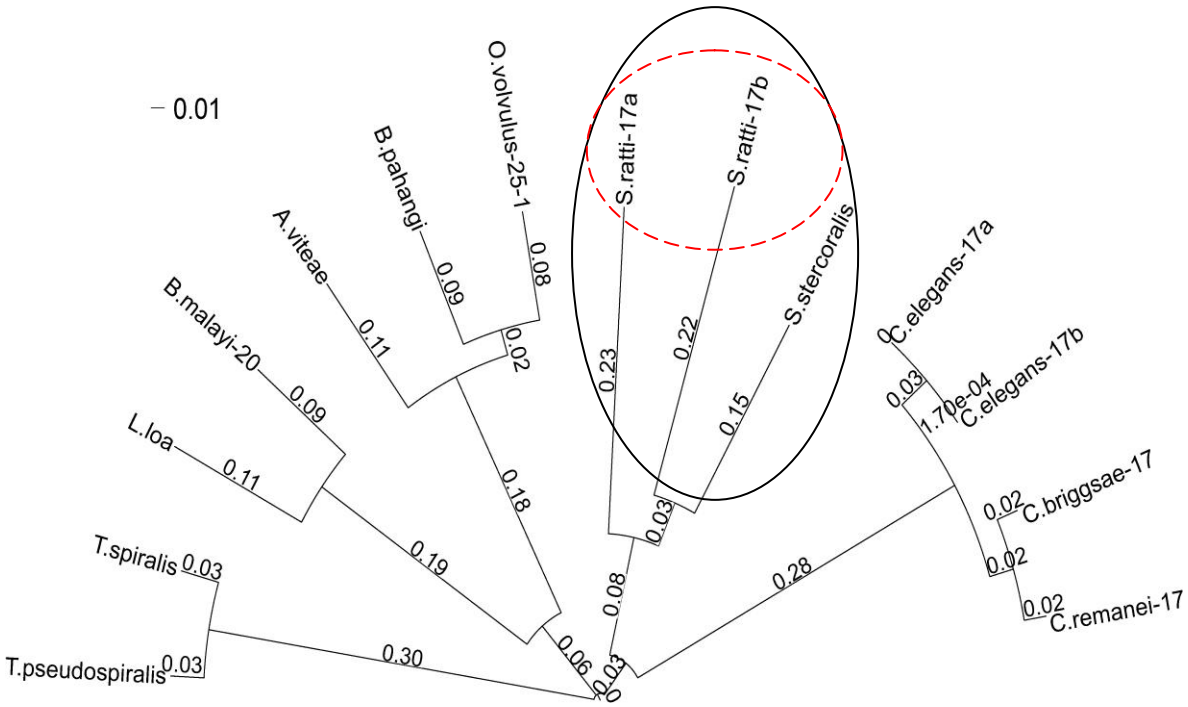

Fig. 8. Sequence and phylogenetic analysis of Sr-HSP17s. (A) Alignment of amino acid sequences of *Sr*-HSP17a and *Sr*-HSP17b with human alphaB-crystallin (ABC). The percentages of identities were relative to the complete aa sequences overall and their alpha-crystallin domains (ACD), highlighted in yellow, green and pink, respectively. Sympols: identical (asterisks), no amino acid residue (dashes), conservation of residue size and hydropathy (colons), conservation of size or hydropathy (periods). (B) Alignment of the *Sr*-HSP17a and *Sr*-HSP17b aa sequences with other 12 related nematodes sHSPs based on CLUSTAL W, neighbor-joining. Highly conserved residues (>10) are shaded in black blocks, median conserved residues (7-9) in dark grey, low conserved residues (4-6) in light grey. (C) Phylogenetic tree of the aligned 14 sHSPs orthologs from nematodes including two HSP17-related proteins identified in *S. ratti* based on CLUSTAL W, neighbor-joining. The compared proteins are: *S. stercoralis* translated mRNA sequence accession no. *N21794*, *C. elegans* HSP17 isoform a accession no. Q20660, *C. elegans* HSP17 isoform b accession no. Q7JP52, *C. briggsae* HSP17 accession no. A8XDE7, *C. remanei* HSP17 accession no. XP_003110614.1, *L. loa* sHSP accession no. E1GRM5, *A. viteae Av*-25 accession no. Q17102, *B. malayi* HSP20 accession no. A8P0X0, *B. pahangi* sHSP accession no. CAA61152.1, *T. pseudospiralis* sHSP accession no. Q000T2, *T. spiralis* sHSP accession no. Q000T3 and *O. volvulus Ov*-25-1 accession no P29778).

5.2.2.2. *Sr*-MIF

Pfam pattern and profile searches predicted one hit of MIF domain features. The translated sequence of *Sr*-MIF has no signal peptide. The alignment of the amino acid sequences revealed (i) high degree of identity (94%) between both *Strongyloides* MIFs, *Sr*-MIF and *Ss*-MIF, (ii) a similar high degree of identidy (90 %) between the proteins of both hosts, rat and human MIFs, while (iii) pronounced differences exist between the MIF sequences of the parasites and the hosts (25% - 28%) (Fig. 9A). *Strongyloides* MIFs lack the Cys57-Xaa-Xaa-Cys60 motif, which has been reported to mediate catalytic oxidoreductase activity (Kleemann *et al*., 1998), and share only two residues, Pro2 and Lys33 with the mammalian MIFs, out of the five (Pro2, Lys33, Il65, Tyr95 and Asn95) that constitute the MIF active site of tautomerase activity (Lubetsky *et al*., 1999).

The comparison of the complete amino acid sequence of *Sr*-MIF (123 aa, ~13.5 kDa) with other members of the MIF proteins from other nematodes (Fig. 9B), showed 65 conserved residues with 6 invariants. The aligned amino acid sequences of MIF-2 in all free-living species of the genus *Caenorhabditis* are highly homologous, showing ≥ 91% identity and ≥ 68% in case of MIF-1. *Sr*-MIF differed from the other nematode MIFs (except that of *Ss*-MIF; 94% identity), with low overall sequence identities (13%-30%). Phylogenetic analysis using Phylogeny.fr program (Dereeper *et al*., 2008) for protein sequence is displayed in Fig. 9C. Identities and phylogenetic distances of the aligned MIFs showed that the *Sr*-MIF is very closely related to that of the human pathogen *S. stercoralis*, and both are related to MIF type-2.

9A

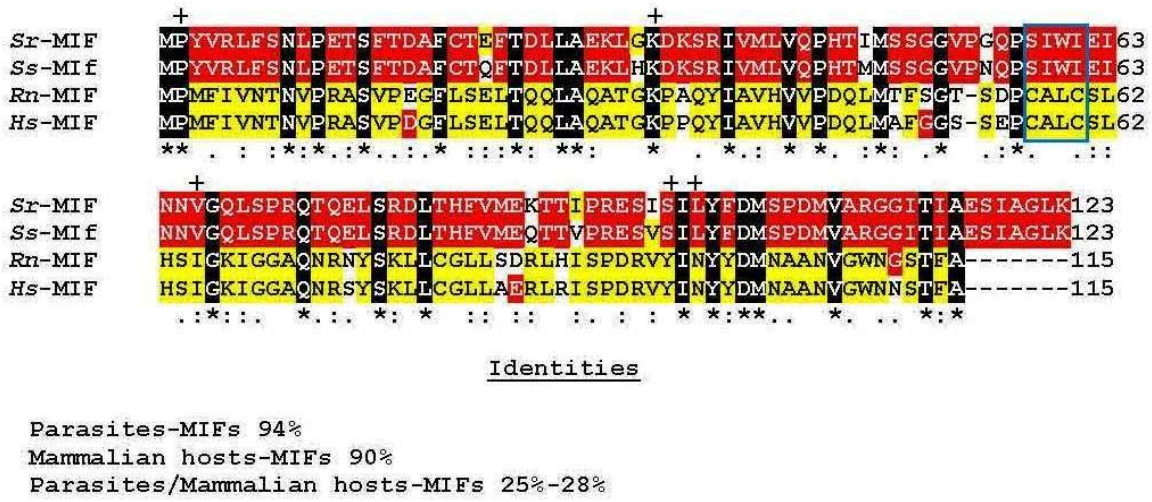

9B

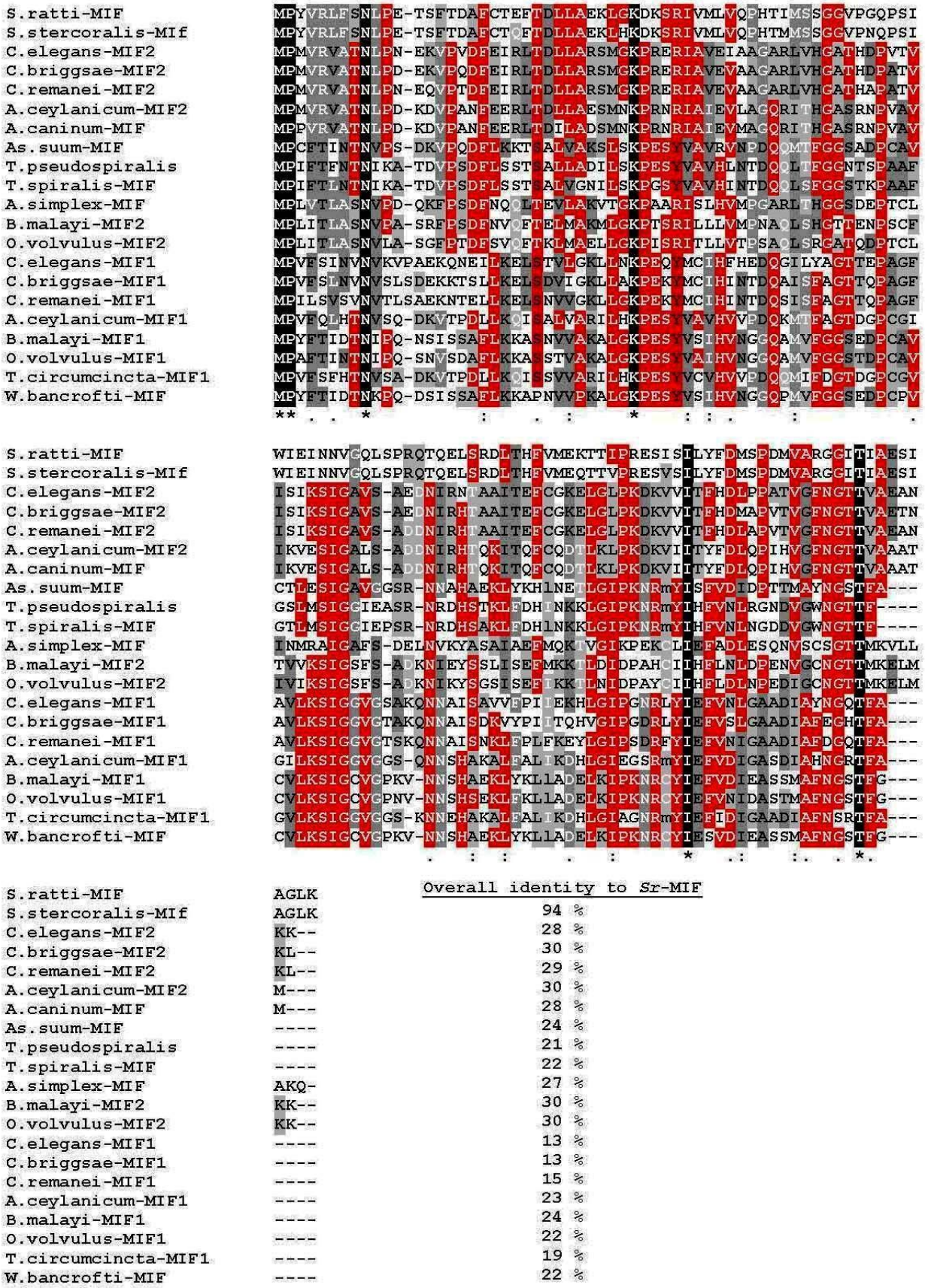
S.ratti-MIF
S.stercoralis-MIf
C.elegans-MIF2
C.briggsae-MIF2
C.remanei-MIF2
A.ceylanicum-MIF2
A.caninum-MIF
As.suum-MIF
T.pseudospiralis
T.spiralis-MIF
A.simplex-MIF
B.malayi-MIF2
O.volvulus-MIF2
C.elegans-MIF1
C.briggsae-MIF1
C.remanei-MIF1
A.ceylanicum-MIF1
B.malayi-MIF1
O.volvulus-MIF1
T.circumcincta-MIF1
W.bancrofti-MIF
Overall identity to Sr-MIF
94 %
28 %
30 %
29 %
30 %
28 %
24 %
21 %
22 %
27 %
30 %
30 %
13 %
13 %
15 %
23 %
24 %
22 %
19 %
22 %

9C

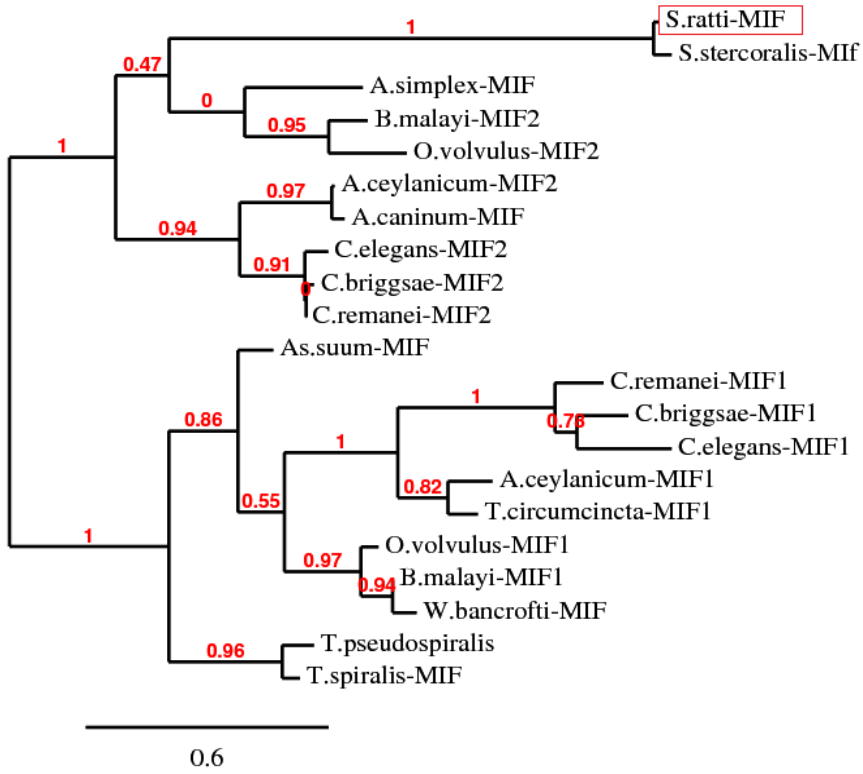

Fig. 9. *Sr*-MIF gene, sequence and phylogenetic analysis. (A) Alignment of amino acid sequences of *Strongyloides ratti* MIF (*Sr*-MIF) and *S. stercoralis* MIF (*Ss*-MIF; EST acc. no. BG224821) with homologues from their hosts: *Homo sapiens* (*Hs*-MIF; acc. no. P14174) and *Rattus norvegicus* (*Rn*-MIF acc. no P30904). Sympols: identical (asterisks), no amino acid residue (dashes), conservation of residue size and hydropathy (colons), conservation of size or hydropathy (periods), residues of the tautomerase catalytic site in the human MIF (+), CXXC TPOR motif (blue/green boundary). (B) Alignment of the *Sr*-MIF aa sequence with other 20 related nematode MIFs based on CLUSTAL W, neighbor-joining. Sympols: identical (asterisks; black blocks), highly conserved residues (≥10) are shaded in red, median conserved residues (7-9) in dark grey, low conserved residues (5-6) in light grey. (C) Phylogenetic tree of the aligned 21 MIF orthologs from nematodes including MIF identified from the *S. ratti* using Phylogeny.fr program. The compared proteins are: *S. stercoralis*, *C. elegans* MIF-1 (acc. no. Q9U228) and MIF-2 (acc. no. Q18785) , *C. briggsae* MIF-1 (acc. no. A8XHI7) and MIF-2 (acc. no. A8Y453), *C. remanei* MIF-1 (acc. no. E3MI52) and MIF2 (acc. no. E3LPW1), *Ancylostoma ceylanicum* MIF1 (acc. no. B6RTC1) and MIF2 (acc. no. A4GRE3), *A. caninum* MIF (acc. no. A7XPN9), *A. simplex* MIF (acc. no. A1Z1S6), *Ascaris suum* MIF (acc. no. Q6I6Y5), *B. malayi* MIF-1 (acc. no. P91850) and MIF-2 (acc. no. Q9NAS2), *Trichinella pseudospiralis* MIF (acc. no. Q95UI7), *T. spiralis* MIF (acc. no. P81529), *Onchocerca volvulus* MIF-1 (acc. no. Q963F7) and MIF-2 (acc. no. Q963F6), *Wuchereria bancrofti* MIF (acc. no. O44786) and *T. circumcincta* MIF (acc. no. D2ECG6).

5.2.3. Genomic organization

5.2.3.1. *Sr*-HSP17s

The PCR products (Fig. 10A) from gDNA were larger than the PF cDNA products, indicating the presence of at least one short intron in each gene. When cloned, sequenced and aligned, these PCR products confirmed the presence of a single intron (Figs. 10B and 10C) in each sHSP located in the second third of the ACDs ORFs with lengths of 63 bp at 321 bases and 49 bp at 315 bases in *Sr*-HSP17a and *Sr*-HSP17b, respectively (Fig. 10D).

Both introns are phase 0 (between two codons); their splice site sequences followed the GU-AG convention and were found to have similar distributions but differed in position, length and in sequence. In addition, the genomic organization of the *Sr*-HSP17 genes did not reflect the pseudosymmetrical domain structure of the protein. In our study, we did not identify the gene-link between the two genes of *Sr*-HSP17a and *Sr*-HSP17b using different primers pairs and different PCR conditions, indicating that they are not in tandem or close connection.

10A

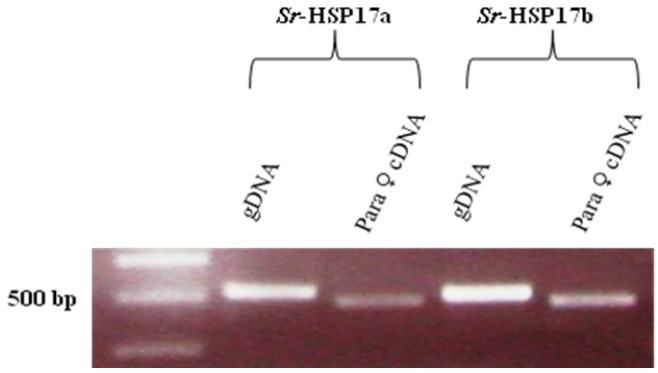

10B

```
gSrHSP17a       ATGAACGACCGTTGGATGACTCCATTTGTCCGTGATCCTCTCTCTGTTTGTCCATTAGGA 60
cSrHSP17a       ATGAACGACCGTTGGATGACTCCATTTGTCCGTGATCCTCTCTCTGTTTGTCCATTAGGA 60
                ************************************************************

gSrHSP17a       TACGGTGGACCAGCAAACCTCTTCAACGAGATGAACATGTTGGAGCGTAAAATGATGAAC 120
cSrHSP17a       TACGGTGGACCAGCAAACCTCTTCAACGAGATGAACATGTTGGAGCGTAAAATGATGAAC 120
                ************************************************************

gSrHSP17a       TCCCTCAACATGGTTGATCGTAATCTCACCAACAACATGGAACTTATGGAACCATGTCCA 180
cSrHSP17a       TCCCTCAACATGGTTGATCGTAATCTCACCAACAACATGGAACTTATGGAACCATGTCCA 180
                ************************************************************

gSrHSP17a       GAGGTAGTAAATAACGACAAGGAATTCAGAGTCAAAATGGATGTATCTCACTATGGACCA 240
cSrHSP17a       GAGGTAGTAAATAACGACAAGGAATTCAGAGTCAAAATGGATGTATCTCACTATGGACCA 240
                ************************************************************

gSrHSP17a       AATGAATTGAAGGTTACCGTTAGAGATAACTACCTCCAAGTTGAAGGAAAACATGAAGAG 300
cSrHSP17a       AATGAATTGAAGGTTACCGTTAGAGATAACTACCTCCAAGTTGAAGGAAAACATGAAGAG 300
                ************************************************************

gSrHSP17a       AAAACTGACAAATACGGAACCGTAAGTTTACTTTATACCTCTAAGTATTTAACTGTGGTA 360
cSrHSP17a       AAAACTGACAAATACGGAACC------------------------------------- 321
                **********************

gSrHSP17a       AAATCTATTCCTTTTAATTTTTAGATCCAAAGAAGTTTCGTCCGTAAATATGCTCTCCCA 420
cSrHSP17a       ----------------------ATCCAAAGAAGTTTCGTCCGTAAATATGCTCTCCCA 357
                                      ************************************

gSrHSP17a       AAAGGACTCACAGAGGAGAATGTCAAAAGTGAACTTACTAAGGACGGTGTCCTCACAGTC 480
cSrHSP17a       AAAGGACTCACAGAGGAGAATGTCAAAAGTGAACTTACTAAGGACGGTGTCCTCACAGTC 417
                ************************************************************

gSrHSP17a       GGAGGTAACAAGATGGCTATTGAGGACAAGAATGTCAAGACTGTCCCAATTGAATATAGA 540
cSrHSP17a       GGAGGTAACAAGATGGCTATTGAGGACAAGAATGTCAAGACTGTCCCAATTGAATATAGA 477
                ************************************************************

gSrHSP17a       AAATAA 546
cSrHSP17a       AAATAA 483
                ******
```

10C

```
gSrHSP17b       ATGTTTGACAACCACATGATGACACCATTCACTCGTATGCCACTTACCTCCTGTCCCTAC 60
cSrHSP17b       ATGTTTGACAACCACATGATGACACCATTCACTCGTATGCCACTTACCTCCTGTCCCTAC 60
                ************************************************************

gSrHSP17b       AAGAGTAAGTACGTCAATGAATGGGATCGTGCTATGAAACGCTACATGGCTAATACTCTT 120
cSrHSP17b       AAGAGTAAGTACGTCAATGAATGGGATCGTGCTATGAAACGCTACATGGCTAATACTCTT 120
                ************************************************************

gSrHSP17b       TCATGGGCAAACAAATCTCTTATGGAAAGCCATAAATTTGCTGACACCCACCCAGATATT 180
cSrHSP17b       TCATGGGCAAACAAATCTCTTATGGAAAGCCATAAATTTGCTGACACCCACCCAGATATT 180
                ************************************************************

gSrHSP17b       ATCGACAATGACAAGGAATTCAAAGTCAAGATGGACGTATCACACTTTAGTCCAGATGAA 240
cSrHSP17b       ATCGACAATGACAAGGAATTCAAAGTCAAGATGGACGTATCACACTTTAGTCCAGATGAA 240
                ************************************************************

gSrHSP17b       TTGAAAGTCACCTTCAGAGATGGATACCTCCAAGTTGAAGGTAATCATGAAGAGAAGAGT 300
cSrHSP17b       TTGAAAGTCACCTTCAGAGATGGATACCTCCAAGTTGAAGGTAATCATGAAGAGAAGAGT 300
                ************************************************************

gSrHSP17b       GACAAATATGGAACCGTAAGTTTTATGCTACTTACTTAGTGTTGTTATCTTATTCGTTTT 360
cSrHSP17b       GACAAATATGGAACC--------------------------------------------- 315
                ***************

gSrHSP17b       TAAGATCCAAAGAAGCTTTGTAAGAAAGTATTCTTTACCACCAAACTTCAATGAAGACGA 420
cSrHSP17b       ----ATCCAAAGAAGCTTTGTAAGAAAGTATTCTTTACCACCAAACTTCAATGAAGACGA 371
                    ********************************************************

gSrHSP17b       CTCCGTCTGTGAGATTTCAAAGGATGGTGTTTTAACTGTTGGAGTTGCCAAACTTGCCAT 480
cSrHSP17b       CTCCGTCTGTGAGATTTCAAAGGATGGTGTTTTAACTGTTGGAGTTGCCAAACTTGCCAT 431
                ************************************************************

gSrHSP17b       CGGAGAGAAAAAGGGAAAAAATATTCCTATCAAGTTTAAGTAA 523
cSrHSP17b       CGGAGAGAAAAAGGGAAAAAATATTCCTATCAAGTTTAAGTAA 474
                *********************************************
```

10D

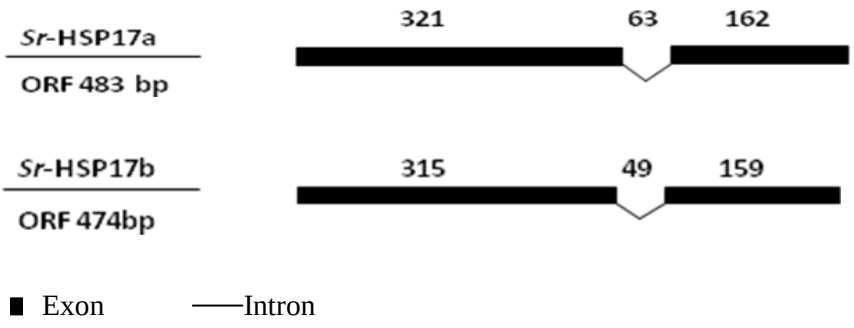

Fig. 10. Genomic organization of *Sr*-HSP17s. (A) The PCR products analysis by ethidium bromide-stained gel of the amplified products using *S. ratti* gDNA or PF cDNA. (B, C) Alignment of the cloned and sequenced PCR products amplified from the PF cDNA and gDNA. Identical (asteriks) and introns (no amino acid residue, dashes); (B) *Sr*-HSP17a, (C) *Sr*-HSP17b. A single intron in each sHSP located in the second third of the ACDs ORFs. Both introns are phase 0, their splice sites sequences followed the GU-AG convention. (C) Illustration of the genomic organization of the *Sr*-HSP17 genes from *S. ratti*. Introns are shown as broken lines and exons are filled boxes. The size of each region (in bases) is indicated above introns and exons.

5.2.3.2. *Sr*-MIF

The PCR products (Fig. 11A) from gDNA and iL3 cDNA were the same size, indicating the absence of introns in the *Sr*-MIF gene structure. When cloned, sequenced and aligned, these PCR products (372 bp) confirmed the absence of introns in the *Sr*-MIF (Fig. 11B), which differs from other eukaryotic MIFs (Fig. 11C and 11D).

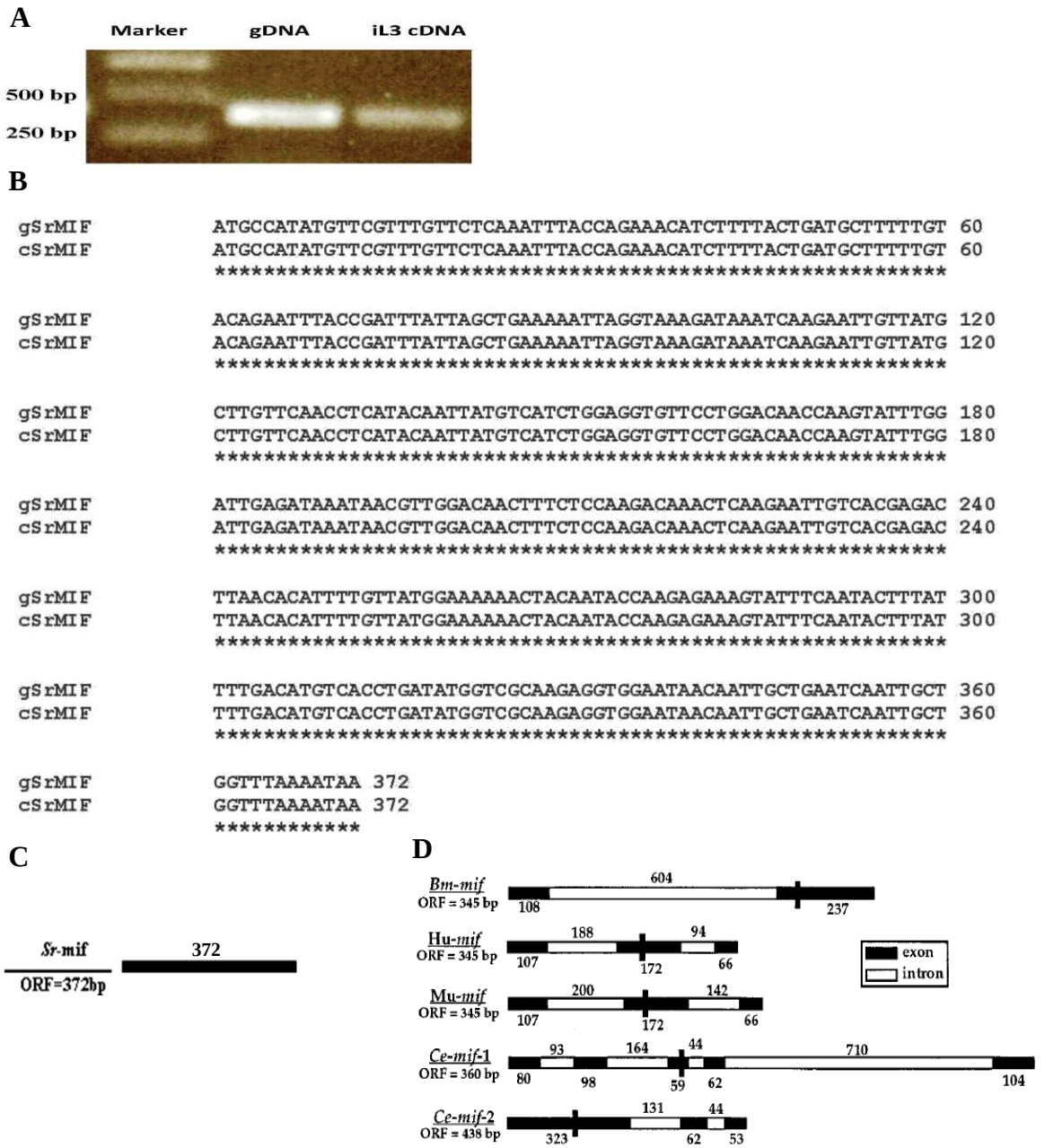

Fig. 11. Genomic organization of *Sr*-MIF. (A) The PCR product analysis by ethidium bromide-stained gel of the amplified products using *S. ratti* gDNA or PF cDNA. (B) Alignment of the cloned and sequenced PCR products amplified from the PF cDNA and gDNA. Symbols: identical (asteriks). (C) Illustration of the genomic organization of the Sr-MIF with (D) a captured illustration of some MIF genes from *B. malayi* (*Bm-MIF*), human (Hu-MIF), mouse (Mu-MIF), and *C. elegans* (*Ce*-mif-1 and *Ce*-mif-2) from (Pastrana et al., 1998).). Introns are shown as open boxes, and exons are filled boxes. The size of each region (in bases) is indicated above introns and beneath exons. Vertical bars indicate the axis of the pseudo-twofold symmetry of the MIF protein (nucleotides 159 to 165 of the ORF).

5.2.4. Expression and purification of recombinant proteins

Sr-HSP17a, *Sr*-HSP17b and *Sr*-MIF were recombinantly expressed in *E. coli* as his-tagged proteins and purified after 8 M urea denaturation by Ni-affinity chromatography. The bacterial lipopolysaccharide (LPS) was removed by washing the Ni-agarose-bound protein with a buffer containing the LPS-binding antibiotic polymyxin B (PMB) and TritonX-114. The remaining LPS concentrations in the different proteins fractions varied between 0.001 - 0.005 EU/µg protein (Table 3), while fractions purified in parallel without the use of TritonX-114 or PMB showed high LPS levels (>1 EU/µg protein). The r*Sr*-HSP17a (~23 kDa), *Sr*-HSP17b (~22 kDa) and *Sr*-MIF (17.5 kDa) containing a his-tail and an enterokinase cleavage site were purified as a single protein band shown in (Fig. 12A,C). Western blot analysis with anti-his tag antibodies (Fig. 12B,D) confirmed the presence of the his-tagged proteins. Since the yield of the *Sr*-HSP17s protein was less than 10% following the removal of the his-tag by enterokinase cleavage (the buffer conditions of the protein and the enzyme were not compatible), only the his-tagged protein was used for functional studies. The his-tag was successfully removed by enterokinase cleavage, producing a high pure yield of the r*Sr*-MIF (Fig. 12C).

Table 3. Buffers used in protein purification procedures and the resulting LPS concentrations. All purification procedures were carried out at RT. Dialysis was carried out at 8 ºC -10 ºC. Buffers were chilled on ice before use. Highly pure water was used for buffer preparation (Aqua B. Braun, Melsungen AG, Germany).

Buffer	Constitution	PH	Uses	Time	LPS con.
B1	8 M urea, 50 mM Tris, 10 mM imidazole, 500 mM NaCl, 10 % glycerol, 0.1 % Triton X-100.	8	Lysis, binding	1 h	Not determined
B2	8 M urea, 50 mM Tris, 10 mM imidazole, 500 mM NaCl, 10 % glycerol, 0.4 % Triton X-114.	8	Washing 1	3x10 min	Not determined
B3	8 M urea, 50 mM Tris, 20 mM imidazole, 500 mM NaCl, 10 % glycerol, 0.1 % Triton X-100, 250 µg/ml PMB .	8	Washing 2	3x10 min	Not determined
B4	8 M urea, 50 mM Tris, 250 mM imidazole, 500 mM NaCl, 10 % glycerol, 0.1 % Triton X-100.	8	Elution	2x2 min	0.008-0.02 EU/µg
B5	2 M urea, 20 mM Tris, 150 mM NaCl, 0.1 % Triton X-100, 30 µg/ml PMB .	7.8	Dialysis 3	12 h	Not determined
B6	PBS, 30 µg/ml PMB or TBS, 30µg/ml PMB	7.8	Dialysis 3	2 h	Not determined

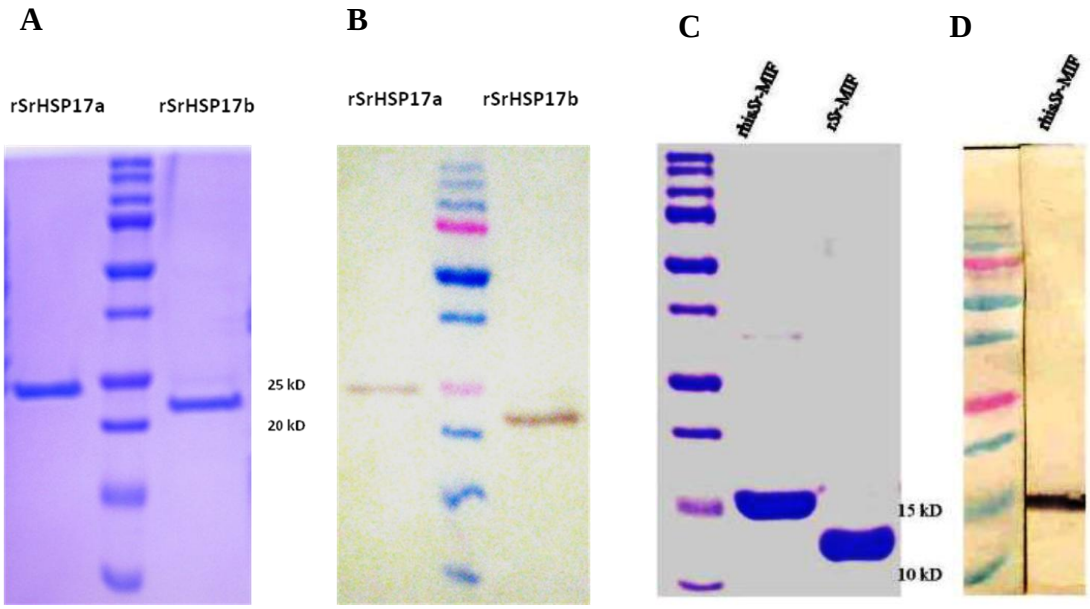

Fig. 12. Expression and purification of recombinant proteins. (A, C) SDS/PAGE and Coomassie staining of r*Sr*-HSP17a, r*Sr*-HSP17b and r*Sr*-MIF, under reducing conditions, purified with nickel affinity chromatography. (B, D) Western blot detection: the recombinant his-tag proteins from identical gels were transferred to nitrocellulose membranes and treated with anti-his POD.

5.2.5. *Sr*-HSP17s lack chaperone-like activity

To determine whether the *Sr*-HSP17s possessed the molecular chaperone activity that has been reported for many sHSPs, we studied the ability of both r*Sr*-HSP17s to alter the thermally-induced aggregation of citrate synthase and malate dehydrogenase substrates, which aggregate irreversibly when incubated at >45°C (Fig. 13A,B). In addition, insulin was used as a non-thermal, DTT-aggregated substrate. Addition of different preparations and different concentrations of the recombinant parasite proteins did not influence the aggregation of the substrates (Fig. 13C).

13 A

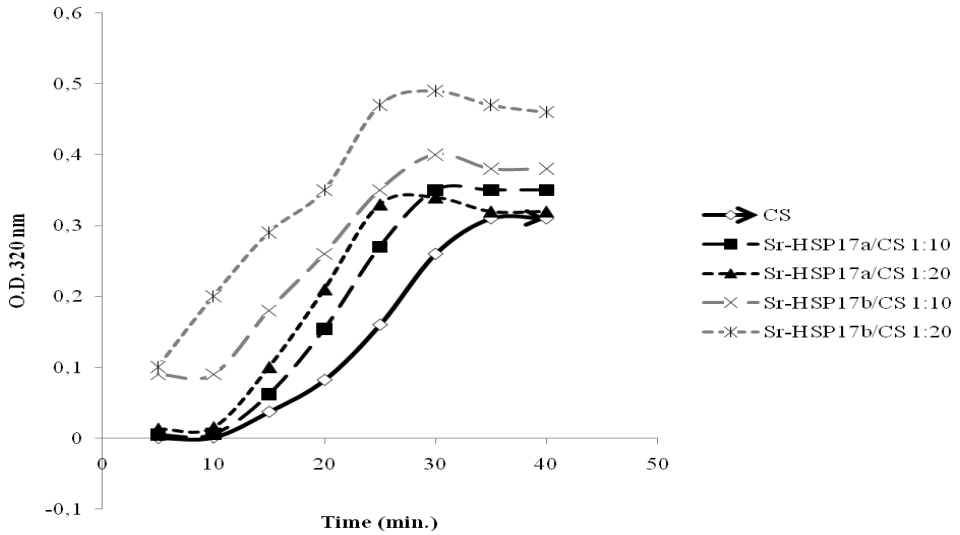

13 B

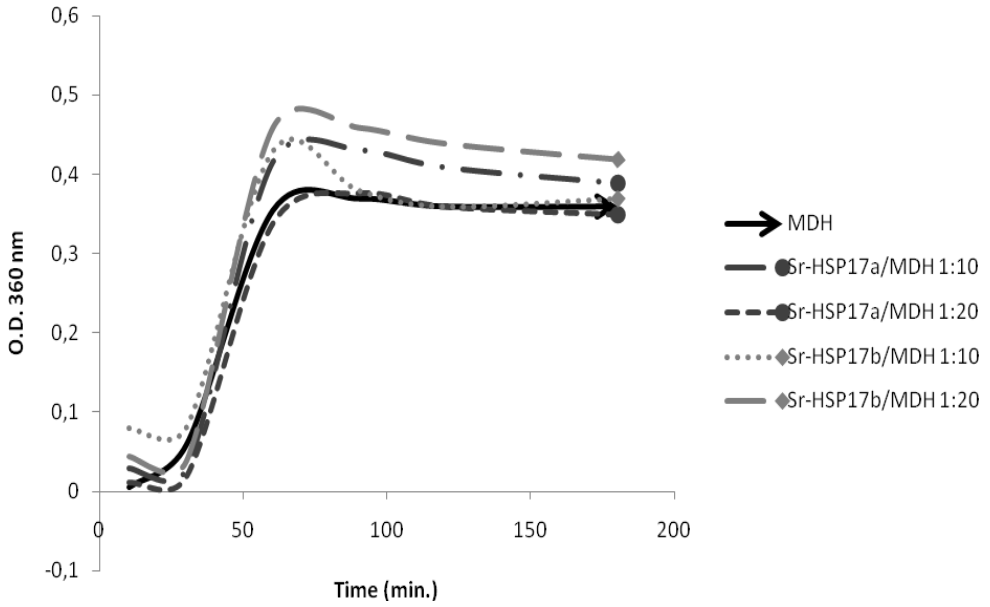

13 C

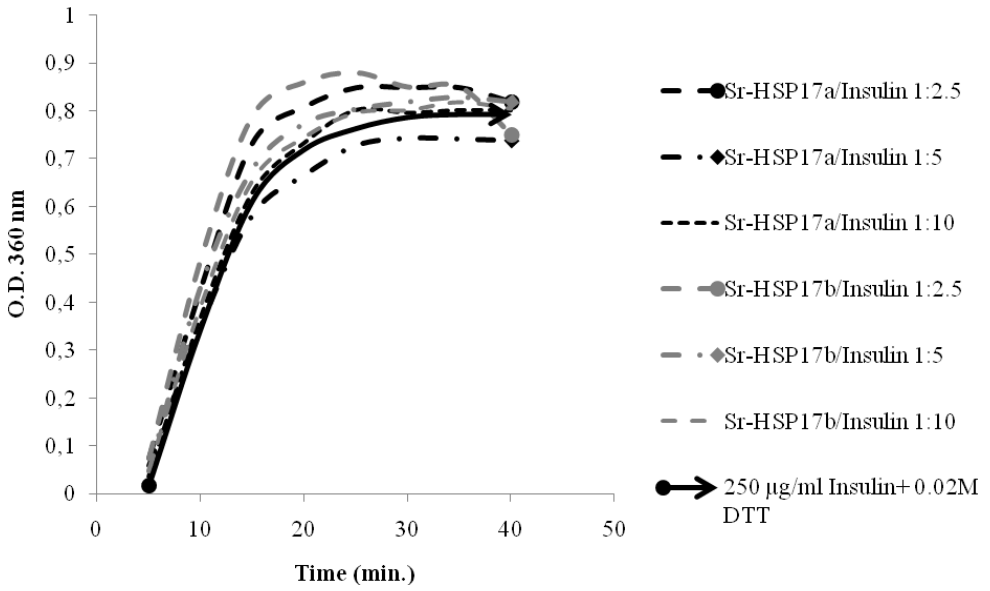

Fig. 13. Recombinant *Sr*-HSP17s lack the molecular chaperone activity *in vitro*. Neither r*Sr*-HSP17a nor r*Sr*-HSP17b were able to reduce the thermally aggregated proteins: (A): citrate synthase (CS) from porcine heart, provided in 2.2 M $(NH_4)_2SO_4$, 6 mM phosphate, 0.5 mM citrate (sigma) used in concentration of 75 µg/ml at 45 °C or (B): malate dehydrogenase (MDH) from porcine heart provided in ammonium sulfate (sigma) used in concentration of 41.5 µg/ml at 48 °C. For both substrates the molar ratios (HSP/substrate) were 1:10 and 1:20. Absorbance was recorded at O.D. 360 nm for insulin and MDH and 320 nm for CS aggregations each 5 min. for 40 min using ultrospec 2000 spectrophotometer (Pharmacia, Biotech.) for 40 min in 1 mL semi microquartz tubes. (C): Both r*Sr*-HSP17s showed no inhibition of chemically-induced insulin aggregation at 37 °C in a molar ratio (HSP/insulin) of 1:2.5, 1:5 and 1:10. The bovine pancreas insulin (250 µg/ml), provided in 25mM HEPES pH 8.2 (Sigma), induced for aggregation by 0.02 M DTT.

5.2.6. *Sr*-MIF lacks the tautomerase activity

Results were presented in Fig. 14A and 14B showing that the recombinant *Sr*-MIF neither with nor without a his-tag has the tautomerase activity either using HPP or LDME as a substrate.

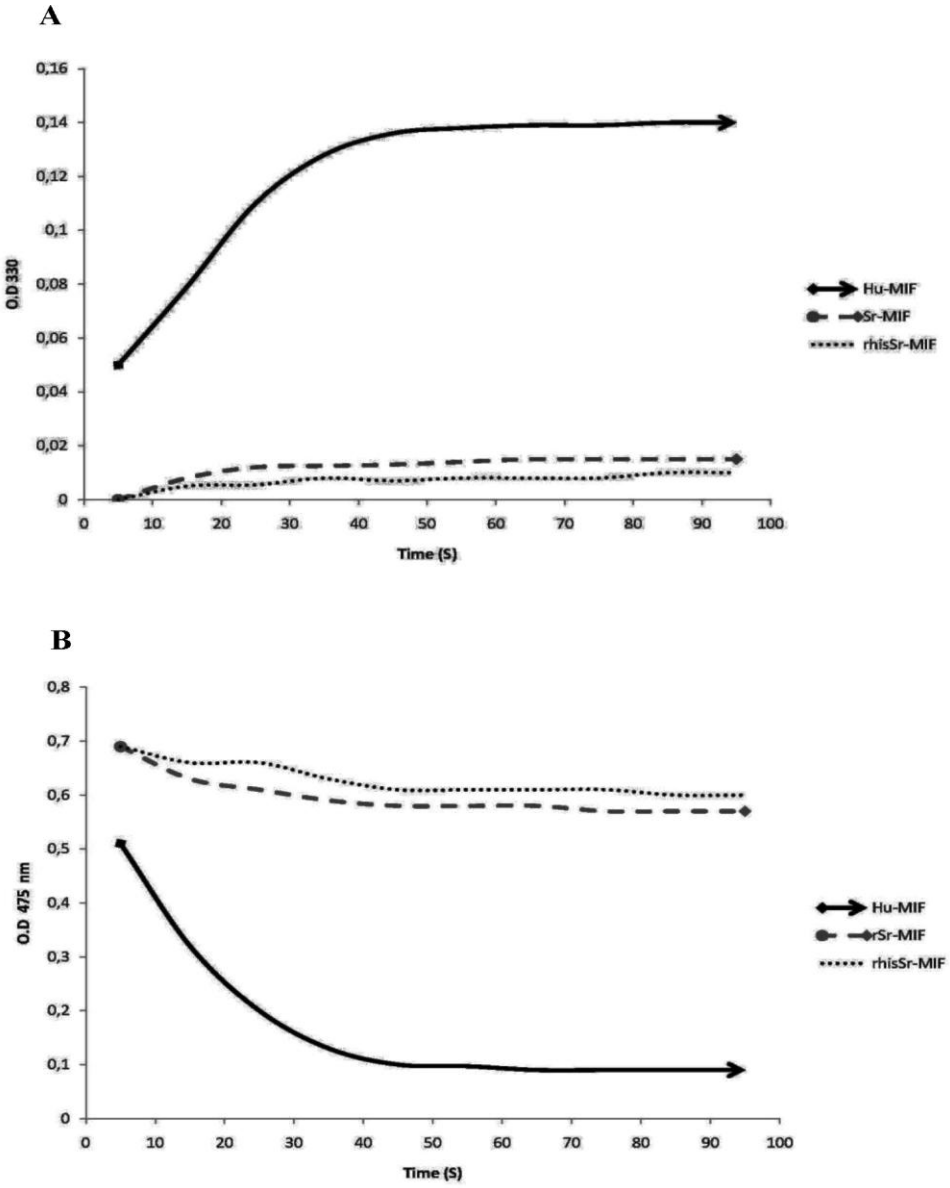

Fig. 14. Recombinant *Sr*-MIF lacks the *in vitro* tautomerase activity. Neither rhis*Sr*-MIF nor r*Sr*-MIF were able to induce tautomerase catalytic reaction: (A) HPP (p-hydroxyphenylpyruvate), purchased from Sigma, was dissolved in 50 mM ammonium acetate pH 6.0, allowed to equilibrate at room temperature overnight, and stored at 4°C. Activity was determined at ~ 25 °C by adding HPP to 1 µg of rhis*Sr*-MIF, r*Sr*-MIF or recombinant human MIF (rHu-MIF), purchased from Applichem GmbH, Darmstadt, Germany, in a quartz cuvette containing 0.435 M boric acid, pH 6.2, and measuring the increase in absorbance at 330 nm spectrophotometrically by following the increase in absorbance for 5-100 s due to the formation of the borate-enol complex. (B) L-dopachrome methyl ester (LDME) which was prepared by adding 4 mM L-3,4-dihydroxyphenylalanine methyl ester (Sigma) with 8 mM sodium periodate for 5 min at room temperature and then placed directly on ice for 20 min before use. Activity was determined at ~ 25°C by adding dopachrome methyl ester to 1µg of rhis*Sr*-MIF, r*Sr*-MIF or rHu-MIF, in a cuvette containing 25 mM potassium phosphate buffer pH 6, 0.5 mM EDTA and measuring the decrease in absorbance for 5-100 s at 475 nm. In both assays blanks containing only substrate and no MIFs were used.

5.2.7. Production of antibody and antibody purification

After immunization of seven rats in two independent experiments with r*Sr*-HSP17a, r*Sr*-HSP17b or r*Sr*-MIF, the post-immunization sera showed high levels of IgG antibodies against *Sr*-HSP17s and against *Sr*-MIF. IgG antibodies against *Sr*-HSP17s were still detectable at serum dilutions of >1:64,000 by ELISA (Fig. 15A,D) and of >1:4,000 by Western blots (Fig. 15B,E). After purification and concentration, the IgG antibodies recognized the r*Sr*-HSP17s at dilutions >1:800 by ELISA (Fig. 15C,F). A restricted cross-reactivity of the immune sera against the two HSP17s was observed using the immunized sera (at 1:3,000), which was found to be much lower after purification of the antibodies at 1:300 (Fig. 16A,B). Similarly, high levels of IgG antibodies against r*Sr*-MIF were still detectable at serum dilutions of >1:250,000 by ELISA (Fig. 17A) and of 1:160,000 by Western blots (Fig. 17B). After purification, the IgG antibodies recognized the r*Sr*-MIF at dilutions >1:800 by ELISA (Fig. 17C).

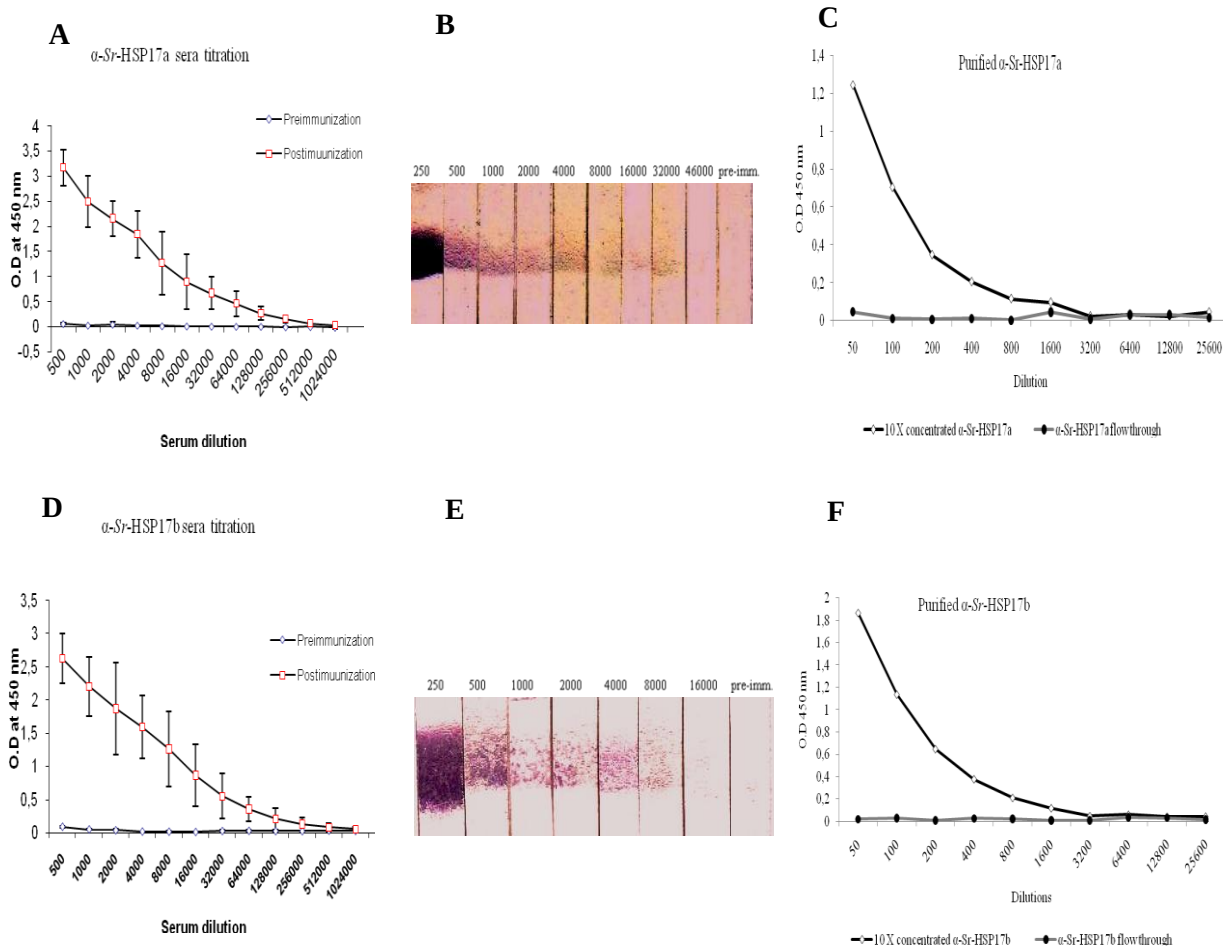

Fig. 15. Recognition of r*Sr*-HSP17s by IgG in the serum from r*Sr*-HSP17s-immunised rats. A, D: The ELISA titration of the immunized sera against the pre-immune sera using r*Sr*-HSP17s proteins as the antigens. B, E: Western blot titration of the immunized sera using r*Sr*-HSP17s proteins as the antigens tested with pre-immune serum (1:50) or r*Sr*-HSP17s-specific rat immune serum taken post immunization (in different dilutions). C, F: ELISA using the recombinant proteins as antigens and titration of the affinity-purified antibodies compared to the concentrated flow through.

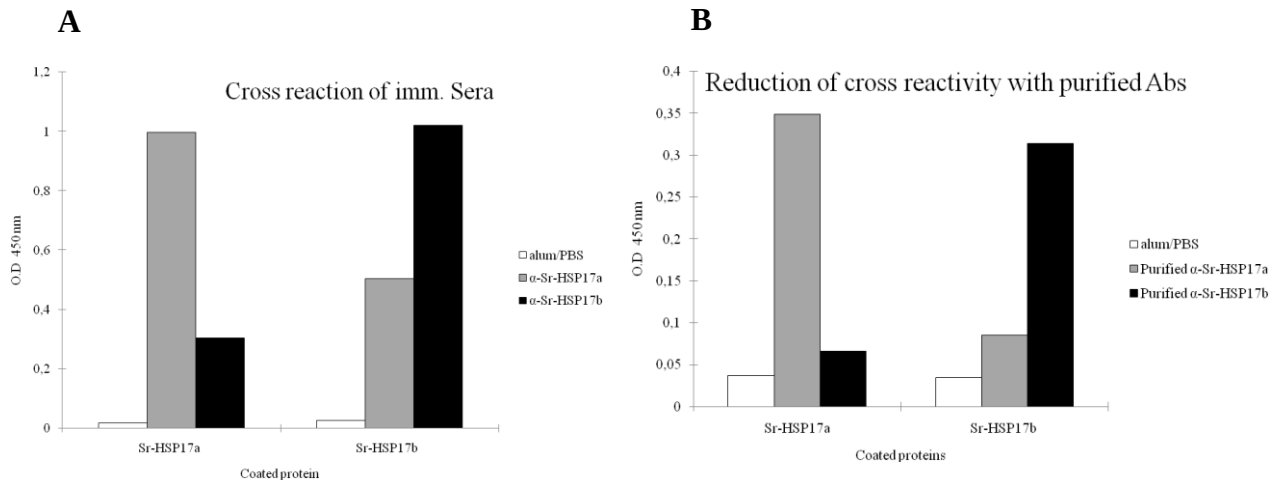

Fig. 16. Cross-reactivities in ELISA titration of the (A) 1:3000 immune sera and (B) 1:300 purified antibodies against the respective *Sr*-HSP17s, by using the recombinant *Sr*-HSP17 proteins as antigens. Sera from mock-immunized rats (1:50) served as controls.

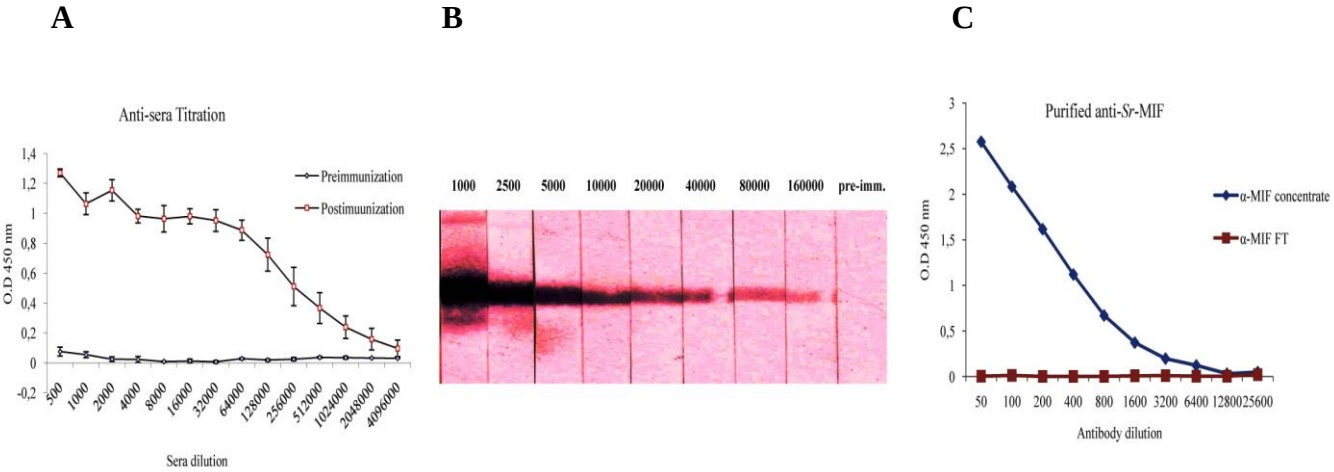

Fig. 17. Recognition of r*Sr*-MIF by IgG in the serum from r*Sr*-MIF-immunised rats. (A) The ELISA titration of the immunized sera against the pre-immune sera using r*Sr*-MIF as the antigen (B) Western blot titration of the immunized sera using r*Sr*-MIF as the antigen tested with pre-immune serum (1:50) or r*Sr*-MIF-specific rat immune serum taken post immunization (in different dilutions). (C) ELISA using the r*Sr*-MIF as antigens and titration of the concentrated affinity-purified antibody compared to the flow through.

5.2.8. Lack of cross reactivity of antibodies against *Strongyloides* MIF and human MIF

To determine the cross reactivity between the anti-Hu-MIF and anti-*Sr*-MIF, immunoblot analysis was performed. Interestingly, both antibodies recognized only the corresponding MIF. The anti-Hu-MIF recognized only the rHu-MIF but neither r*Sr*-MIF nor native *Sr*-MIF from the iL3 extract (Fig. 18A). Similarly, the anti-*Sr*-MIF reacted with the *Sr*-MIF but not the Hu-MIF (Fig 18B).

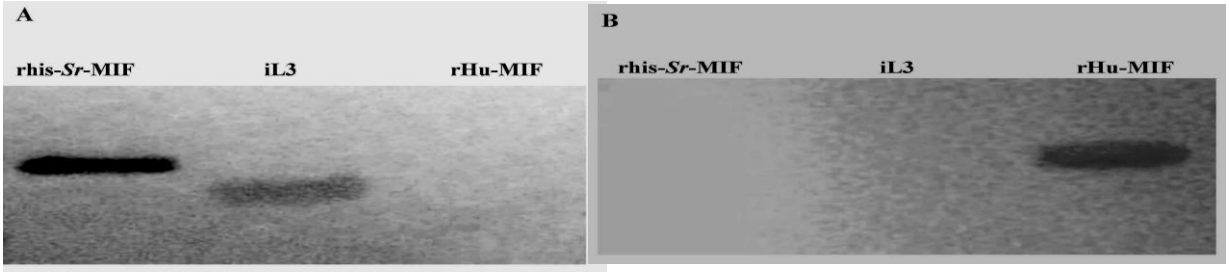

Fig. 18. Lack of cross-reactivity between anti-*Sr*-MIF and anti-Hu-MIF. (A) Western blot analysis showed the recognition of the purified anti-*Sr*-MIF antibody of both recombinant and *Sr*-MIF from iL3 stage extract but not the rHu-MIF. (B) The anti-Hu-MIF recognized only the rHu-MIF but neither recombinant nor native *Sr*-MIF in the Western blots.

5.2.9. Detection of native *Sr*-HSP17s and *Sr*-MIF in ESP and somatic extracts

While sera from naïve, not-immunized rats, did not recognize *Sr*-HSP17a, *Sr*-HSP17b nor *Sr*-MIF in somatic extracts or in ESPs of iL3, PF and FF (Fig. 19), the IgG antibodies from rat sera after immunization with *Sr*-HSP17a, *Sr*-HSP17b or *Sr*-MIF recognized not only the recombinant proteins, but also the native *Sr*-HSP17s and *Sr*-MIF proteins, respectively, in the extracts and in ESPs of *S. ratti* stages (Fig. 19A,B,C). ELISA tests clearly confirmed the predominant presence of *Sr*-HSP17s in the PF as compared to other stages. Thus, the mean optical density (OD) for *Sr*-HSP17a was found about 4.8-fold (extracts) and about 2.4-fold (ESP) higher in the PF than in the FF (Fig. 19A). Similarly, for *Sr*-HSP17b, the OD levels appeared >7.4- fold (extracts) but only > 1.3-fold (ESP) higher in the PF than that in the FF. ELISA tests showed the presence of *Sr*-MIF in all stages with higher expression in iL3 as compared to other stages (Fig. 19B). The mean optical density (OD) for *Sr*-MIF was found to be ~ 2-fold higher in either the extract or ESP from iL3 as compared to the other stages. Interestingly, the OD in the ESP was higher than that of extracts (Fig. 19C).

19A

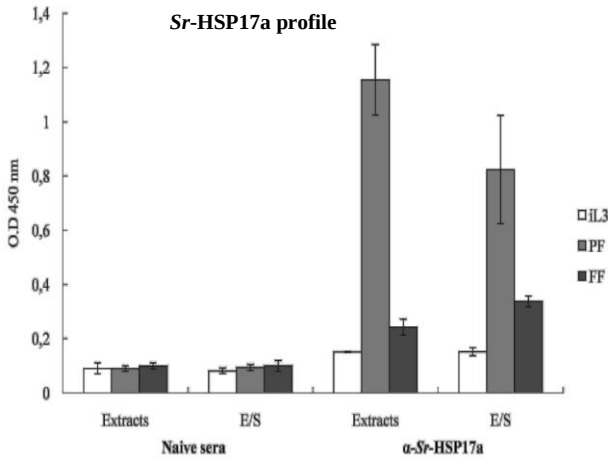

19B

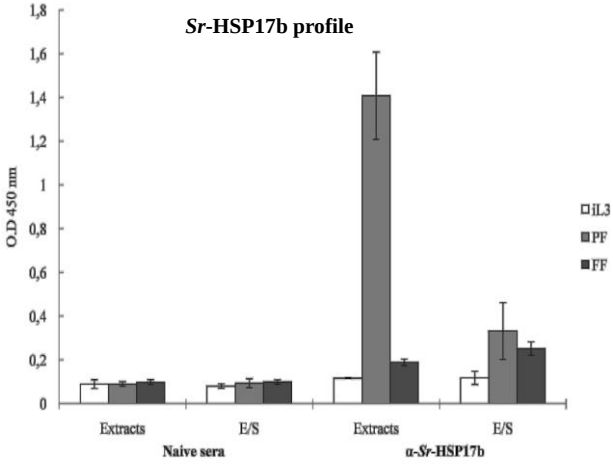

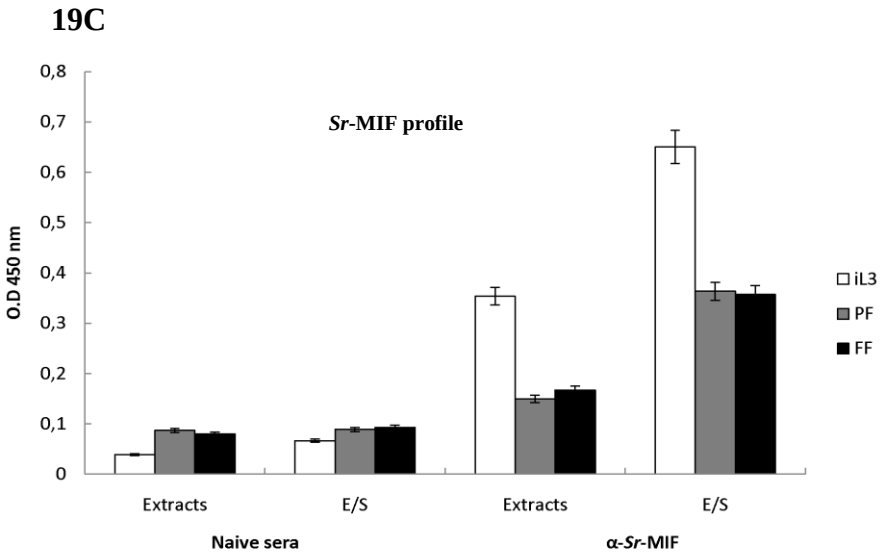

Fig. 19. Detection of native *Sr*-HSP17s and *Sr*-MIF. (A) Detection of native *Sr*-HSP17a using purified antibody against *Sr*-HSP17a. (B) Detection of native *Sr*-HSP17b using purified antibody against *Sr*-HSP17b. (C) Detection of native *Sr*-MIF using purified antibody against *Sr*-MIF. Native *S. ratti* HSP17s and MIF in the ESPs and extracts, of the iL3, PF and FF detected by ELISA using *Sr*-HSP17s and *Sr*-MIF-specific antibodies (1:300). As a negative control, sera from naïve rats before immunization were used diluted 1:50. The ESPs and extracts were used as antigens.

5.2.10. Immune recognition of *Sr*-HSP17s and *Sr*-MIF by sera from *Strongyloides*-infected rats and exposed humans

Serological analysis was performed to determine if the *Sr*-HSP17s and/or *Sr*-MIF are targets for immune recognition during an infection by *Strongyloides*. Sera from rats 37 and 112 days after infection were used in ELISA tests, resulting in time-dependent significantly increasing IgG reactivity toward *S. ratti* recombinant proteins 37 and 112 days post-infection ($P<0.01$; Fig. 20A). Furthermore, sera of 50 individuals living in areas endemic for intestinal nematodes, including *S. stercoralis*, reacted significantly with *Sr*-HSP17s and *Sr*-MIF in contrast to 10 non-exposed healthy Europeans, indicating a significant IgG1 recognition (Fig. 20B).

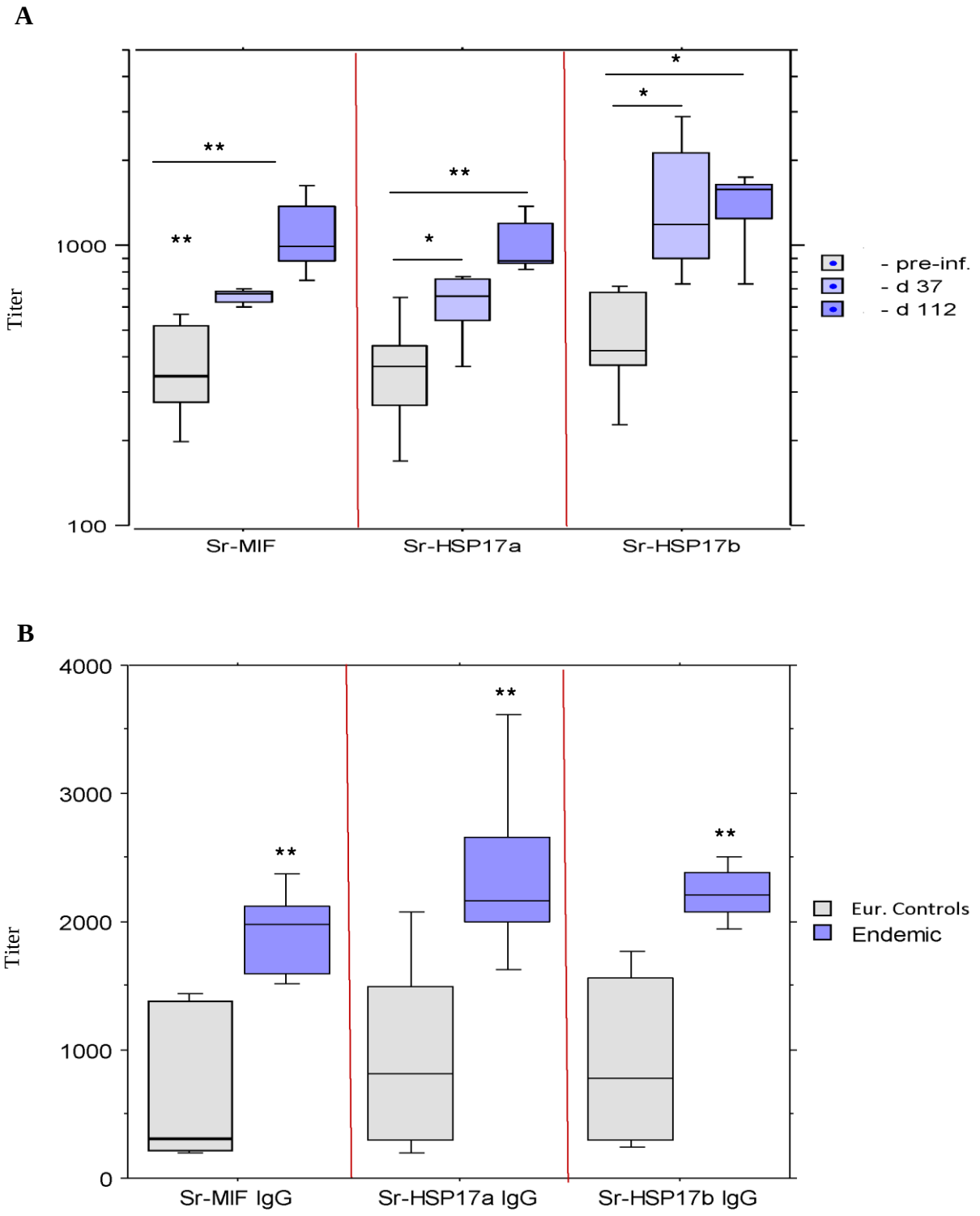

Fig. 20. Immune recognition of *Sr*-HSP17s and *Sr*-MIF. (A) IgG antibody reactivities with r*Sr*-HSP17a, r*Sr*-HSP17b and r*Sr*-MIF proteins in sera of 5 rats 37 and 112 days after infection with *S. ratti* as compared with pre-infection sera. (B) IgG1 antibody recognition of r*Sr*-HSP17s from 50 Africans living in areas endemic for intestinal nematodes including *S. stercoralis*. Mann-Whitney U test: * P<0.05 and **P<0.01.

5.2.11. *Sr*-HSP17s and *Sr*-MIF bind differentially to host immune cells

Using flow cytometry (FACS), the binding of r*Sr*-HSP17s and r*Sr*-MIF to host cells was investigated. The host cells were incubated with biotin-labeled r*Sr*-Hsp17a, r*Sr*-HSP17b or r*Sr*-MIF.

5.2.11.1. *Sr*-HSP17s

Using freshly isolated human MNC, *Sr*-HSP17b strongly bound to the monocyte population, gated by CD14 but *Sr*-HSP17a bound only marginally (Fig. 22A,B). Preincubation with the respective antibodies against the *Sr*-HSP17s resulted in a pronounced (>50%) reduction in the binding of *Sr*-HSP17b. Further, the presence of different concentrations of unlabelled HSP17s resulted in dose-dependent reductions of the fluorescence and binding competition with the labeled HSP17s (85%-100%). This indicates the specific binding of *Sr*-HSP17s to the monocyte/macrophage lineage (Fig. 23A,B).

In contrast, the CD14-negative non-activated lymphocytes showed no binding with both proteins (Fig. 24A). Similarly, CD16-positive neutrophilic granulocytes (PMN) showed no binding with both labeled proteins (Fig. 24 B,C). The binding to the monocyte-lineage was confirmed by a CD14-positive macrophage cell line (J774) showing strong binding of both *Sr*-HSP17s and pronounced reduction of the binding by antibodies against *Sr*-HSP17a (Fig. 22C,D) and weak reduction by antibodies against *Sr*-HSP17b. Only *Sr*-HSP17a showed a dose dependent, moderate binding to the rat intestinal epithelial cell line (IEC-6) that was not inhibitable by the preincubation with antibody (Fig. 22E,F). These experiments were repeated up to six times.

5.2.11.2. *Sr*-MIF

Sr-MIF strongly bound to the monocyte population, gated by CD14 (Fig. 21A). Preincubation with the recombinant human CD74 resulted in significant reduction (> 60%) of the fluorescence (Fig. 25A). In contrast, the CD14-negative lymphocytes showed no binding with *Sr*-MIF (Fig. 25B). The binding to the monocyte-lineage was confirmed by a CD14-positive macrophage cell line (J774) showing strong binding of r*Sr*-MIF and pronounced reduction by antibody against *Sr*-MIF (Fig. 25C). Similarly, CD16-positive neutrophils (PMN) showed marginal binding with labeled protein (Fig. 25D), which reduced by preincubation with the purified anti-*Sr*-MIF.

The differential binding of *S. ratti* proteins to monocyte/MØ is shown (Fig. 26). Further, the preferential binding to the studied host immune cells is summarized (Table 4).

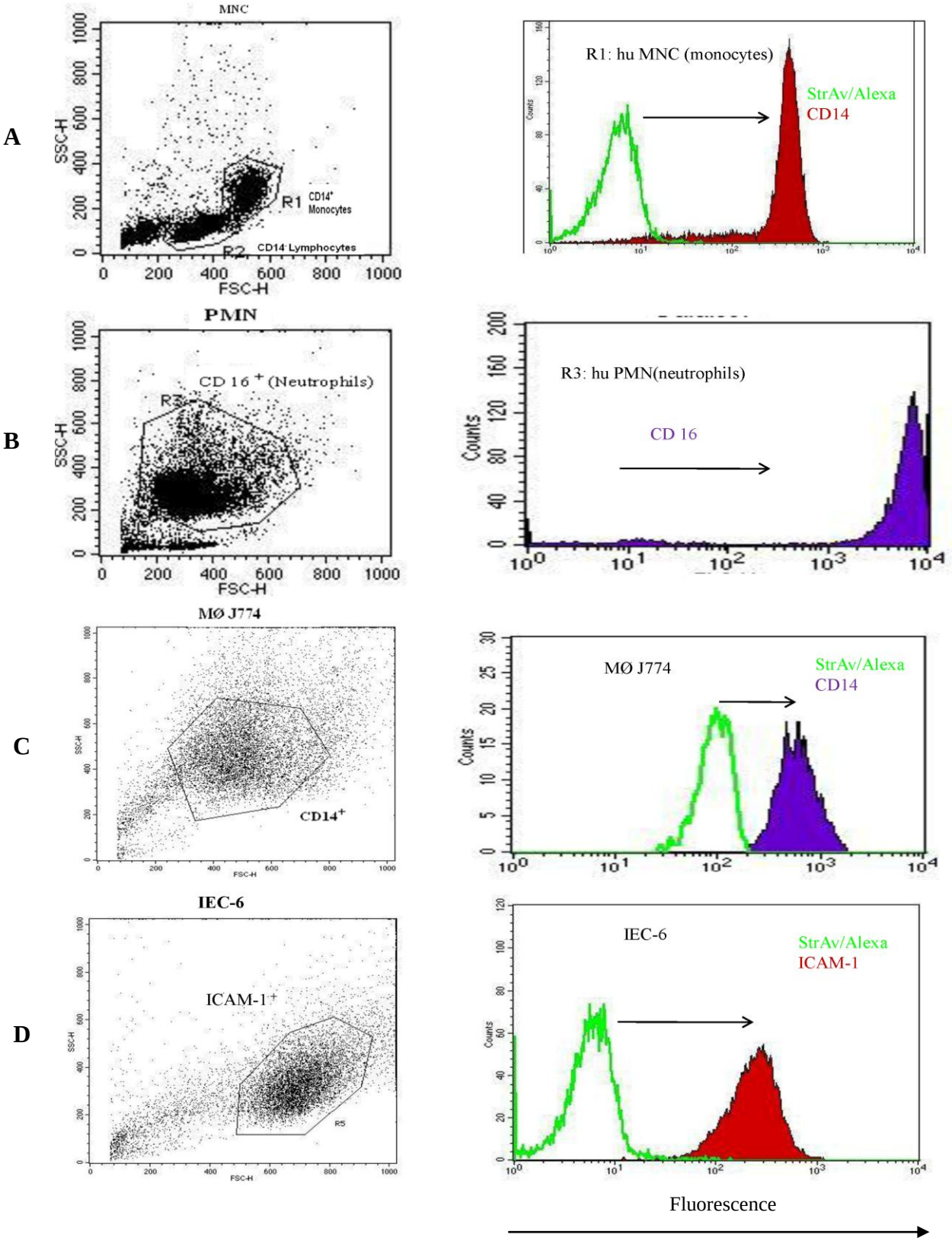

Fig. 21. Host cell characteristics. **(A)** Peripheral blood mononuclear cells (MNC) and gating of the $CD14^+$ monocytes. **(B)** Peripheral blood polymorphonuclear cells (PMN) and gating of the $CD16^+$ neutrophils. **(C)** MØ J774 cell line shows positive binding to CD14. **(D)** Rat intestinal epithelial cell line IEC-6 bound to ICAM-1. Left figures: forward-site-scatter plot of host cells showing their morphological distribution according to cell size and granularity. Right figures: cell gating and positive controls.

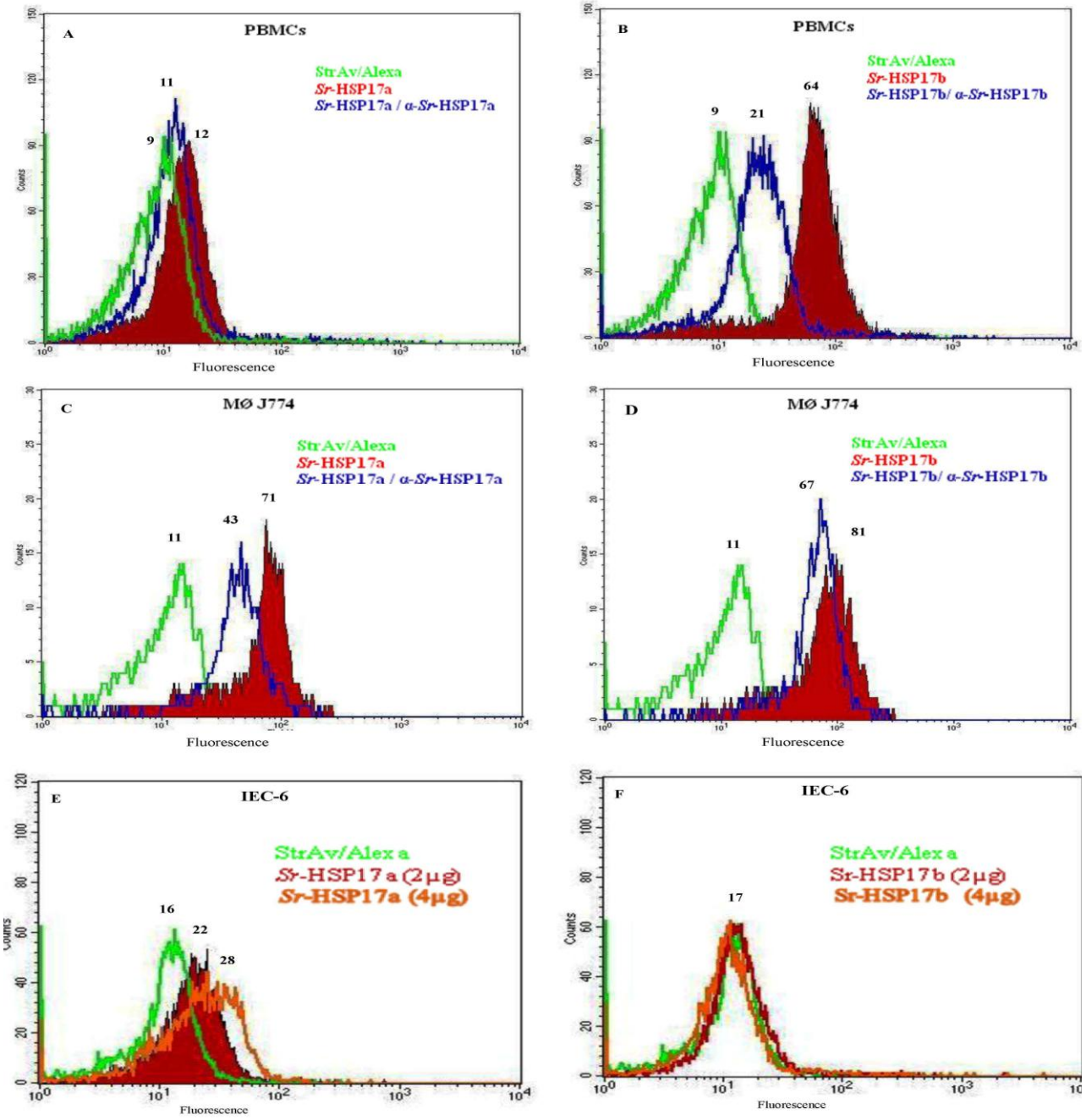

Fig. 22. Binding of *Sr*-Hsp17a and *Sr*-HSP17b to host immune cells. (A, B) CD14-positive, gated monocytes. (C, D) J774 MØ cell line. (E, F) IEC-6 cell line. 2 x 10^5 cells were incubated at 4 °C for 45 min with biotin-labeled *Sr*-HSP17s. Intensity of surface fluorescence (F.I., x-axis) is plotted against cell counts. The noted counts in the figures represent the mean fluorescence index values. Representative results of three independent experiments are shown.

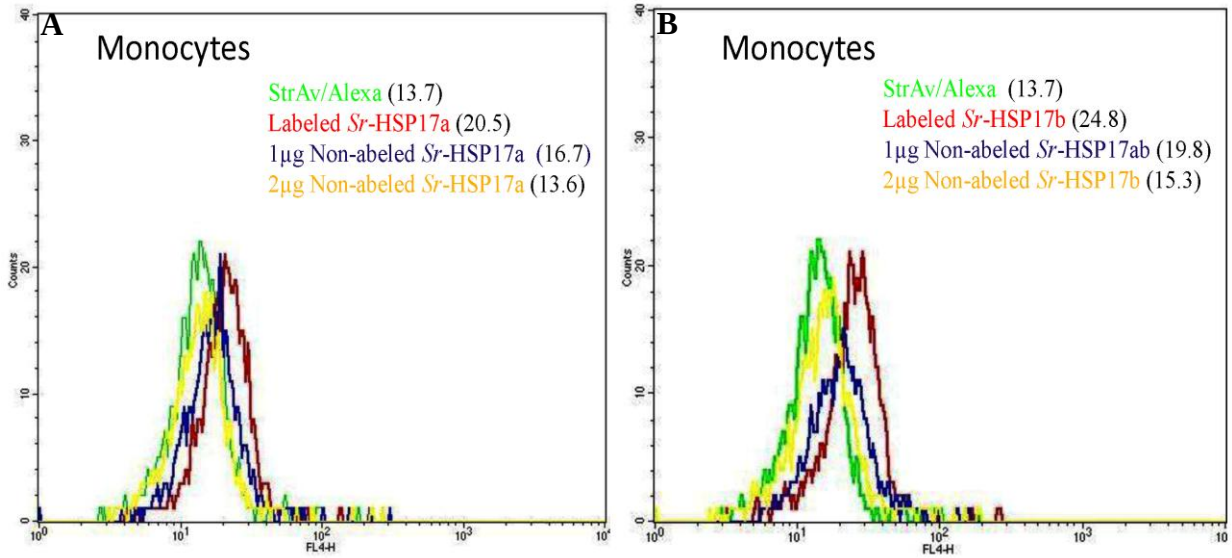

Fig. 23. Binding specificity of *Sr*-Hsp17s to monocytes. Binding of biotin-labeled *Sr*-HSP17a (A) and biotin-labeled *Sr*-HSP17b (B) to CD14-positive, gated monocytes was highly reduced (100% and 85%) in the presence of the unlabelled corresponding *Sr*-HSP17. The conditions and figure were processed like figure 22.

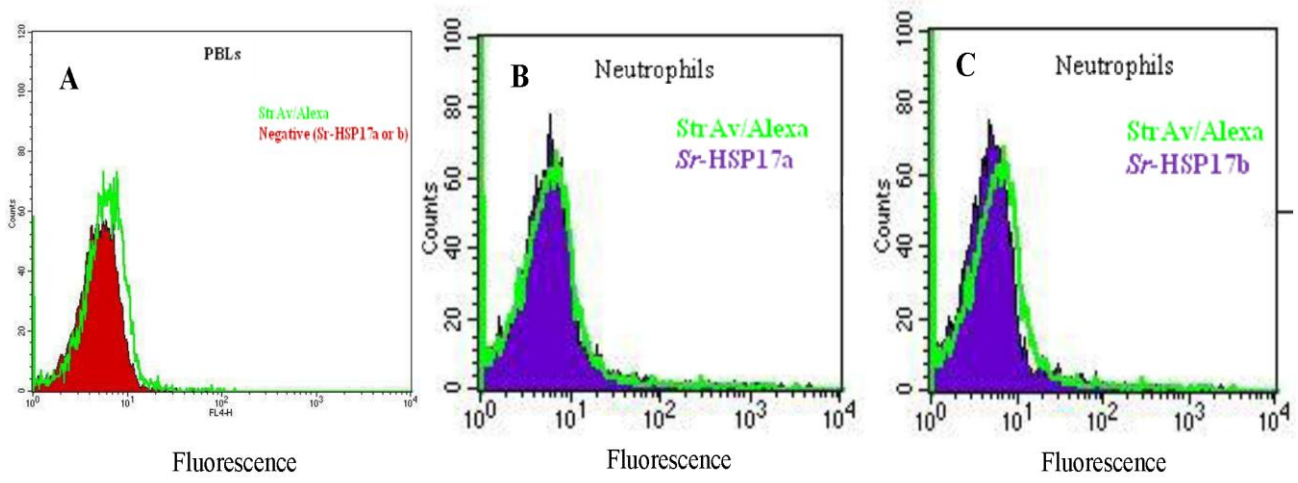

Fig. 24. r*Sr*-Hsp17s did not bind to lymphocytes nor neutrophils. Binding of biotin-labeled *Sr*-HSP17s to (A) CD14-negative lymphocytes and (B, C) CD16-positive neutrophils to CD14-positive. The conditions and figure were processed like figure 22.

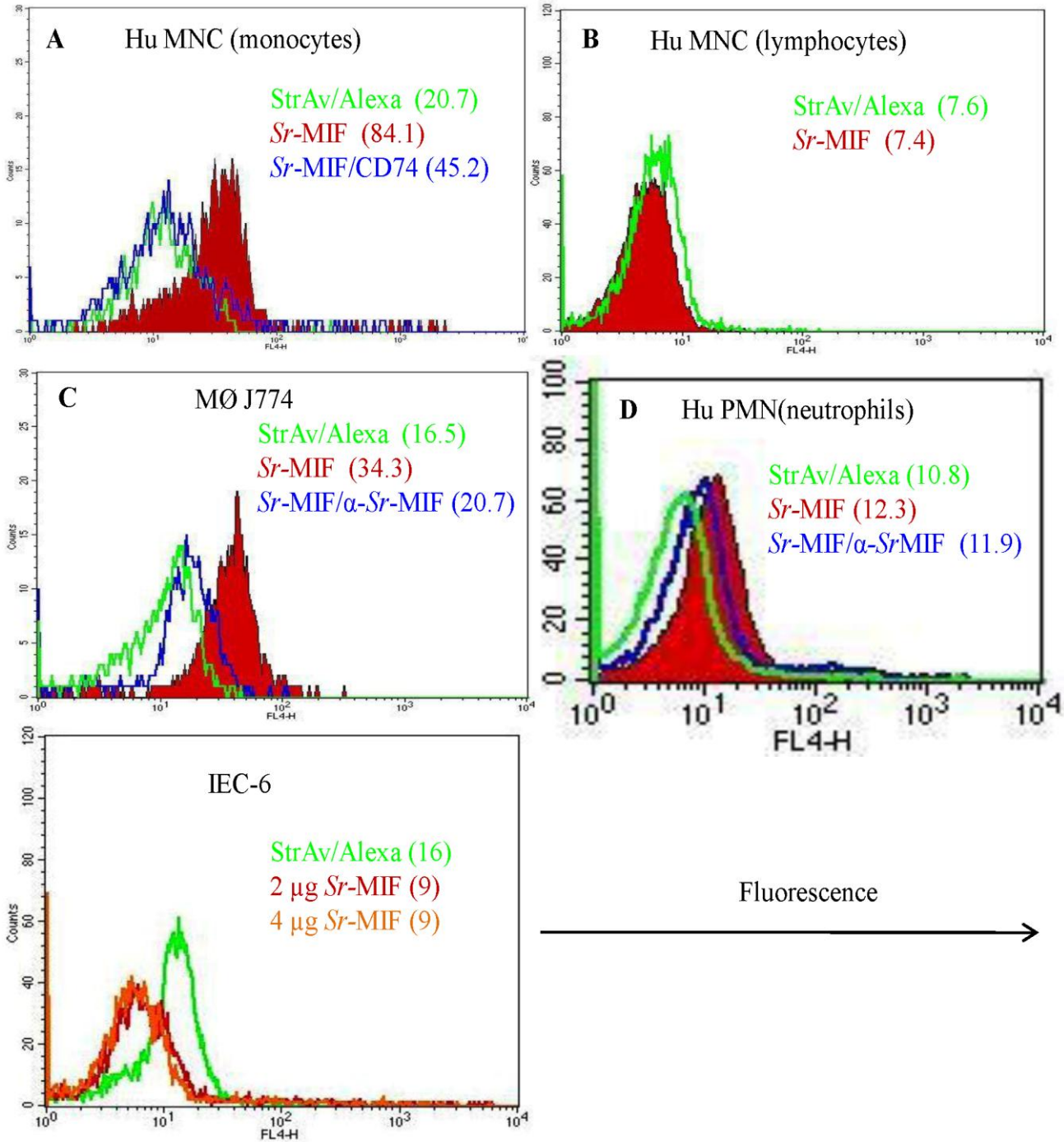

Fig. 25. Binding of *Sr*-MIF to host immune cells. (A) CD14-positive, gated monocytes. (B) CD14-negative lymphocytes. (C) J774 MØ cell line. (D) CD16-positive neutrophils. 2 x 10^5 cells were incubated at 4 °C for 45 min with biotin-labeled r*Sr*-MIF. Intensity of surface fluorescence (F.I., x-axis) is plotted against cell counts. The noted counts in the figures represent the mean fluorescence index values. Representative results of three independent experiments are shown.

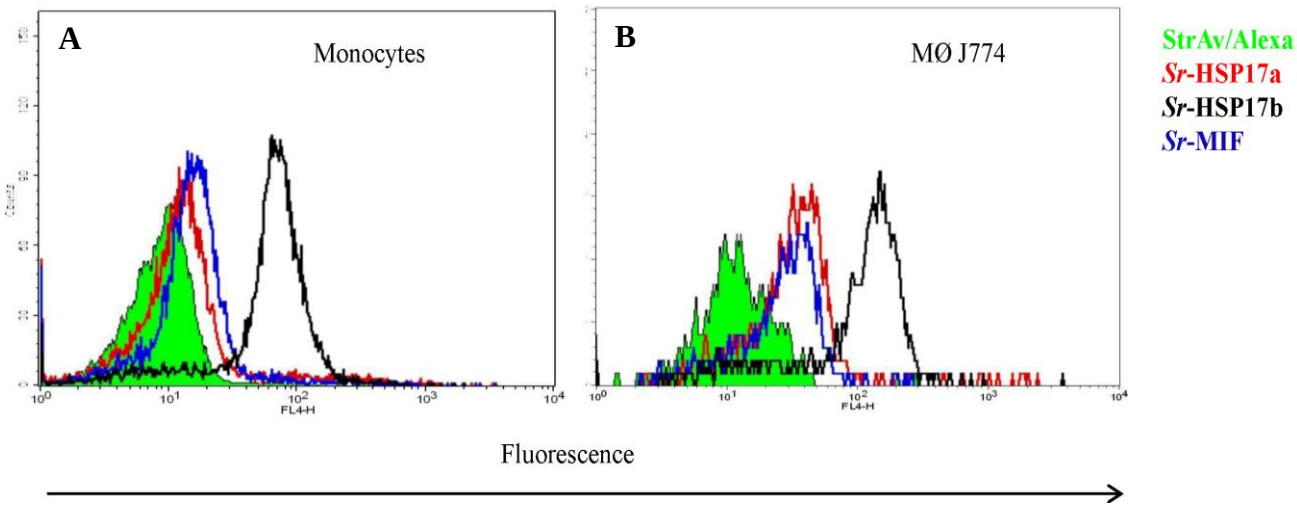

Fig. 26. Differential binding of *S. ratti* proteins to monocytes. (A) CD14-positive, gated monocytes. (B) J774 MØ cell line.

Table 4. Differential binding of *S. ratti* proteins to host immune cells.

Cell type	*Sr*-MIF	*Sr*-HSP17a	*Sr*-HSP17b
Monocytes	++	+	+++
MØ J774	+/++	++	+++
Lymphocytes	-	-	-
Neutrophils	+	-	-
IEC-6	-	+	-

5.2.12. *S. ratti* protein induced cytokine release

The recombinant *S. ratti* proteins *Sr*-HSP17s and *Sr*-MIF were examined for their capacity to induce cytokine secretion in human MNC cultures. Different preparations of the highly purified r*Sr*-HSP17s and r*Sr*-MIF induced a pronounced increase in release of the anti-inflammatory cytokine IL-10 but not of the inflammatory cytokine TNF-alpha (Tables 5 and 6). Cytokine release was observed in the presence as well as in the absence of supplemented PMB, indicating the high purity of the r*Sr*-proteins from LPS. In contrast to the cultures exposed to r*Sr*-HSP17s and r*Sr*-MIF, the stimulatory effect of the monocyte activator LPS was strongly blocked by PMB.

Table 5. Cytokine responses of MNC exposed to r*Sr*-HSP17s. $2x10^5$ MNC were cultured for 72 h with r*Sr*-HSP17a or r*Sr*-HSP17b (each at 2 µg/ml) in the presence of polymyxin B (50 µg/ml). As a control, LPS (1 µg/ml) with or without PMB or PHA (1 µg/ml) was used. Cell-free culture supernatants were analysed for released IL-10 and TNF-alpha by commercial ELISAs. Data from two separate experiments are shown (mean ± SD).

	IL-10 (pg/ml)	TNF-alpha (pg/ml)
unstimulated	165 ± 86	10 ± 14
LPS[1)]	1300 ± 66	191 ± 88
LPS / polymyxin	81 ± 78	57 ± 66
PHA	1750 ± 353	361 ± 329
Sr-HSP17a	870 ± 232	10 ± 12
Sr-HSP17b	827 ± 527	58 ± 55

1) culture in the absence of polymyxin B

Table 6. Cytokine responses of MNC exposed to r*Sr*-MIF. $2x10^5$ MNC were cultured for 72 h with r*Sr*-MIF (at 2 µg/ml and 10 µg/ml) in the presence of polymyxin B (50 µg/ml). As a control, LPS (1 µg/ml) with or without PMB or PHA (1 µg/ml) was used. Cell-free culture supernatants were analysed for released IL-10 and TNF-alpha by commercial ELISAs. Data from 3-5 separate experiments were shown (mean ± SD).

	N° Experiments	IL-10 (pg/ml)	TNF-alpha (pg/ml)
unstimulated	5	90 ± 83	16 ± 13
LPS[1)]	3	1088 ± 370[2)]	150 ± 97
LPS / polymyxin	3	72 ± 58	54 ± 47
PHA	4	1547 ± 315[3)]	242 ± 294[2)]
Sr-MIF (2 µg/ml)	5	548 ± 402[3)]	51 ± 44
Sr-MIF (10 µg/ml)	4	775 ± 461[3)]	149 ± 239

1) culture in the absence of polymyxin B. 2) $P<0.05$, 3) $P<0.01$

5.2.13. Preliminary experiment of immunization and subsequent infection

After immunization of rats with r*Sr*-HSP17a, r*Sr*-HSP17b, r*Sr*-MIF or the aluminium adjuvant (mock) (four rats per treatment), the sera obtained 12 day after immunization and 12 day after subsequent infection with *S. ratti* comprised antibodies somewhat reactive with r*Sr*-HSP17a, more reactive with r*Sr*-HSP17b and the most reactive with r*Sr*-MIF (Fig. 27). No IgG responses were observed for the mock immunized rats, and no further significant increase of the antibody responses after infection could be observed (Fig. 27). The differences in the total fecal worm output (F1 count/10 g faeces), which were determined at different times during the infection (6, 12 and 18 d.p.i), were found to be significant for MIF (6 and 18 d.p.i) but were non-significant for the HSP17s (Fig. 28 A). Pronounced decrease of the fecal worm output (F1 count/10 g faeces) in the *Sr*-MIF immunized rats (~ 28.3%, 40.4% and 77.4% at 6, 12 and 18 d.p.i. respectively) and an increase in *Sr*-HSP17a- but not *Sr*-HSP17b-immunised rats (~ 6,4 % and 54.3%, at day 12 and day 18 p.i respectively) were observed (Fig. 28 A, B). The differences in the total fecal worm output can be expressed in terms of protection percentage against infection after immunization by the recombinant *S. ratti* proteins (Fig. 28 B).

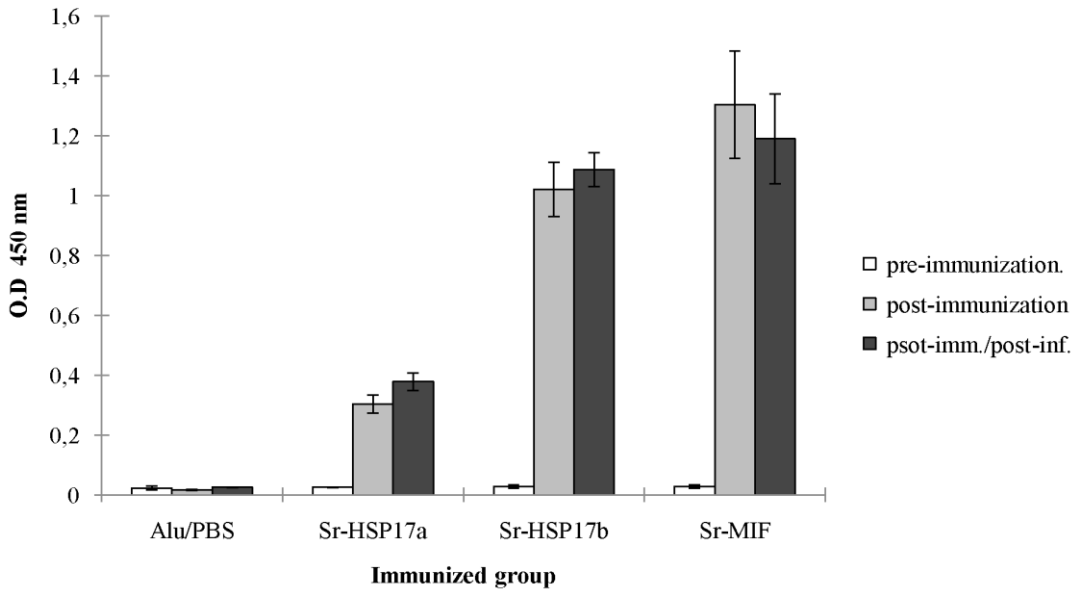

Fig. 27. Induction of antibodies in rats, immunized with r*Sr*-Hsp17a, r*Sr*-HSP17b and r*Sr*-MIF and infected with 1000 *S. ratti* iL3.

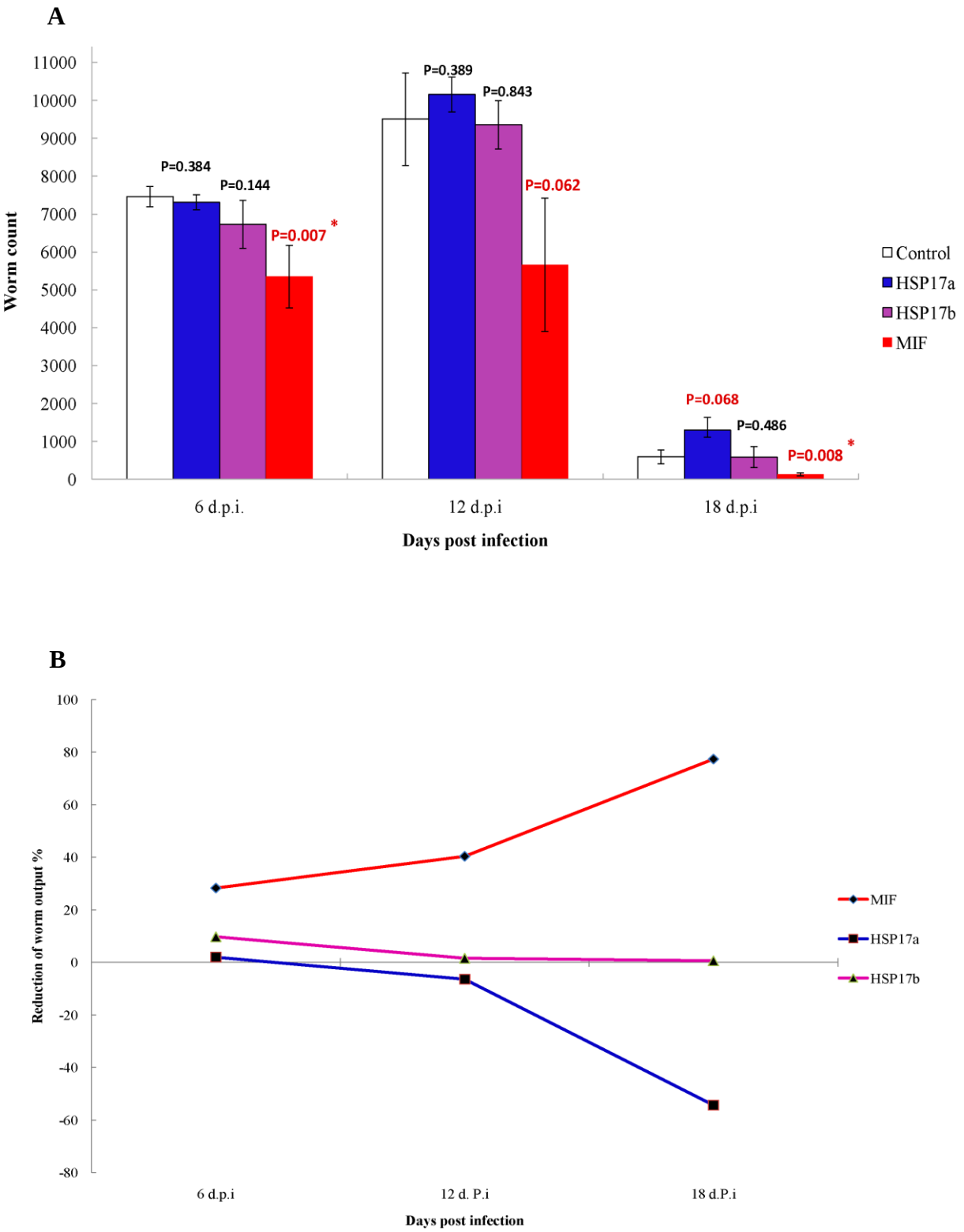

Fig. 28. Effect of immunization with r*Sr*-Hsp17 and r*Sr*-MIF and subsequent infection of rats with 1000 iL3 on the worm load. (A) Differences between F1 counts/10 g faces in rats previously immunised with r*Sr*-HSP17a, r*Sr*-HSP17b or with r*Sr*-MIF in alum/PBS and mock-immunised (alum/PBS) control group. *P<0.05. (B) The same results are expressed as percentage of protection.

6. DISCUSSION

Understanding of the molecular and the immunological basis of helminth infections is still limited, which restricts the development of novel therapeutic approaches. *S. ratti* is a natural parasite of rats, closely related to the human parasite *S. stercoralis*, and is used as a laboratory model for nematode infection and parasitological genetic mapping (Nemetschke *et al*., 2010). The transition from free-living larval stages to the parasitic lifestyle *via* an infective non-feeding stage, is characteristic for *Strongyloides spp.* In a mammalian host this represents a period in which the parasites encounter stress due to dramatic environmental changes. The adaptation of the nematodes to a parasitic lifestyle outlines an evolutionary challenge that is likely to go along with gene duplication and subsequent acquisition of novel gene function among its paralogous members (Mello *et al*., 2009).

Identification of the genes and proteins that differ in their presence, absence or presentation in different amounts from stage to stage, may help in the analysis of the particular signals involved in this transition. This in turn is important for understanding genetic, molecular and functional mechanisms of parasitism, and it may promise novel targets for vaccination and/or treatment development against the parasite itself or for other diseases.

The 19 investigated stage-specific transcripts from the free-living and parasitic stages observed in the qRT-PCR of selected *S. ratti* genes confirmed stage-specific expression found in the proteomic data on this parasite. The remarkable diversity of the expression levels of the various genes in the iL3, PF, and FF as determined in the present study reflects changes associated with the transition to parasitic lifestyle and the adaptation to the host. These include the iL3-specific *Sr* astacin (*Sr*-AST), which is homologous to a vaccine candidate against hookworm infection (*Ancylostoma caninum*) (Hotez *et al*., 2003). This astacin-like metalloprotease, *Ac*-MTP-1 (Gallego *et al*., 2005), is specifically secreted by the iL3 of the hookworm showing the same stage-specificity as *Sr*-AST (SR11111) in this study. Work from our laboratory had characterized a homologous astacin in the filaria *O. volvulus* (Borchert *et al*., 2007), which was reported to induce a strong host immune response. It was of interest that this metalloprotease showed elevated expression in iL3 stages of both *S. ratti* and *S. stercoralis* (Gallego et al., 2005), thus underlining its suggested role to facilitate skin penetration at the initiation of infection. Besides the iL3-specific astacin (SR11111), two other EST clusters (SR03587 and SR02663) were identified that showed similarities to astacins. However, these two astacins were PF-specific, thus indicating that different astacins were expressed during different developmental stages resulting in protease activities tailored

to the needs of each life cycle stage. Similarly, hookworm expresses an astacin (MTP-2) in the adult stage (Feng et al., 2007).

Sr-MIF was detected in the ESP of the iL3 and PF stages but not FF. The iL3 stage-related mRNA transcription could be confirmed by >2-fold higher expression level in iL3 as compared to FF, although the transcript is also detectable in FF. Differential MIF transcription was also reported for other parasitic nematodes, for example in the *Teladorsagia circumcincta* (Nisbet *et al*., 2010). Nisbet *et al*. detected MIF in egg, iL3 and adult but to lower extent in L4 stage. In addition, they detected the absence of the monocyte migration inhibitory effect of the *Tci*-MIF.

Another example of a stage-specific protease was *S. ratti* prolyl oligopeptidase *Sr*-POP, which has exclusively been identified in parasitic females. This protein was only partially covered by the EST clusters used for the protein identification. This may suggest that this protease plays a role in parasite establishment within the host, a notion that was supported by the observation that similar stage-specific gene expression for POP had been reported before in *T. circumcincta* (Nisbet *et al*., 2008). The stage-specificity of POP in *S. ratti* was supported by the fact that the ESTs encoding POP originated only from the EST libraries generated from PF. In addition, the comparative PCR analysis (Fig. 6) showed a positive result for PF cDNA only. The *Strongyloides* POP represents a novel abundant stage-specific protein in nematodes that might have relevance for the containment of parasitism. Interestingly, POPs had also been studied as a potential therapeutic agent for the treatment of celiac sprue, an inflammatory disease of the small intestine (Ehren *et al*., 2008).

Interestingly, the *Sr*-HSP17a and *Sr*-HSP17b showed stage-specific gene expression, as they were >6-fold and 9-fold higher expressed in PF in comparison to FF. Both *Sr*-HSP17s were highly down-regulated in iL3 in agreement with the microarray and EST studies of *S. ratti* (Evans *et al*., 2008), which reported that various orthologues of a *C. elegans* heat-shock gene (hsp-17 in *S. ratti*) were upregulated in PF stage.

Recently, a microarray consisting of 2,227 putative genes was used to identify genes likely to play a key role in the parasitic life of *S. ratti* (Thompson et al., 2008). In this published report, the microarray was probed with cDNA, prepared from parasites subject to low- (harvested 6 days) or high- (harvested 15 days post-infection) immune pressures. Comparison of these transcript expression data with our qRT-PCR data shows that several of the previously termed putative genes are present in our samples prepared from different *S. ratti* stages. For example, the cluster SR00984, which relates to a heat-shock protein 17, is

only observed in ESP from PF and occurred under low-immune pressure. However, cluster SR04440, representing the PF-associated prolyl oligopeptidase sequence (Table 2), is expressed in parasites under high-immune response.

The putative and hypothetical proteins like the *Sr*-ZK (homologue of *B. malayi* hypothetical 35.6 kDa protein), which shows high upregulation in iL3, may be of relevance for penetration and evasion mechanisms. Other interesting proteins which are moderately upregulated in the PF, such as *Sr*-GAL-3, *Sr*-CALUM, *Sr*-TIL, *Sr*-CBP, *Sr*-HSP10 and *Sr*-HSP60, may be involved in the parasite-host mucosal interaction. *Sr*-HSP10 and *Sr*-HSP60 have been partially characterized by our group (Tazir *et al*., 2009), where *Sr*-HSP10 was shown to have a partial protective effect against infection in the immunized rats. Further characterization of such proteins is recommended.

Some transcripts were observed to be free-living stage-specific, like: *Sr*-MFP2B; *Ascaris suum* putative homologue or P40 putative protein of *B. malayi* and *Sr*-Y51F10.7; and *C. elegans* putative uncharacterized protein. In addition, high levels of *Sr*-lysozyme transcript, homologue of Lys-5 from *C. elegans*, were detected in the FF, which may be of relevance in the free-living stages to kill harmful microorganisms in the surrounding environment.

One notable exception to the accordance between proteomic and transcript data was PhRT which was identified only in the PF sample using proteomics, but showed equal transcript levels throughout *S. ratti* developmental stages. A possible explanation for this observation is that while the majority of the stage-specific E/S proteins are controlled at the transcriptional level, the excretion/secretion of PhRT may be controlled post-transcriptionally, i.e. by timed translation or by post-translational events, such as stage-specific post-translational modifications.

In the present study, for the first time, we identified and characterized two novel sHSPs from *S. ratti*, *Sr*-HSP17a and *Sr*-HSP17b. The two HSPs proteins were identified on the basis of the previous study by Hanns Soblik (BNI, Hamburg), using mass spectrometry from culture supernatants of the *S. ratti* PF stage. The low molecular weight of 18-19 kDa suggested that they belong to the sHSPs family. A number of secreted HSPs have been identified in helminth pathogens such as *Oo*-HSP18 in ESP from *Ostertagia ostertagi* (Vercauteren *et al*., 2006), the heat shock protein homolog r38 found in the secretions of parasite eggs of *Schistosoma mansoni* (Cai *et al*., 1996), HSP70 in the secretome of the *Fasciola hepatica* (Robinson *et al*., 2009) and HSP10 and HSP60 in the secretion of *S. ratti* recently reported by our group (Tazir *et al*., 2009). Interestingly, one of the two hsp16 genes

in *C. elegans* shows tissue-specific expression in the excretory canal and in a few neuronal cells (Shim *et al*., 2003). A nonclassical secretion pathway has been reported for several HSPs exhibiting no signal peptides e.g. for HSP70 secretion by exosome-dependent trafficking (Lancaster and Febbraio, 2005) or lysosomal endosomes (Calderwood *et al*., 2007; Mambula *et al*., 2007).

Secretion of *Sr*-HSPs by the PF into the intra-host environment of the parasite may be of relevance for parasite–host interactions. This was also suggested for the small heat shock protein 12.6 from *B. malayi*, which functions as a human IL-10 receptor binding protein (Gnanasekar *et al*., 2008). It was also recently reported for the alpha-crystallin (Deng *et al*., 2010), which upregulates components of the TGF-beta pathway and can enhance the activity of the activating protein-1 (AP-1) through modulating the function of the MAP kinase and thereby retarding the cell migration. It has been suggested that this sHSP negatively regulates pancreatic carcinogenesis.

The full-length cDNAs of the two sHSPs homologues (*Sr*-HSP17s) were identified. The size and sequence properties suggest the presence of distinct sHSP17 genes within *S. ratti* (paralogues) rather than splice variants of the same gene. The primary structure of both *Sr*-sHSPs contains the three domains, N-terminal, ACD, and C-terminal domain, confirming the conservation of the ancient ACD domain that is uniform in size (80–100 amino acids) and comprises about one quarter of highly conserved or invariant amino acids.

Phylogenetic comparisons of sHSP originated from other nematodes showed low overall sequence identities (21% - 35%). However, a higher homology of 59 and 61% identity between *Sr*-HSP17a, *Sr*-HSP17b and the deduced *S. stercoralis* sHSP (*Ss*-HSP17) partial sequence was observed (Moore *et al*., 1996). The higher similarity of the *Strongyloides* sHSPs to *Caenorhabditis* than to the other parasitic nematodes may be related to the fact that the *Strongyloides* cycle comprises free-living stages in contrast to *Brugia* and *Trichinella* which cannot survive outside the host. Each of both *Sr*-HSP17 genes has a single intron of ancient GU-AG origin interrupting the genes at the ACDs. The HSPs are likely ancient genes that have diverged through evolution as an adaptation to parasitism.

Many sHSPs, like *Ce*-HSP12.2 and *Ce*-HSP12.3 (Kokke *et al*., 1998), lack chaperone activity, probably due to the sequence features of the ACD (Kokke *et al*., 2001). Similarly, it was reported that *Bm*-HSP-s1 from *B. malayi* (Raghavan *et al*., 1999) lacks the chaperone activity *in vitro*, similar to the r*Sr*-HSP17s that also did not express a chaperone-like activity *in vitro.* Previous reports suggest that small heat-shock proteins are not necessarily involved in stress responses in parasitic nematodes (Hartman *et al*., 2003).

The native *Sr*-HSP17s in both extracts and ESPs were detected by specific antibodies and were found to be increased in the PF when compared to iL3 and FF. All together, the previous Ms/Ms analysis as well as the present qRT-PCR data and ELISA analysis of both *Sr*-HSP17s indicated the stage-specificity of *Sr*-HSP17s in PF. The stage-related expression of sHSPs has been observed in many nematodes, for example, in *Trichinella spiralis* (Wu *et al*., 2007), *B. malayi* (Raghavan *et al*., 1999), *B. pahangi* (Devaney *et al*., 1992), *Nippostrongylus brasiliensis* (Tweedie *et al*., 1993), *O. ostertagi* (Vercauteren *et al*., 2006) and *Haemonchus contortus* (Hartman *et al*., 2003). The strong expression of HSPs in the intestine supports the possibility that HSPs are involved in the adaptation of the parasite to its new environment in the intestine, also hypothesized before (Jecock and Devaney, 1992). In the present study, the secreted *Sr*-HSP17s were recombinantly expressed and LPS was effectively removed by adding TritonX114 and PMB (Table 3).

Furthermore, a novel MIF homologue has been described in the present study from the parasitic nematode *Strongyloides ratti*. Based on MS/MS ESP data and sequence analysis, the full-length cDNA of *Sr*-MIF was identified. MIF similarly was detected in the secretion of other nematodes like *B. malayi* (Pastrana *et al*., 1998) and *Trichinella spp*. (Tan *et al*., 2001). A previous report indicated that the leaderless MIF is secreted by a non-classical means via ABC transporters (Flieger *et al*., 2003). The sequence and phylogenetic comparisons of MIF homologues showed that *Sr*-MIF was highly identical to the deduced *S. stercoralis* MIF and both are related to MIF type-2 and highly differ from those of the hosts MIFs.

While MIF orthologs are known to have at least one intron (Pastrana *et al*., 1998), comparison of the sequences of *Sr*-MIF PCR products from both cDNA and gDNA showed that *Sr*-MIF has no intron. This indicates one major difference between *Sr*-MIF and other MIF genes and may result in different properties of the *Sr*-MIF protein, for example the absence of splice variant products. Comparative functional future analysis may lead to the understanding of the significance of MIF genes with or without introns.

At present, the MIF function in the non-pathogenic organisms is scarcely understood**.** Four MIF-like genes were found in the free-living nematode *C. elegans (Marson et al., 2001).* Two of them were highly upregulated in the dauer stage larvae; it has been hypothesized that these genes may have a homeostatic role during developmental arrest. The stage-related expression of *Sr*-MIF was confirmed using the purified anti-*Sr*-MIF in extracts and ESP of the stages in ELISA. Similar to the previous finding that MIF homologue secreted by hookworms (*Ace*-MIF) was upregulated in iL3 (Cho *et al*., 2007), in the present study the expression of native *Sr*-MIF protein (extracts and ESP) was found to be ~2-fold upregulated in the iL3 stage

compared to FF, suggesting a potential role in modulation of the host immune responses, during evasion and tissue migration (iL3) and/or intestinal mucosa modulation (PF).

The present results document that a produced polyclonal anti-*Sr*-MIF IgG recognizes both, native and recombinant *Sr*-MIF, but fails to react with the human MIF. On the other hand, anti-Hu-MIF reacted only with the rHu-MIF but not *Sr*-MIF, suggesting that the recombinant human and *Strongyloides* MIF, which are 28% amino acid sequence identical, differ in immunoreactive epitopes. This finding suggests that *Sr*-MIF may be a target of vaccine or drug development without interfering with host MIF. The nematode and host MIFs appear to function differentially.

In vitro tests indicated that r*Sr*-MIF lacks the tautomerase-like activity. Several reports, however, suggested that the MIF tautomerase activity, detected only *in vitro*, without the determination of the possible physiological substrate and the lack or inhibition of the tautomerase-like activity is not adequate to reduce the MIF biological functions (El-Turk *et al*., 2008; Fingerle-Rowson *et al*., 2009). Further, amongst the two characterized MIF-like proteins in *Leishmania major* (Richardson *et al*., 2009), one of them lacks the tautomerase activity.

The purified r*Sr*-HSP17s and r*Sr*-MIF were used for immunizing rats, cellular assays, and other functional analyses. *Sr*-HSP17s and *Sr*-MIF, when exposed to the host immune system, were highly immunogenic as demonstrated by strong IgG responses after repeated immunization. In addition, significant increasing antibody reactions against each of them were documented after infection of rats with *S. ratti* as well as in sera of *S. stercoralis*-exposed individuals from endemic countries.

In the preliminary immunization/infection experiments the immunization with the r*Sr*-HSP17s showed no protection effect against the subsequent infection by iL3. A possible interpretation for an increased larval output may be due to a possible cross-reaction of the high titer antibodies with the highly conserved host HSPs important for its defense subsequently may render it more susceptible for the parasite. In contrast, *Sr*-MIF immunized rats showed a decrease in the larval output. This small scale experiment suggests a putative role of *Sr*-MIF as strongyloidiasis vaccine candidate, however, larger scale experiments are needed. Interestingly, no further increase of the high antibody responses after infection could be observed.

The cellular results obtained in the present study indicated that *Sr*-HSP17s can interact and subsequently activate host cells, namely of the monocyte/macrophage lineage and intestinal epithelial cells, while neither lymphocytes nor granulocytes are affected. Of putative

importance, the first line host cells exposed to *Sr*-Hsp17s after their release from parasitic females in the intestine represent the intestinal epithelial cells and these appear to interact with the *Sr*-Hsp17a as indicated by flow cytometry analysis. Furthermore, directly adjacent to the epithelial cells occur monocyte-lineage cells, to which *Sr*-HSP17b appear to bind more strongly than *Sr*-HSP17a. Similarly, *Sr*-MIF interacts with the monocyte/macrophage lineage and weakly with neutrophils, but not lymphocytes. The strong reduction of the binding of r*Sr*-MIF after preincubation with the CD74 to monocytes indicated that r*Sr*-MIF binds to the previously characterized cell surface mammalian MIF receptor, CD74, as reported for human (Leng *et al*., 2003) and hookworm MIF (Cho *et al*., 2007). Interestingly, PF also can express *Sr*-MIF and the adjacent host cell lineage, the intestinal epithelial cells, also can express CD74 (Maharshak *et al*., 2010).

Extensive work has suggested that HSPs may be potent activators of the innate immune system capable of inducing proinflammatory cytokine production by the monocyte-macrophage lineage. However, recent evidence suggests that the reported cytokine effects of HSP may be influenced as a result of contaminating LPS and LPS-associated molecules (Gao and Tsan, 2004; Tsan and Gao, 2004). Similarly, several reports suggested that MIF may be able to induce proinflammatory mechanisms (Aeberli et al., 2006; Conroy et al., 2010). Our results, however, indicate that the highly purified r*Sr*-HSP17s and r*Sr*-MIF , containing none or extremely low endotoxin, were found to induce IL-10 but not TNF-alpha by MNC and importantly, in the presence or absence of PMB. The effectiveness of PMB was confirmed by neutralization of the LPS-induced cytokines. These results agree with the results of (Park et al., 2009), who reported that the IL-10 and TGF-β levels in the bronchoalveolar lavage fluid were significantly higher following the treatment with the recombinant *Anisakis simplex* MIF (r*AS*-MIF). Furthermore, TGF-β and IL-10 were found increased in the spleen and mesenteric lymph nodes from r*AS*-MIF treated mice (Cho *et al*., 2010), but there was no effect on the levels of IFN-γ, IL-6, and IL-13. The r*As*-MIF appears to ameliorate dextran sodium sulfate-induced colitis, suggesting that MIF may be of therapeutic relevance for the treatment of intestinal inflammatory disease. The recombinant MIF from *B. malayi* was able to induce cytokine production in human monocytes including endogenous human MIF (Hu-MIF), suggesting that a positive feedback loop might exist in parasite-stimulated Hu-MIF expression due to the presence of high levels of MIF, creating a local or possibly systemic anti-inflammatory host environment (Zang *et al*., 2002). In addition, the secretion of MIF at the site of infection by the helminths, which might induce production of endogenous host MIF, may lead to blockade of AP-1-dependent proinflammatory gene expression by binding the

transcription factor Jun activation domain-binding protein 1 (Jab1) (Kleemann et al., 2000).

Thus, the present study confirms the stage-related expression of the E/S proteins. Furthermore, three secreted and stage-related proteins from *S. ratti* (*Sr*-HSP17a, *Sr*-HSP17b and *Sr*-MIF) were identified and molecularly characterized. Their biological role in the parasite-host interaction was initiated. This should help to increase our knowledge and understanding about the parasite-host relationship. Also, it represents a strong motivation for further investigations of the biological role of these proteins and to identify other putative relevant proteins secreted by the parasite.

7. REFERENCES

Aeberli, D., Leech, M., and Morand, E.F. (2006). Macrophage migration inhibitory factor and glucocorticoid sensitivity. Rheumatology (Oxford) *45*, 937-943.

Anderson, R.C. (2000). Nematode parasites of vertebrates : their development and transmission, 2nd ed. edn (Wallingford, CABI Pub).

Behnke, J.M., Barnard, C.J., and Wakelin, D. (1992). Understanding chronic nematode infections: evolutionary considerations, current hypotheses and the way forward. Int J Parasitol *22*, 861-907.

Blankenhaus, B., Klemm, U., Eschbach, M.L., Sparwasser, T., Huehn, J., Kuhl, A.A., Loddenkemper, C., Jacobs, T., and Breloer, M. (2011). Strongyloides ratti Infection Induces Expansion of Foxp3+ Regulatory T Cells That Interfere with Immune Response and Parasite Clearance in BALB/c Mice. J Immunol *186*, 4295-4305.

Borchert, N., Becker-Pauly, C., Wagner, A., Fischer, P., Stocker, W., and Brattig, N.W. (2007). Identification and characterization of onchoastacin, an astacin-like metalloproteinase from the filaria Onchocerca volvulus. Microbes Infect *9*, 498-506.

Brattig, N.W., Lepping, B., Timmann, C., Buttner, D.W., Marfo, Y., Hamelmann, C., and Horstmann, R.D. (2002). Onchocerca volvulus-exposed persons fail to produce interferon-gamma in response to O. volvulus antigen but mount proliferative responses with interleukin-5 and IL-13 production that decrease with increasing microfilarial density. J Infect Dis *185*, 1148-1154.

Bungiro, R., and Cappello, M. (2004). Hookworm infection: new developments and prospects for control. Curr Opin Infect Dis *17*, 421-426.

Burglin, T.R., Lobos, E., and Blaxter, M.L. (1998). Caenorhabditis elegans as a model for parasitic nematodes. Int J Parasitol *28*, 395-411.

Cai, Y., Langley, J.G., Smith, D.I., and Boros, D.L. (1996). A cloned major Schistosoma mansoni egg antigen with homologies to small heat shock proteins elicits Th1 responsiveness. Infect Immun *64*, 1750-1755.

Calandra, T., Echtenacher, B., Roy, D.L., Pugin, J., Metz, C.N., Hultner, L., Heumann, D., Mannel, D., Bucala, R., and Glauser, M.P. (2000). Protection from septic shock by neutralization of macrophage migration inhibitory factor. Nat Med *6*, 164-170.

Calandra, T., and Roger, T. (2003). Macrophage migration inhibitory factor: a regulator of innate immunity. Nat Rev Immunol *3*, 791-800.

Calderwood, S.K., Mambula, S.S., and Gray, P.J., Jr. (2007). Extracellular heat shock proteins in cell signaling and immunity. Ann N Y Acad Sci *1113*, 28-39.

Chan, M.S. (1997). The global burden of intestinal nematode infections--fifty years on. Parasitol Today *13*, 438-443.

Cherepkova, O.A., Lyutova, E.M., Eronina, T.B., and Gurvits, B.Y. (2006). Chaperone-like activity of macrophage migration inhibitory factor. Int J Biochem Cell Biol *38*, 43-55.

Cho, M.K., Lee, C.H., and Yu, H.S. (2010). Amelioration of intestinal colitis by macrophage migration inhibitory factor isolated from intestinal parasites through Toll-like receptor 2. Parasite Immunol.

Cho, Y., Jones, B.F., Vermeire, J.J., Leng, L., DiFedele, L., Harrison, L.M., Xiong, H., Kwong, Y.K., Chen, Y., Bucala, R., *et al.* (2007). Structural and functional characterization of a secreted hookworm Macrophage Migration Inhibitory Factor (MIF) that interacts with the human MIF receptor CD74. J Biol Chem *282*, 23447-23456.

Clos, J., and Brandau, S. (1994). pJC20 and pJC40--two high-copy-number vectors for T7 RNA polymerase-dependent expression of recombinant genes in Escherichia coli. Protein Expr Purif *5*, 133-137.

Collins, P.L., and Hightower, L.E. (1982). Newcastle disease virus stimulates the cellular accumulation of stress (heat shock) mRNAs and proteins. J Virol *44*, 703-707.

Concha, R., Harrington, W., Jr., and Rogers, A.I. (2005). Intestinal strongyloidiasis: recognition, management, and determinants of outcome. J Clin Gastroenterol *39*, 203-211.

Conroy, H., Mawhinney, L., and Donnelly, S.C. (2010). Inflammation and cancer: macrophage migration inhibitory factor (MIF)--the potential missing link. QJM *103*, 831-836.

Cooper, E.S., and Bundy, D.A. (1988). Trichuris is not trivial. Parasitol Today *4*, 301-306.

Currie, R.W. (1987). Effects of ischemia and perfusion temperature on the synthesis of stress-induced (heat shock) proteins in isolated and perfused rat hearts. J Mol Cell Cardiol *19*, 795-808.

Deng, M., Chen, P.C., Xie, S., Zhao, J., Gong, L., Liu, J., Zhang, L., Sun, S., Ma, H., Batra, S.K., *et al.* (2010). The small heat shock protein alphaA-crystallin is expressed in pancreas and acts as a negative regulator of carcinogenesis. Biochim Biophys Acta *1802*, 621-631.

Dereeper, A., Guignon, V., Blanc, G., Audic, S., Buffet, S., Chevenet, F., Dufayard, J.F., Guindon, S., Lefort, V., Lescot, M., *et al.* (2008). Phylogeny.fr: robust phylogenetic analysis for the non-specialist. Nucleic Acids Res *36*, W465-469.

Devaney, E., Egan, A., Lewis, E., Warbrick, E.V., and Jecock, R.M. (1992). The expression of small heat shock proteins in the microfilaria of Brugia pahangi and their possible role in development. Mol Biochem Parasitol *56*, 209-217.

Ehren, J., Govindarajan, S., Moron, B., Minshull, J., and Khosla, C. (2008). Protein engineering of improved prolyl endopeptidases for celiac sprue therapy. Protein Eng Des Sel *21*, 699-707.

El-Turk, F., Cascella, M., Ouertatani-Sakouhi, H., Narayanan, R.L., Leng, L., Bucala, R., Zweckstetter, M., Rothlisberger, U., and Lashuel, H.A. (2008). The conformational flexibility of the carboxy terminal residues 105-114 is a key modulator of the catalytic activity and stability of macrophage migration inhibitory factor. Biochemistry *47*, 10740-10756.

Eschbach, M.L., Klemm, U., Kolbaum, J., Blankenhaus, B., Brattig, N., and Breloer, M. (2010). Strongyloides ratti infection induces transient nematode-specific Th2 response and reciprocal suppression of IFN-gamma production in mice. Parasite Immunol *32*, 370-383.

Evans, H., Mello, L.V., Fang, Y., Wit, E., Thompson, F.J., Viney, M.E., and Paterson, S. (2008). Microarray analysis of gender- and parasite-specific gene transcription in Strongyloides ratti. Int J Parasitol *38*, 1329-1341.

Farrell, R.E. (1993). RNA methodologies : a laboratory guide for isolation and characterization (San Diego ; London, Academic Press).

Feder, M.E., and Hofmann, G.E. (1999). Heat-shock proteins, molecular chaperones, and the stress response: evolutionary and ecological physiology. Annu Rev Physiol *61*, 243-282.

Feng, J., Zhan, B., Liu, Y., Liu, S., Williamson, A., Goud, G., Loukas, A., and Hotez, P. (2007). Molecular cloning and characterization of Ac-MTP-2, an astacin-like metalloprotease released by adult Ancylostoma caninum. Mol Biochem Parasitol *152*, 132-138.

Fingerle-Rowson, G., Kaleswarapu, D.R., Schlander, C., Kabgani, N., Brocks, T., Reinart, N., Busch, R., Schutz, A., Lue, H., Du, X., *et al.* (2009). A tautomerase-null macrophage migration-inhibitory factor (MIF) gene knock-in mouse model reveals that protein interactions and not enzymatic activity mediate MIF-dependent growth regulation. Mol Cell Biol *29*, 1922-1932.

Flaster, H., Bernhagen, J., Calandra, T., and Bucala, R. (2007). The macrophage migration inhibitory factor-glucocorticoid dyad: regulation of inflammation and immunity. Mol Endocrinol *21*, 1267-1280.

Flieger, O., Engling, A., Bucala, R., Lue, H., Nickel, W., and Bernhagen, J. (2003). Regulated secretion of macrophage migration inhibitory factor is mediated by a non-classical pathway involving an ABC transporter. FEBS Lett *551*, 78-86.

Gallego, S.G., Loukas, A., Slade, R.W., Neva, F.A., Varatharajalu, R., Nutman, T.B., and Brindley, P.J. (2005). Identification of an astacin-like metallo-proteinase transcript from the infective larvae of Strongyloides stercoralis. Parasitology International *54*, 123-133.

Gao, B., and Tsan, M.F. (2004). Induction of cytokines by heat shock proteins and endotoxin in murine macrophages. Biochem Biophys Res Commun *317*, 1149-1154.

Gething, M.-J. (1997). Guidebook to molecular chaperones and protein-folding catalysts (Oxford, Sambrook & Tooze at Oxford University Press).

Gnanasekar, M., Anandharaman, V., Anand, S.B., Nutman, T.B., and Ramaswamy, K. (2008). A novel small heat shock protein 12.6 (HSP12.6) from Brugia malayi functions as a human IL-10 receptor binding protein. Mol Biochem Parasitol *159*, 98-103.

Grove, D.I. (1989). Strongyloidiasis : a major roundworm infection of man (Taylor & Francis).

Grove, D.I. (1996). Human strongyloidiasis. Adv Parasitol *38*, 251-309.

Guyatt, H. (2000). Do intestinal nematodes affect productivity in adulthood? Parasitology today (Personal ed) *16*, 153-158.

Hartman, D., Cottee, P.A., Savin, K.W., Bhave, M., Presidente, P.J., Fulton, L., Walkiewicz, M., and Newton, S.E. (2003). Haemonchus contortus: molecular characterisation of a small heat shock protein. Exp Parasitol *104*, 96-103.

Hewitson, J.P., Grainger, J.R., and Maizels, R.M. (2009). Helminth immunoregulation: the role of parasite secreted proteins in modulating host immunity. Mol Biochem Parasitol *167*, 1-11.

Hotez, P.J. (2008). Tropical diseases research: thirty years and counting. PLoS Negl Trop Dis *2*, e329.

Hotez, P.J., Ashcom, J., Zhan, B., Bethony, J., Loukas, A., Hawdon, J., Wang, Y., Jin, Q., Jones, K.C., Dobardzic, A., *et al.* (2003). Effect of vaccination with a recombinant fusion protein encoding an astacinlike metalloprotease (MTP-1) secreted by host-stimulated Ancylostoma caninum third-stage infective larvae. J Parasitol *89*, 853-855.

Hunter, T., Bannister, W.H., and Hunter, G.J. (1997). Cloning, expression, and characterization of two manganese superoxide dismutases from Caenorhabditis elegans. J Biol Chem *272*, 28652-28659.

Janeway, C.A. (2001). Immunobiology 5 : the immune system in health and disease, 5th ed. edn (New York, Garland ; Edinburgh : Churchill Livingstone).

Jecock, R.M., and Devaney, E. (1992). Expression of small heat shock proteins by the third-stage larva of Brugia pahangi. Mol Biochem Parasitol *56*, 219-226.

Jehle, S., Rajagopal, P., Bardiaux, B., Markovic, S., Kuhne, R., Stout, J.R., Higman, V.A., Klevit, R.E., van Rossum, B.J., and Oschkinat, H. (2010). Solid-state NMR and SAXS studies

provide a structural basis for the activation of alphaB-crystallin oligomers. Nat Struct Mol Biol *17*, 1037-1042.

Junod, C. (1987). [Retrospective study of 1,934 cases of strongyloidiasis diagnosed in Paris (1970-1986). I. Geographic origin. Epidemiology]. Bull Soc Pathol Exot Filiales *80*, 357-369.

Keiser, J., Thiemann, K., Endriss, Y., and Utzinger, J. (2008). Strongyloides ratti: in vitro and in vivo activity of tribendimidine. PLoS Negl Trop Dis *2*, e136.

Keiser, P.B., and Nutman, T.B. (2004). Strongyloides stercoralis in the Immunocompromised Population. Clin Microbiol Rev *17*, 208-217.

Kim, K.K., Kim, R., and Kim, S.H. (1998). Crystal structure of a small heat-shock protein. Nature *394*, 595-599.

Kleemann, R., Hausser, A., Geiger, G., Mischke, R., Burger-Kentischer, A., Flieger, O., Johannes, F.J., Roger, T., Calandra, T., Kapurniotu, A., *et al.* (2000). Intracellular action of the cytokine MIF to modulate AP-1 activity and the cell cycle through Jab1. Nature *408*, 211-216.

Kleemann, R., Kapurniotu, A., Frank, R.W., Gessner, A., Mischke, R., Flieger, O., Juttner, S., Brunner, H., and Bernhagen, J. (1998). Disulfide analysis reveals a role for macrophage migration inhibitory factor (MIF) as thiol-protein oxidoreductase. J Mol Biol *280*, 85-102.

Kobayashi, M., Nasuhara, Y., Kamachi, A., Tanino, Y., Betsuyaku, T., Yamaguchi, E., Nishihira, J., and Nishimura, M. (2006). Role of macrophage migration inhibitory factor in ovalbumin-induced airway inflammation in rats. Eur Respir J *27*, 726-734.

Kokke, B.P., Boelens, W.C., and de Jong, W.W. (2001). The lack of chaperonelike activity of Caenorhabditis elegans Hsp12.2 cannot be restored by domain swapping with human alphaB-crystallin. Cell Stress Chaperones *6*, 360-367.

Kokke, B.P., Leroux, M.R., Candido, E.P., Boelens, W.C., and de Jong, W.W. (1998). Caenorhabditis elegans small heat-shock proteins Hsp12.2 and Hsp12.3 form tetramers and have no chaperone-like activity. FEBS Lett *433*, 228-232.

Korenaga, M., Nawa, Y., Mimori, T., and Tada, I. (1983). Strongyloides ratti: the role of enteral antigenic stimuli by adult worms in the generation of protective immunity in rats. Exp Parasitol *55*, 358-363.

Kramme, S., Nissen, N., Soblik, H., Erttmann, K., Tannich, E., Fleischer, B., Panning, M., and Brattig, N. (2010). Novel real-time PCR for the universal detection of Strongyloides spp. J Med Microbiol.

Laemmli, U.K. (1970). Cleavage of structural proteins during the assembly of the head of bacteriophage T4. Nature *227*, 680-685.

Laganowsky, A., Benesch, J.L., Landau, M., Ding, L., Sawaya, M.R., Cascio, D., Huang, Q., Robinson, C.V., Horwitz, J., and Eisenberg, D. (2010). Crystal structures of truncated alphaA and alphaB crystallins reveal structural mechanisms of polydispersity important for eye lens function. Protein Sci *19*, 1031-1043.

Lancaster, G.I., and Febbraio, M.A. (2005). Exosome-dependent trafficking of HSP70: a novel secretory pathway for cellular stress proteins. J Biol Chem *280*, 23349-23355.

Leech, M., Lacey, D., Xue, J.R., Santos, L., Hutchinson, P., Wolvetang, E., David, J.R., Bucala, R., and Morand, E.F. (2003). Regulation of p53 by macrophage migration inhibitory factor in inflammatory arthritis. Arthritis Rheum *48*, 1881-1889.

Leng, L., and Bucala, R. (2006). Insight into the biology of macrophage migration inhibitory factor (MIF) revealed by the cloning of its cell surface receptor. Cell Res *16*, 162-168.

Leng, L., Metz, C.N., Fang, Y., Xu, J., Donnelly, S., Baugh, J., Delohery, T., Chen, Y., Mitchell, R.A., and Bucala, R. (2003). MIF signal transduction initiated by binding to CD74. J Exp Med *197*, 1467-1476.

Liao, J.H., Lee, J.S., Wu, S.H., and Chiou, S.H. (2009). COOH-terminal truncations and site-directed mutations enhance thermostability and chaperone-like activity of porcine alphaB-crystallin. Mol Vis *15*, 1429-1444.

Liebau, E., Hoppner, J., Muhlmeister, M., Burmeister, C., Luersen, K., Perbandt, M., Schmetz, C., Buttner, D., and Brattig, N. (2008). The secretory omega-class glutathione transferase OvGST3 from the human pathogenic parasite Onchocerca volvulus. FEBS J *275*, 3438-3453.

Lightowlers, M.W., and Rickard, M.D. (1988). Excretory-secretory products of helminth parasites: effects on host immune responses. Parasitology *96 Suppl*, S123-166.

Lim, S., Katz, K., Krajden, S., Fuksa, M., Keystone, J.S., and Kain, K.C. (2004). Complicated and fatal Strongyloides infection in Canadians: risk factors, diagnosis and management. CMAJ *171*, 479-484.

Liu, C., Young, A.L., Starling-Windhof, A., Bracher, A., Saschenbrecker, S., Rao, B.V., Rao, K.V., Berninghausen, O., Mielke, T., Hartl, F.U., *et al.* (2010). Coupled chaperone action in folding and assembly of hexadecameric Rubisco. Nature *463*, 197-202.

Liu, L.X., and Weller, P.F. (1993). Strongyloidiasis and other intestinal nematode infections. Infect Dis Clin North Am *7*, 655-682.

Livak, K.J., and Schmittgen, T.D. (2001). Analysis of relative gene expression data using real-time quantitative PCR and the 2(-Delta Delta C(T)) Method. Methods *25*, 402-408.

Lubetsky, J.B., Swope, M., Dealwis, C., Blake, P., and Lolis, E. (1999). Pro-1 of macrophage migration inhibitory factor functions as a catalytic base in the phenylpyruvate tautomerase activity. Biochemistry *38*, 7346-7354.

Maharshak, N., Cohen, S., Lantner, F., Hart, G., Leng, L., Bucala, R., and Shachar, I. (2010). CD74 is a survival receptor on colon epithelial cells. World J Gastroentero *16*, 3258-3266.

Maizels, R.M., and Yazdanbakhsh, M. (2003). Immune regulation by helminth parasites: cellular and molecular mechanisms. Nat Rev Immunol *3*, 733-744.

Mambula, S.S., Stevenson, M.A., Ogawa, K., and Calderwood, S.K. (2007). Mechanisms for Hsp70 secretion: crossing membranes without a leader. Methods *43*, 168-175.

Marcos, L.A., Terashima, A., Dupont, H.L., and Gotuzzo, E. (2008). Strongyloides hyperinfection syndrome: an emerging global infectious disease. Trans R Soc Trop Med Hyg *102*, 314-318.

Marson, A.L., Tarr, D.E., and Scott, A.L. (2001). Macrophage migration inhibitory factor (mif) transcription is significantly elevated in Caenorhabditis elegans dauer larvae. Gene *278*, 53-62.

Martin, J., Abubucker, S., Wylie, T., Yin, Y., Wang, Z., and Mitreva, M. (2009). Nematode.net update 2008: improvements enabling more efficient data mining and comparative nematode genomics. Nucleic Acids Res *37*, D571-578.

Maruyama, H., El-Malky, M., Kumagai, T., and Ohta, N. (2003). Secreted adhesion molecules of Strongyloides venezuelensis are produced by oesophageal glands and are components of the wall of tunnels constructed by adult worms in the host intestinal mucosa. Parasitology *126*, 165-171.

Mello, L.V., O'Meara, H., Rigden, D.J., and Paterson, S. (2009). Identification of novel aspartic proteases from Strongyloides ratti and characterisation of their evolutionary relationships, stage-specific expression and molecular structure. BMC Genomics *10*, 611.

Mimori, T., Tanaka, M., and Tada, I. (1987). Strongyloides ratti: formation of protection in rats by excretory/secretory products of adult worms. Exp Parasitol *64*, 342-346.

Montes, M., Sawhney, C., and Barros, N. (2010). Strongyloides stercoralis: there but not seen. Curr Opin Infect Dis *23*, 500-504.

Moore, T.A., Ramachandran, S., Gam, A.A., Neva, F.A., Lu, W., Saunders, L., Williams, S.A., and Nutman, T.B. (1996). Identification of novel sequences and codon usage in Strongyloides stercoralis. Mol Biochem Parasitol *79*, 243-248.

Morand, E.F. (2005). New therapeutic target in inflammatory disease: macrophage migration inhibitory factor. Intern Med J *35*, 419-426.

Mpagi, J.L., Buttner, D.W., Tischendorf, F.W., Erttmann, K.D., and Brattig, N.W. (2000). Humoral responses to a secretory Onchocerca volvulus protein: differences in the pattern of antibody isotypes to recombinant Ov20/OvS1 in generalized and hyperreactive onchocerciasis. Parasite Immunol *22*, 455-460.

Muller, N., Hemphill, A., Imboden, M., Duvallet, G., Dwinger, R.H., and Seebeck, T. (1992). Identification and characterization of two repetitive non-variable antigens from African trypanosomes which are recognized early during infection. Parasitology *104 Pt 1*, 111-120.

Nagaraj, S.H., Gasser, R.B., and Ranganathan, S. (2008). Needles in the EST haystack: large-scale identification and analysis of excretory-secretory (ES) proteins in parasitic nematodes using expressed sequence tags (ESTs). PLoS Negl Trop Dis *2*, e301.

Nemetschke, L., Eberhardt, A.G., Viney, M.E., and Streit, A. (2010). A genetic map of the animal-parasitic nematode Strongyloides ratti. Mol Biochem Parasitol *169*, 124-127.

Newton, S.E., and Munn, E.A. (1999). The development of vaccines against gastrointestinal nematode parasites, particularly Haemonchus contortus. Parasitol Today *15*, 116-122.

Nisbet, A.J., Bell, N.E., McNeilly, T.N., Knox, D.P., Maizels, R.M., Meikle, L.I., Wildblood, L.A., and Matthews, J.B. (2010). A macrophage migration inhibitory factor-like tautomerase from Teladorsagia circumcincta (Nematoda: Strongylida). Parasite Immunol *32*, 503-511.

Nisbet, A.J., Redmond, D.L., Matthews, J.B., Watkins, C., Yaga, R., Jones, J.T., Nath, M., and Knox, D.P. (2008). Stage-specific gene expression in Teladorsagia circumcincta (Nematoda: Strongylida) infective larvae and early parasitic stages. Int J Parasitol *38*, 829-838.

Nokes, C., Grantham-McGregor, S.M., Sawyer, A.W., Cooper, E.S., Robinson, B.A., and Bundy, D.A. (1992). Moderate to heavy infections of Trichuris trichiura affect cognitive function in Jamaican school children. Parasitology *104 (Pt 3)*, 539-547.

Ogawa, H., Nishihira, J., Sato, Y., Kondo, M., Takahashi, N., Oshima, T., and Todo, S. (2000). An antibody for macrophage migration inhibitory factor suppresses tumour growth and inhibits tumour-associated angiogenesis. Cytokine *12*, 309-314.

Olsen, A., van Lieshout, L., Marti, H., Polderman, T., Polman, K., Steinmann, P., Stothard, R., Thybo, S., Verweij, J.J., and Magnussen, P. (2009). Strongyloidiasis--the most neglected of the neglected tropical diseases? Trans R Soc Trop Med Hyg *103*, 967-972.

Park, S.K., Cho, M.K., Park, H.K., Lee, K.H., Lee, S.J., Choi, S.H., Ock, M.S., Jeong, H.J., Lee, M.H., and Yu, H.S. (2009). Macrophage migration inhibitory factor homologs of anisakis simplex suppress Th2 response in allergic airway inflammation model via CD4+CD25+Foxp3+ T cell recruitment. J Immunol *182*, 6907-6914.

Pastrana, D.V., Raghavan, N., FitzGerald, P., Eisinger, S.W., Metz, C., Bucala, R., Schleimer, R.P., Bickel, C., and Scott, A.L. (1998). Filarial nematode parasites secrete a homologue of the human cytokine macrophage migration inhibitory factor. Infect Immun *66*, 5955-5963.

Pfaffl, M.W. (2001). A new mathematical model for relative quantification in real-time RT-PCR. Nucleic Acids Res *29*, e45.

Playfair, J.H.L., and Bancroft, G.J. (2008). Infection and immunity, 3rd ed. edn (Oxford, Oxford University Press).

Plesset, J., Palm, C., and McLaughlin, C.S. (1982). Induction of heat shock proteins and thermotolerance by ethanol in Saccharomyces cerevisiae. Biochem Biophys Res Commun *108*, 1340-1345.

Pouyssegur, J., Shiu, R.P., and Pastan, I. (1977). Induction of two transformation-sensitive membrane polypeptides in normal fibroblasts by a block in glycoprotein synthesis or glucose deprivation. Cell *11*, 941-947.

Quaroni, A., Wands, J., Trelstad, R.L., and Isselbacher, K.J. (1979). Epithelioid cell cultures from rat small intestine. Characterization by morphologic and immunologic criteria. J Cell Biol *80*, 248-265.

Raghavan, N., Ghosh, I., Eisinger, W.S., Pastrana, D., and Scott, A.L. (1999). Developmentally regulated expression of a unique small heat shock protein in Brugia malayi. Mol Biochem Parasitol *104*, 233-246.

Richardson, J.M., Morrison, L.S., Bland, N.D., Bruce, S., Coombs, G.H., Mottram, J.C., and Walkinshaw, M.D. (2009). Structures of Leishmania major orthologues of macrophage migration inhibitory factor. Biochem Biophys Res Commun *380*, 442-448.

Robinson, M.W., Menon, R., Donnelly, S.M., Dalton, J.P., and Ranganathan, S. (2009). An integrated transcriptomics and proteomics analysis of the secretome of the helminth pathogen Fasciola hepatica: proteins associated with invasion and infection of the mammalian host. Mol Cell Proteomics *8*, 1891-1907.

Rook, G.A. (2007). The hygiene hypothesis and the increasing prevalence of chronic inflammatory disorders. Trans R Soc Trop Med Hyg *101*, 1072-1074.

Rook, G.A. (2009). Review series on helminths, immune modulation and the hygiene hypothesis: the broader implications of the hygiene hypothesis. Immunology *126*, 3-11.

Rook, G.A. (2010). 99th Dahlem conference on infection, inflammation and chronic inflammatory disorders: darwinian medicine and the 'hygiene' or 'old friends' hypothesis. Clin Exp Immunol *160*, 70-79.

Rook, G.A., and Lowry, C.A. (2008). The hygiene hypothesis and psychiatric disorders. Trends Immunol *29*, 150-158.

Sambrook, J., Fritsch, E.F., and Maniatis, T. (1989). Molecular cloning, 2nd ed. edn (Cold Spring Harbor, N.Y., Cold Spring Harbor Laboratory Press).

Sampson, I.A., and Grove, D.I. (1987). Strongyloidiasis is endemic in another Australian population group: Indochinese immigrants. Med J Aust *146*, 580-582.

Scaglia, M., Brustia, R., Gatti, S., Bernuzzi, A.M., Strosselli, M., Malfitano, A., and Capelli, D. (1984). Autochthonous strongyloidiasis in Italy: an epidemiological and clinical review of 150 cases. Bull Soc Pathol Exot Filiales *77*, 328-332.

Sher, A., Pearce, E., and Kaye, P. (2003). Shaping the immune response to parasites: role of dendritic cells. Curr Opin Immunol *15*, 421-429.

Shi, X., Leng, L., Wang, T., Wang, W., Du, X., Li, J., McDonald, C., Chen, Z., Murphy, J.W., Lolis, E., *et al.* (2006). CD44 is the signaling component of the macrophage migration inhibitory factor-CD74 receptor complex. Immunity *25*, 595-606.

Shim, J., Im, S.H., and Lee, J. (2003). Tissue-specific expression, heat inducibility, and biological roles of two hsp16 genes in Caenorhabditis elegans. FEBS Lett *537*, 139-145.

Smits, H.H., Everts, B., Hartgers, F.C., and Yazdanbakhsh, M. (2010). Chronic helminth infections protect against allergic diseases by active regulatory processes. Curr Allergy Asthma Rep *10*, 3-12.

Smits, H.H., and Yazdanbakhsh, M. (2007). Chronic helminth infections modulate allergen-specific immune responses: Protection against development of allergic disorders? Ann Med *39*, 428-439.

Sprott, V., Selby, C.D., Ispahani, P., and Toghill, P.J. (1987). Indigenous strongyloidiasis in Nottingham. Br Med J (Clin Res Ed) *294*, 741-742.

Stone, A.R., Platt, H.M., and Khalil, L.F. (1983). Concepts in nematode systematics (London, Published for the Systematics Association by Academic Press).

Swope, M., Sun, H.W., Blake, P.R., and Lolis, E. (1998). Direct link between cytokine activity and a catalytic site for macrophage migration inhibitory factor. EMBO J *17*, 3534-3541.

Tan, T.H., Edgerton, S.A., Kumari, R., McAlister, M.S., Roe, S.M., Nagl, S., Pearl, L.H., Selkirk, M.E., Bianco, A.E., Totty, N.F., *et al.* (2001). Macrophage migration inhibitory factor of the parasitic nematode Trichinella spiralis. Biochem J *357*, 373-383.

Tazir, Y., Steisslinger, V., Soblik, H., Younis, A.E., Beckmann, S., Grevelding, C.G., Steen, H., Brattig, N.W., and Erttmann, K.D. (2009). Molecular and functional characterisation of the heat shock protein 10 of Strongyloides ratti. Mol Biochem Parasitol *168*, 149-157.

Thompson, F.J., Barker, G.L., Hughes, L., and Viney, M.E. (2008). Genes important in the parasitic life of the nematode Strongyloides ratti. Mol Biochem Parasitol *158*, 112-119.

Tsan, M.F., and Gao, B. (2004). Cytokine function of heat shock proteins. Am J Physiol Cell Physiol *286*, C739-744.

Tweedie, S., Grigg, M.E., Ingram, L., and Selkirk, M.E. (1993). The expression of a small heat shock protein homologue is developmentally regulated in Nippostrongylus brasiliensis. Mol Biochem Parasitol *61*, 149-153.

Van Montfort, R., Slingsby, C., and Vierling, E. (2001). Structure and function of the small heat shock protein/alpha-crystallin family of molecular chaperones. Adv Protein Chem *59*, 105-156.

van Riet, E., Hartgers, F.C., and Yazdanbakhsh, M. (2007). Chronic helminth infections induce immunomodulation: consequences and mechanisms. Immunobiology *212*, 475-490.

Vercauteren, I., De Maere, V., Vercruysse, J., Stevens, M., Gevaert, K., and Claerebout, E. (2006). A small heat shock protein of Ostertagia ostertagi: stage-specific expression, heat inducibility, and protection trial. J Parasitol *92*, 1244-1250.

Vermeire, J.J., Cho, Y., Lolis, E., Bucala, R., and Cappello, M. (2008). Orthologs of macrophage migration inhibitory factor from parasitic nematodes. Trends Parasitol *24*, 355-363.

Viney, M.E. (1994). A genetic analysis of reproduction in Strongyloides ratti. Parasitology *109 (Pt 4)*, 511-515.

Viney, M.E. (1999). Exploiting the life cycle of Strongyloides ratii. Parasitol Today *15*, 231-235.

Viney, M.E., and Lok, J.B. (2007). Strongyloides spp. WormBook, 1-15.

Wakelin, D. (1996). Immunology and genetics of zoonotic infections involving parasites. Comp Immunol Microbiol Infect Dis *19*, 255-265.

Wakelin, D., and Walliker, D. (1996). Genetics of host and parasite--implications for immunity, epidemiology and evolution. Parasitology *112 Suppl*, S1-4.

Walzer, P.D., Milder, J.E., Banwell, J.G., Kilgore, G., Klein, M., and Parker, R. (1982). Epidemiologic features of Strongyloides stercoralis infection in an endemic area of the United States. Am J Trop Med Hyg *31*, 313-319.

Woolhouse, M.E., Webster, J.P., Domingo, E., Charlesworth, B., and Levin, B.R. (2002). Biological and biomedical implications of the co-evolution of pathogens and their hosts. Nat Genet *32*, 569-577.

Wu, Z., Nagano, I., Boonmars, T., and Takahashi, Y. (2007). Thermally induced and developmentally regulated expression of a small heat shock protein in Trichinella spiralis. Parasitol Res *101*, 201-212.

Wylie, T., Martin, J.C., Dante, M., Mitreva, M.D., Clifton, S.W., Chinwalla, A., Waterston, R.H., Wilson, R.K., and McCarter, J.P. (2004). Nematode.net: a tool for navigating sequences from parasitic and free-living nematodes. Nucleic Acids Res *32*, D423-426.

Young, J.C., Agashe, V.R., Siegers, K., and Hartl, F.U. (2004). Pathways of chaperone-mediated protein folding in the cytosol. Nat Rev Mol Cell Biol *5*, 781-791.

Zang, X., Taylor, P., Wang, J.M., Meyer, D.J., Scott, A.L., Walkinshaw, M.D., and Maizels, R.M. (2002). Homologues of human macrophage migration inhibitory factor from a parasitic nematode. Gene cloning, protein activity, and crystal structure. J Biol Chem *277*, 44261-44267.

Zugel, U., and Kaufmann, S.H. (1999). Role of heat shock proteins in protection from and pathogenesis of infectious diseases. Clin Microbiol Rev *12*, 19-39.

8. PUBLICATIONS

Parts of this thesis have been published, after modification, in peer-reviewed international journals:

Younis AE, Geisinger F, Ajonina-Ekoti I, Soblik H, Steen H, Mitreva M, Erttmann KD, Perbandt M, Liebau E, Brattig NW (2011) Stage-specific excretory-secretory small heat shock proteins from the parasitic nematode *Strongyloides ratti*- putative links to host's intestinal mucosal defense system. *FEBS J*. 278, 3319-3336.

Younis AE, Soblik H, Ajonina I, Erttmann KD, Liebau E, Brattig NW (2011) Excretory/secretory macrophage migration inhibitory factor homologue from the parasitic nematode *Strongyloides ratti* interacts with host´s immune system. *Microbes Infect* (*in Press*).

Soblik H, **Younis AE**, Mitreva M, Renard BY, Geisinger F, Steen H, Brattig NW (2011) Life cycle stage-resolved proteomic analysis of the excretome/secretome from *Strongyloides ratti* – identification of stage-specific protease. *Mol Cell Proteomics* (*in Press*).

Tazir Y, Steisslinger V, Soblik , **Younis AE**, Beckmann S, Grevelding CG, Steen H, Brattig NW, Erttmann KD (2009) Molecular and functional characterization of the heat shock protein 10 of *Strongyloides ratti*. *Mol. Biochem. Parasitol*. 168, 149-157